1967-09

An analysis of single stage axial-flow turbine performance using three-dimensional calculating methods.

Harrison, Robert Glen

Monterey, California. U.S. Naval Postgraduate School

AN ANALYSIS OF SINGLE STAGE AXIAL-FLOW TURBINE PERFORMANCE USING THREE-DIMENSIONAL CALCULATING METHODS

ROBERT GLEN HARRISON

AN ANALYSIS OF SINGLE STAGE

AXIAL-FLOW TURBINE PERFORMANCE USING

THREE-DIMENSIONAL CALCULATING METHODS

by

Robert Glen Harrison
Lieutenant, United States Navy
B.M.E., University of Louisville, 1959

Submitted in partial fulfillment of the
requirements for the degree of

AERONAUTICAL ENGINEER

from the

NAVAL POSTGRADUATE SCHOOL
September 1967

ABSTRACT

The method of turbine performance prediction developed by Vavra and Eckert has been refined in this analysis to realize more of the potential of the three-dimensional calculating methods. Mach number and rotor tip clearance effects on blade outlet angles and loss coefficients have been localized rather than averaged over the blade height. An approximation for streamline curvature has been used.

Performance curves were determined for two single stage axial-flow turbines located at the Propulsion Laboratory of the Naval Postgraduate School. Test results were available for one of the turbines. Agreement between predicted and experimental performance values was generally within 3 per cent.

Thesis by Robert G. Harrison entitled: "An Analysis of Single-Stage Axial-Flow Turbine Performance Using Three-Dimensional Calculating Methods"

ERRATA SHEET

Page	Line	Change	To
3	10	Developement	Development
13	21	( )	(γ/δ)
13	22	518.4	$T_{to}/518.4$
18	13	developement	development
21	Eq.13	reads: $\xi = 1 - \sum \frac{\delta^*}{a} = \frac{H^{***}-1}{H^{***}-\zeta/2}$	
21	Eq.14	reads: $dA = \xi Z \frac{a}{a_m} dX\ a_m\ r_m$	
24	13	respresenting	representing
26	7/8	calculat-ing	calcula-ting
27	2		insert "α_1" after "the" at end of line.
27	27/28	proce-dur	proce-dure
36	10	$(\ \ )_w$	$(\eta)_w$
39	16		insert "ζ_R" after "of" at end of line.
44	13/14	opera-ting	operat-ing
45	23	b unt	blunt
49	8/9	coeffici-ents	coeffi-cients
107	7	glade	blade
147	Item 10	Item 10. should read:	"This document is subject to special export controls and each transmittal to foreign nationals may be made only with prior approval of the Naval Postgraduate School"

TABLE OF CONTENTS

Section		Page
1.	Introduction	17
2.	Basis for the Analysis	18
3.	Technique for Obtaining a Solution	23
4.	MOD I and MOD II Turbines	37
5.	Conclusions and Recommendations	48
6.	Bibliography	88
Appendix		
A.	Developement of Equations	89
B.	Computations of Outlet Angles and Loss Coefficients	101
C.	Computer Program	112

LIST OF TABLES

Table		Page
I.	Sample Calculations for Stator Outlet Angles	104
II.	Sample Calculations for Rotor Outlet Angles	105
III.	Sample Calculations for Stator Loss Coefficient	109
IV.	Sample Calculations for Stalling Incidence and Rotor Loss Coefficients	110
V.	Sample Computer Output for Stator Solution	144
VI.	Sample Computer Output for Rotor Solution	145

LIST OF ILLUSTRATIONS

Figure		Page
1.	Turbine Thermodynamic Process	50
2.	Coordinates and Streamlines	51
3.	Velocity Diagrams	52
4.	Stator and Rotor Blade Profiles (MOD I)	53
5.	Stator and Rotor Blade Profiles (MOD II)	54
6.	Stator and Rotor Throat Openings versus Radial Position (MOD I & MOD II)	55
7.	Variation of Stator Outlet Angle with Radius (MOD I)	56
8.	Variation of Stator Outlet Angle with Mach Number (MOD I)	56
9.	Variation of Stator Outlet Angle with Radius (MOD II)	57
10.	Variation of Stator Outlet Angle with Mach Number (MOD II)	57
11.	Variation of Rotor Outlet Angle with Radius (MOD I)	58
12.	Variation of Rotor Outlet Angle with Mach Number (MOD I)	58
13.	Variation of Rotor Outlet Angle with Radius (MOD II)	59
14.	Variation of Rotor Outlet Angle with Mach Number (MOD II)	59
15.	Stator Loss Coefficients as Function of Radius (MOD I & MOD II)	60
16.	Variation of Blade Inlet and Stall Incidence Angles with Radius (MOD I & MOD II)	61
17.	Rotor Loss Coefficients as Function of Incidence Ratio (MOD I)	62
18.	Rotor Loss Coefficients as Function of Incidence Ratio (MOD II)	63

Figure		Page

19. Variation of Referred Flowrate with Referred RPM (MOD I) 64

20. Referred Moment versus Referred RPM (MOD I) 65

21. Total-Static Efficiency versus Referred RPM (MOD I, k=0.020 in.) 66

22. Total-Static Efficiency versus Referred RPM (MOD I, k=0.033 in.) 67

23. Total-Static Efficiency versus Isentropic Head Coefficient (MOD I) 68

24. Referred Power versus Referred RPM (MOD I) 69

25. Theoretical Degree of Reaction versus Isentropic Head Coefficient (MOD I) 70

26. Theoretical Degree of Reaction versus Referred RPM (MOD I, P_{t_o}/P_2=1.40) 71

27. Variation of Referred Flowrate with Referred RPM (MOD II, k=0.015 in.) 72

28. Variation of Referred Flowrate with Referred RPM (MOD II, k=0.033 in.) 73

29. Referred Moment versus Referred RPM (MOD II, k=0.015 in.) 74

30. Referred Moment versus Referred RPM (MOD II, k=0.033 in.) 75

31. Total-Static Efficiency versus Referred RPM (MOD II, P_{t_o}/P_2=1.30, 1.31) 76

32. Total-Static Efficiency versus Referred RPM (MOD II, P_{t_o}/P_2=1.40) 77

33. Total-Static Efficiency versus Referred RPM (MOD II, P_{t_o}/P_2=1.50, 1.51) 78

34. Total-Static Efficiency versus Referred RPM (MOD II, P_{t_o}/P_2=1.60) 79

35. Total-Static Efficiency versus Isentropic Head Coefficient (MOD II) 80

Figure | Page

36. Referred Power versus Referred RPM (MOD II, k=0.015 in.) [illegible]

37. Referred Power versus Referred RPM (MOD II, k=0.033 in.) 82

38. Theoretical Degree of Reaction versus Isentropic Head Coefficient (MOD II) 8[illegible]

39. Theoretical Degree of Reaction versus Referred RPM (MOD II, P_{t_o}/P_2=1.40) 84

40. Absolute Flow Outlet Angles as Function of Radius (MOD II, k=0.015 in., P_{t_o}/P_2=1.40, RPM/$\sqrt{\theta}$ =13,934) 85

41. Referred Velocities as Function of Radius (MOD II, k=0.015 in., P_{t_o}/P_2=1.40, RPM/$\sqrt{\theta}$ =13,934) 8[illegible]

42. Relative Rotor Flow Outlet Angle as Function of Radius (MOD II, k=0.015 in., P_{t_o}/P_2=1.40, RPM/$\sqrt{\theta}$ =13,934) 86

43. Plots of Axial Velocity Ratios versus Radius Ratios at Peak Efficiency (MOD I & MOD II, P_{t_o}/P_2=1.40) 87

44. Expansion from Plenum 94

45. Conditions at Exit of Blade Row 96

46. Blade Geometry 102

47. Tip Clearance Factor X as Function of Radius 103

TABLE OF SYMBOLS

Symbols

A	Area (in.^{2})
a	Throat opening of blade channel (in.)
B	Shroud factor used in rotor loss coefficient calculations (dimensionless)
b	Blade's departure from being straight-backed (in.)
C_1	Conversion factor, 2gJ(ft^2-lb$_m$/sec^2-BTU)
c	Blade Chord (in.)
c_p	Specific heat, constant pressure (BTU/lb$_m$-^{o}R)
$\dot{E}$	Kinetic energy rate (ft-lb/sec)
e	Mean radius of curvature of back of blade (in.)
g	Universal gravitational constant (32.174 lb$_m$-ft/lb-sec^2)
H	Total enthalpy (BTU/lb$_m$)
H***	Boundary layer energy parameter ($\frac{\delta^{***}}{\delta^*}$)
h	Static enthalpy (BTU/lb$_m$)
h	Blade height (in.)
HP	Horsepower
I	Integrand
i	Incidence angle (deg. or radians)
$\vec{i}$	Unit vector
i_s	Stalling incidence angle (deg. or radians)
J	Conversion factor (778.16 ft-lb/BTU)
j	Distance from throat to trailing edge of blade (in.)
k	Tip clearance (in.)
k_{is}	Isentropic head coefficient (dimensionless)

Symbols

L	Distance between stations 0 and 1 and between stations 1 and 2 (in.)
M	Mach number
M	Moment (ft-lb)
$\dot{m}$	Mass flowrate (slugs/sec)
m	Exponent used in boundary layer calculations, see Eq. 146 (dimensionless)
P	Pressure (psia)
R	Gas constant for air (53.345 ft-lb/lb_m-^oR)
r	Radius (in.)
r^*	Theoretical degree of reaction (dimensionless)
s	Blade spacing (in.)
s	Entropy (BTU/lb_m-^oR)
s^*	Non-dimensional entropy ($\frac{s}{c_p}$)
T	Temperature (^oR)
t	Blade thickness (in.)
t	Blade trailing edge thickness (in.)
t^*	Projection of blade trailing edge thickness on the exit plane of the blade row (in.)
U	Peripheral velocity (ft/sec)
u	Velocity within a boundary layer (ft/sec)
V	Absolute velocity (ft/sec)
W	Relative velocity (ft/sec)
$\dot{w}$	Weight flowrate (lb_m/sec)
W_f	Fraction of the total flowrate which passes between the hub and any other streamline (dimensionless)
W_{ref}	Reference flowrate (in.^{2})

Symbols

X	Non-dimensional radius $\frac{r}{r_m}$ where r_m is the mean streamline radius
X	Shroud factor for calculation of rotor outlet angles (dimensionless)
X_e	See Eq. 145
Y	Non-dimensional axial velocity $\frac{V_A}{V_{A_m}}$ where V_{A_m} is the mean streamline axial velocity
Y	Pressure loss parameter, see Eq. 167
y	Distance from wall of a point in a boundary layer (in.)
Z	Number of blades

Greek Letters

α	Absolute gas flow angles (deg. or radians)
β	Gas flow angles relative to rotor (deg. or radians)
β_o	Blade inlet angle (deg. or radians)
γ	Specific heat ratio (dimensionless)
ΔR	Streamline displacement, see Fig. 2 (in.)
δ	Boundary layer thickness (in.)
δ	Referred pressure $\frac{P_{t_o}}{14.7}$ (dimensionless)
δr	Streamline displacement, see Fig. 2 (in.)
δ^*	Boundary layer displacement thickness (in.)
δ^{***}	Boundary layer energy thickness (in.)
ζ	Loss coefficient (dimensionless)
η	Efficiency (dimensionless)
η	Non-dimensional distance from the wall in a boundary layer ( )
θ	Referred temperature 518.4 (dimensionless)
K	Streamline curvature factor (dimensionless)

Greek Letters

λ	Angle between flow and axis of turbine in a meridional plane (deg. or radians)
λ	Factor used in predicting secondary loss coefficients, see Eq. 171 (dimensionless)
ξ	Area restriction factor (dimensionless)
ρ	Density (lb_m/ft^3)
Φ	Non-dimensional flow function
ω	Angular velocity (radians/sec)

Subscripts

A	Axial
d	Discharge
E	Equivalent
H	Hub
is	Isentropic expansion from total inlet conditions
m	Mean streamline
o	Station ahead of stator
P	Profile
R	Relative
r	Radial
ref	Referred
req.	Required
S	Stator
S	Shroud
s	Isentropic expansion from equivalent total conditions
T	Tip
t	Total

Subscripts

th	Theoretical
u	Tangential
z	Axial direction, cyclindrical coordinates
θ	Peripheral direction, cyclindrical coordinates
1	Station between stator and rotor
2	Station after rotor

Superscript

**	Refers to predicted values for the mean streamline

1. Introduction

Turbines form an important part of propulsion systems. To optimize a design it is necessary to know the performance at off-design conditions as well as the performance at the design point. Since the testing of a prototype is very costly and time consuming, it is of great advantage to be able to predict the performance characteristics by means of theoretical methods. The more advanced a system is the more important it becomes to improve the accuracy of these methods. Hence it is necessary to base these methods on the fundamental laws of fluid dynamics rather than on rule-of-thumb approximations. The latter basis is possible only when data on previous designs are available. For new and advanced configurations, it will be necessary to apply refined methods which enable the designer and systems engineer to predict the effect of proposed design changes.

The principal equations that describe the flow properties in turbomachines are well known. These same equations are used as a basis for all proper "three-dimensional" calculating methods that have been cited in the technical literature. The methods differ however in the manner in which these equations are manipulated and applied.

This thesis is concerned with the refinement of the three-dimensional method of analysis developed by Vavra and Eckert. Based on the physical dimensions of particular test turbines that are available at the Turbo-Propulsion Laboratory of the Naval Postgraduate School, performance curves were determined for these machines. Concurrently with the performance analysis, experimental tests were conducted on one of these turbines so that actual experimental results could be used to judge the accuracy of the proposed theoretical performance evaluation.

In addition to his publications and classroom lectures which constituted the foundation for this analysis, Professor Vavra was very generous in providing guidance and counsel during the period of this work. For this I am greatly appreciative. I would also like to thank Lieutenants P. M. Commons and J. A. Messegee for making their experimental results available.

2. Basis for the Analysis

The two conservation equations that must be satisfied to obtain a solution for the flow in a turbine are the equations of motion and continuity. These equations are satisfied at stations between blade rows. The method used is that given by Vavra.[1] Vavra developed the equations of motion and continuity for absolute flows. The equations in this form are readily useable for the position after the stator. Eckert later developed these equations for relative flows to be used for rotor calculations.[2] Eckert's conversion allows relative flow quantities to be handled directly without conversion to an absolute system. Eckert's approach also avoids iteration procedures to determine the total enthalpy after the rotor.

The assumptions made for the developement of the equations used in the performance analysis are:

1. An infinite number of blades in each row so that downstream effects are not felt upstream.

2. Axisymmetric flow at the stations where the equations of motion are solved.

3. Adiabatic and steady flow so that the total enthalpy along any given streamline is constant through the stator and the relative total enthalpy is constant through the rotor.

4. All entropy changes are assumed to occur in the blade channels that are located ahead of the stations where the equations of motion are satisfied. Hence at the calculating stations the flow is assumed to be isentropic along particular streamlines.

With the above assumptions, the equations of motion for absolute and relative flows, respectively, are

$$\nabla H = \bar{V} \times (\nabla \times \bar{V}) + T \nabla s \tag{1}$$

$$\nabla H_R = \bar{W} \times (\nabla \times \bar{W} + 2\bar{\omega}) + T \nabla s \tag{2}$$

---

[1] Vavra, M. H., Aero-Thermodynamics and Flow in Turbomachines. New York, London: John Wiley and Sons, Inc., 1960, Chapter 16.

[2] Eckert, R. H., Performance Analysis and Initial Tests of a Transonic Turbine Test Rig (USNPGS Thesis, May 1966), pp. 149-155.

Relative total enthalpy can be written as

$$H_R = h_1 + \frac{W_1^2}{2} - \frac{U_1^2}{2} = h_2 + \frac{W_2^2}{2} - \frac{U_2^2}{2} = h_{2s} + \frac{W_{2th}^2}{2} - \frac{U_2^2}{2} \quad (3)$$

Equivalent enthalpy is defined as

$$H_E = h_{2s} + \frac{W_{2th}^2}{2} = H_R + \frac{U_2^2}{2} \quad (4)$$

Similar to H_R, the equivalent enthalpy H_E is constant along a streamline for the adopted assumptions. Equivalent enthalpy can also be written as

$$H_E = h_2 + \frac{W_2^2}{2} = h_1 + \frac{W_1^2}{2} + \frac{U_2^2 - U_1^2}{2} \quad (5)$$

The introduction of the equivalent enthalpy allows this quantity to be used for the rotor in a manner analogous to the way total enthalpy is used for the stator.

For equations used in this analysis, the subscripts refer to:

0 - station ahead of stator

1 - station ahead of rotor

2 - station after rotor

is - isentropic expansion from P_{t_0}

s - isentropic expansion from P_{t_E}

th - the theoretical value

Figure 1 is a temperature-entropy diagram showing the thermodynamic process along a particular streamline for a single stage turbine. In general, the fluid properties will vary from streamline to streamline. The method in which the loss coefficients are applied is also indicated in Fig. 1. The loss coefficients are defined as

$$y_S = \frac{V_{1th}^2 - V_1^2}{V_{1th}^2} \qquad \text{For the Stator} \quad (6)$$

$$y_R = \frac{W_{2th}^2 - W_2^2}{W_{2th}^2} \qquad \text{For the Rotor} \quad (7)$$

The coordinate system that will be used in the analysis is indicated in Fig. 2. This figure also shows the general layout of the type turbine to which the prediction performance analysis is applied.

Sign convention for the various angles that are needed in the analysis is indicated in Fig. 3.

The modification of Eq. 2 into a form that can be used for the analysis is given in Appendix A, Section 1. The appropriate form of Eq. 1 can be obtained from the modification of Eq. 2 if the angular velocity ω is set equal to zero. Other differences of the final equations derived from Eqs. 1 and 2 are listed in Appendix A, Section 1. Equation 1 can then be written

$$\frac{d(\ln Y_1^2)}{dX_1} = -\cos^2\alpha_1\left[\left(-K2r_m\frac{\delta r}{L^2}\right)-\left(\frac{L^2+(\Delta R/2)^2}{L^2}\right)\frac{ds_1^*}{dX_1}\right]-2\,\mathrm{TAN}\,\alpha_1\frac{d\alpha_1}{dX_1}$$

$$-\frac{2}{X_1}\mathrm{SIN}^2\alpha_1+\frac{C_1\cos^2\alpha_1}{Y_1^2V_{A_{1m}}^2}\frac{dH}{dX_1}-\left[\frac{C_1H\cos^2\alpha_1}{Y_1^2V_{A_{1m}}^2}-\mathrm{SIN}^2\alpha_1\right]\frac{ds_1^*}{dX_1} \tag{8}$$

Equation 2 becomes

$$\frac{d(\ln Y_2^2)}{dX_2} = -\cos^2\beta_2\left[\left(K2r_m\frac{\delta r}{L^2}\right)-\left(\frac{L^2+(\Delta R/2)^2}{L^2}\right)\frac{ds_2^*}{dX_2}\right]-2\,\mathrm{TAN}\,\beta_2\frac{d\beta_2}{dX_2}-\frac{2}{X_2}\mathrm{SIN}^2\beta_2$$

$$-\frac{4U_m\cos\beta_2\sin\beta_2}{W_{A_m}Y_2}-\frac{2U_mU_2\cos^2\beta_2}{W_{A_m}^2Y_2^2}+\frac{C_1\cos^2\beta_2}{W_{A_m}^2Y_2^2}\frac{dH_E}{dX_2}-\left[\frac{C_1H_E\cos^2\beta_2}{W_{A_m}^2Y_2^2}-\mathrm{SIN}^2\beta_2\right]\frac{ds_2^*}{dX_2} \tag{9}$$

where:

$Y=\frac{V_A}{V_{A_m}}$ or $\frac{W_A}{W_{A_m}}$	for Eqs. 8 and 9 respectively (subscript m refers to mean streamline)
$X=\frac{r}{r_m}$	
$K=5.0$	streamline curvature factor
δr	streamline displacements shown in Fig. 2
ΔR	
$L=\frac{L_1+L_2}{2}$	(see Fig. 2)
$s^*=\frac{s}{c_p}$	
$C_1=2gJ$	

The equation of continuity is used in its non-dimensional form by introducing a flow function Φ . Developement of Φ is given in Appendix A, Section 2. In differential form the equations for absolute and relative flows can then be expressed by

$$\frac{d\dot{w}\sqrt{T_{t_0}}}{P_{t_0}}\sqrt{\frac{R}{g}} = dA\,\Phi = dA\sqrt{\frac{2\gamma}{\gamma-1}\left[\left(\frac{P}{P_{t_0}}\right)^{\frac{2}{\gamma}}-\left(\frac{P}{P_{t_0}}\right)^{\frac{\gamma+1}{\gamma}}\right]} \tag{10}$$

and

$$\frac{d\dot{w}\sqrt{T_{t_E}}}{P_{t_E}}\sqrt{\frac{R}{g}} = dA\,\Phi = dA\sqrt{\frac{2\gamma}{\gamma-1}\left[\left(\frac{P}{P_{t_E}}\right)^{\frac{2}{\gamma}}-\left(\frac{P}{P_{t_E}}\right)^{\frac{\gamma+1}{\gamma}}\right]} \tag{11}$$

The differential element of area dA is

$$dA = \xi\, Z\, a\, dr \tag{12}$$

where:

Z = number of blades

a = blade exit opening (see Fig. 46)

ξ = area restriction coefficient

Since Φ is valid for isentropic flow only, the restriction factor ξ must be introduced to correct the actual flow area to an effective area which accounts for the restrictions due to the boundary layers on both sides of the flow channel.

The factor ξ can be expressed by[3]

$$\xi = 1 - \Sigma \frac{\delta^*}{a} = \frac{H^{***} - 1}{H^{***} - 1 + \zeta/2} \qquad (13)$$

In Eq. 13, δ^* is the boundary layer displacement thickness and H^{***} is the so-called energy parameter defined as the energy thickness divided by the displacement thickness. The term $\frac{\zeta}{2}$ represents the loss that is assumed to occur from the inlet to the throat of the blade channel, where ζ is the loss coefficient representing all the losses across the row of blades. The profile loss coefficient was used by Eckert[4] to represent the loss prior to the blade throat. Percentage of the total loss due to profile losses will vary considerably depending on blade geometry, radial position, and the incidence of the flow on the leading edge of the blade. Since secondary flow and tip clearance effects result in losses in the blade channel, half the total loss coefficient provides a better average representation of the losses in the blade channel prior to the throat. The basis for the developement of ξ and H^{***} as used is given in Appendix A, Sections 3 and 4.

By multiplying and dividing by $a_m r_m$ Eq. 12 is

[illegible] (14)

---

[3] Vavra, M. H., Problems of Fluid Mechanics in Radial Turbomachines (Rhode-Saint-Genese, Belgium: Von Kármán Institute for Fluid Dynamics, 1965) VKI Course Note 55b, pp. G46-50.

[4] Eckert, op. cit., p. 44.

After integration Eqs. 10 and 11 become, respectively,

$$\frac{\dot{w}\sqrt{T_{t_o}}}{P_{t_o}}\sqrt{\frac{R}{g}} = a_m Z r_m \int_{X_H}^{X_T} \frac{a}{a_m} \xi \Phi \, dX \tag{15}$$

and

$$\frac{\dot{w}\sqrt{T_{t_E}}}{P_{t_L}}\sqrt{\frac{R}{g}} = a_m Z r_m \int_{X_H}^{X_T} \frac{a}{a_m} \xi \Phi \, dX \tag{16}$$

The flowrate $\dot{w}$ can be computed from the conditions ahead of the stator. Then a reference flowrate is defined by

$$W_{ref} \equiv \left[\frac{\dot{w}\sqrt{T_{t_o}}}{P_{t_o}}\sqrt{\frac{R}{g}}\right] \tag{17}$$

where W_{ref} is in square inches. Continuity will be satisfied for the stator by

$$\left[a_m Z r_m \int_{X_H}^{X_T} \frac{a}{a_m} \xi \Phi \, dX\right]_{STATOR} = W_{ref} \tag{18}$$

Similarly for the rotor

$$\left[a_m Z r_m \int_{X_H}^{X_T} \frac{P_{t_E}}{P_{t_o}}\sqrt{\frac{T_{t_o}}{T_{t_E}}} \frac{a}{a_m} \xi \Phi \, dX\right]_{ROTOR} = W_{ref} \tag{19}$$

The in luence of the leakage flow through the radial tip clearance has not been accounted for in Eq. 19.

The element of area between the blade tips and the shroud is

$$dA = 2\pi r \, dr \tag{20}$$

The flow through the tip clearance area is

$$\left[\frac{\dot{w}\sqrt{T_{t_E}}}{P_{t_E}}\sqrt{\frac{R}{g}}\right]_{TIP\ CLEARANCE} = 2\pi a_m Z r_m^2 \int_{X_T}^{X_S} \frac{X}{Z a_m} \xi \Phi \, dX \tag{21}$$

Since the tip clearance is relatively small, the values of Φ, ξ, P_{t_E}, T_{t_E}, and X_2 for the tip will be used in Eq. 21. With these assumptions Eq. 19 can be expressed by

$$\left[\int_{X_H}^{X_T} \frac{P_{t_E}}{P_{t_o}}\sqrt{\frac{T_{t_o}}{T_{t_E}}} \frac{a}{a_m} \xi \Phi \, dX + 2\pi r_m \int_{X_T}^{X_S} \left(\frac{P_{t_E}}{P_{t_o}}\sqrt{\frac{T_{t_o}}{T_{t_E}}} \xi \Phi X\right)_{TIP} \frac{dX}{Z a_m}\right]_{ROTOR} = \frac{W_{ref}}{\left[a_m Z r_m\right]_{ROTOR}} \tag{22}$$

The assumptions used to arrive at Eq. 22 are obviously incorrect in two respects. First, the flow represented by Φ_T is not

perpendicular to the tip clearance area. Second, the effective area represented by ξ_T is larger than that which probably occurs because of the relatively large boundary layers that exist on the shroud and blade tips. The exact behavior of the flow in the small region between the shroud and the blade tips is impossible to predict without further tests. However, it is felt that the flowrate through this space as represented in Eq. 22 is too large for the reasons just mentioned. Therefore a more accurate approximation of this flowrate will be obtained if the last term on the left side of Eq. 22 is divided by 2, yielding

$$\left[\int_{X_H}^{X_T} \frac{P_{t_E}}{P_{t_o}}\sqrt{\frac{T_{t_o}}{T_{t_E}}}\,\frac{a}{a_m}\,\xi\,\Phi\,dX + \pi r_m \int_{X_T}^{X_S}\left(\frac{P_{t_E}}{P_{t_o}}\sqrt{\frac{T_{t_o}}{T_{t_E}}}\,\xi\,\Phi\,X\right)_{TIP}\frac{dX}{Z a_m}\right]_{ROTOR} = \frac{W_{ref}}{\left[a_m Z r_m\right]_{ROTOR}} \tag{23}$$

The tip clearance flow included in Eq. 23 can be obtained by integration,

$$\pi r_m \int_{X_T}^{X_S}\left(\frac{P_{t_E}}{P_{t_o}}\sqrt{\frac{T_{t_o}}{T_{t_E}}}\,\xi\,\Phi\,X\right)_{TIP}\frac{dX}{Z a_m} = \frac{\pi r_m}{Z a_m}\left(\frac{P_{t_E}}{P_{t_o}}\sqrt{\frac{T_{t_o}}{T_{t_E}}}\,\xi\,\Phi\,X\right)_{TIP}\left[X_S - X_T\right]$$

$$= \frac{\pi r_m}{Z a_m}\left(\frac{P_{t_E}}{P_{t_o}}\sqrt{\frac{T_{t_o}}{T_{t_E}}}\,\xi\,\Phi\,X\right)_{TIP}\frac{k}{r_m} = \frac{\pi k r_T}{a_m Z r_m}\left(\frac{P_{t_E}}{P_{t_o}}\sqrt{\frac{T_{t_o}}{T_{t_E}}}\,\xi\,\Phi\right)_{TIP} \tag{24}$$

Introducing this expression into Eq. 23 gives

$$\left[\int_{X_H}^{X_T} \frac{P_{t_E}}{P_{t_o}}\sqrt{\frac{T_{t_o}}{T_{t_E}}}\,\frac{a}{a_m}\,\xi\,\Phi\,dX + \frac{\pi k r_T}{a_m Z r_m}\left(\frac{P_{t_E}}{P_{t_o}}\sqrt{\frac{T_{t_o}}{T_{t_E}}}\,\xi\,\Phi\right)_{TIP}\right]_{ROTOR} = \frac{W_{ref}}{\left[a_m Z r_m\right]_{ROTOR}} \tag{25}$$

3. Technique for Obtaining Solution

With the equations of motion and continuity in the forms given by Eqs. 8, 9, 18 and 25, a method has been developed to analyze single stage axial turbines, in particular, those available for test in the Turbine Test Rig of the Turbo-Propulsion Laboratory of the Naval Postgraduate School. The method of analysis predicts turbine performance for specified values of inlet total pressure, inlet total temperature, rotor speed and the ratio of total inlet to static discharge pressure P_{t_o}/P_2. This method is similar to that described by Eckert.[5] However, Eckert's analysis neglected some effects which

[5] Ibid, Section 3.

have been accounted for in this developement. Some significant changes made in this method are listed below:

1. Stator and rotor outlet angles for a particular radial location are computed using a calculated Mach number for that location rather than an assumed Mach number or the Mach number of the mean streamline.

2. Variation of loss coefficients due to changes in blade geometry in the radial direction is accounted for.

3. The influence of rotor tip clearance on the rotor outlet angles and loss coefficients is concentrated near the tip of the blade rather than averaging these effects over the full blade height.

4. Fourth order polynomials are used to better approximate the curves respresenting blade characteristics as a function of radius and the curves of rotor loss coefficients as a function of incidence.

5. Streamline curvature effects have been accounted for in the solution of the equations of motion.

In addition to the assumptions that were mentioned in Section 2 for the developement of the particular form of the equation of motion, the conditions ahead of the stator are assumed to be uniform; that is, the total temperature, velocity, and entropy are assumed constant and the flow axial in direction. It is realized that completely uniform conditions are difficult to obtain, but any other assumpt on would be extremely difficult to develop mathematically.

Direct solution of the equations of motion is not possible since they are nonlinear in the dependent variable Y. Likewise, no direct method is possible to satisfy continuity. Solutions of these equations must therefore be gained by making initial assumptions for the values of the axial velocities which must be improved by successive iterations until the equations are satisfied. To account for streamline curvature and slope, a complete solution of the flow through the stator and rotor must first be made by neglecting the effects of curvature in order to determine streamline locations. Then the iteration to account for these effects may progress. These requirements make the use of a high-speed computer a necessity.

This analysis has been programmed for the IBM 360 computer using FORTRAN IV. The program is described in Appendix C. The following paragraphs set forth the procedural steps of the program. The equations are listed in general form without referring to specific streamline locations. In the interest of clarity, however, some relationships will be written in forms similar to those used in the program. For example, $P_1(2)/P_{t_o}=\left[T_{1is}(2)/T_{t_o}\right]^{\frac{\gamma}{\gamma-1}}$ will represent the isentropic relationship for the number 2 streamline.

Five streamlines are utilized for the analysis with the number 1 streamline located at the hub and the number 5 streamline located at the tip as shown in Fig. 2. The number 3 streamline will be used as the mean streamline, and the radius of this streamline will be referred to as the mean radius. The radial locations of the streamlines ahead of the stator will be such that the mass flowrate between adjacent streamlines is 25 per cent of the total flowrate. Positions for the streamlines after the stator and after the rotor are initially assumed. The locations of streamlines 2, 3, and 4 then vary during the solution as necessary so that the percentage of the total flowrate between adjacent streamlines does not change. This continuity requirement will be called streamline continuity.

Besides the radii, sufficient input information must be used to effectively reflect the physical characteristics of the stator and rotor blading. Some of the physical properties are introduced directly; such as, the number of stator blades, the number of rotor blades, and the rotor tip clearance. The other quantities used which reflect blade characteristics are throat opening dimensions for the blade channels, discharge angles, rotor blade inlet angles, loss coefficients, and stalling incidences for the rotor.

Throat opening dimension "a" is a function of radius. The best method for introducing this characteristic into the anaylsis is to enter the measured values of "a" together with the corresponding radii. Then, utilizing the method of least squares, a fourth order polynominal curve is fitted through these points. From the resulting polynomial, the value of "a" for any radius required by streamline continuity can be determined.

Discharge angles are predicted by using a combination of the methods of Vavra and Ainley.[6] Outlet angles are first calculated using the formula which Vavra established from the experimental data of Beer.[7] These angles are then corrected for tip clearance, blade curvature, and Mach number effects with the methods given by Ainley. Stator and rotor discharge angles are predicted at three radii; namely, the hub, mean radius, and tip. The method used for calculating these angles is explained in Appendix B, Section 1.

Values of stator gas outlet angles α_1 for the mean streamline are determined for Mach numbers M_1 of 0.5, 0.7, 0.75, 0.8, and 1.0. These values are represented by two parabolic curves of the form

$$\alpha_1 = a + bM_1 + cM_1^2 \tag{26}$$

The first curve is used for Mach numbers M_1 from 0.5 to 0.75 and the second established interim values of α_1 for M_1 between 0.75 and 1.0. From these curves the flow angle α_1 for the mean streamline can be found for any Mach number M_1.

The flow angle α_1 is also a function of radius r_1. Therefore the changes of α_1 for the hub and tip with reference to the mean radius, called $\Delta\alpha_H$ and $\Delta\alpha_T$ respectively, must be used. The flow angle α_1 can then be determined for any r_1 by assuming a linear variation of α_1 between the hub and the mean radius and between the mean and the tip. With this assumption and using the Mach number M_1 in Eq. 26 corresponding to the number 2 streamline, the flow angle α_1 for this streamline would be

$$\alpha_1(2) = \alpha_1^{**} + \frac{r_1(2) - r_1^{**}}{r_1(1) - r_1^{**}} \Delta\alpha_H \tag{27}$$

---

[6] Ainley, D. G. and Mathieson, G. C. R., A Method of Performance Estimation for Axial-Flow Turbines. Aeronautical Research Council, R & M No. 2974, 1957. pp. 3-4.

[7] Beer, R., Aerodynamic Design and Estimated Performance of a Two-Stage Curtis Turbine for the Liquid Oxygen Turbopump of the M-1 Engine. NASA CR 54764 (AGC 8800-12), Nov. 19, 1965. p. 29.

The superscript ** is used with r_1 and α_1 in Eq. 27 to indicate the radius initially assumed for the mean streamline and the computed for that radius. Equation 27 can then be used throughout the analysis even though the radial location of the mean streamline may change due to streamline continuity requirements. A similar approach is used to establish the flow angle β_2 at the rotor discharge.

The rotor blade inlet angles β_0 are measured from the manufacturing drawings of the blade profiles. Using the values of β_0 for the hub, mean, and tip streamlines, a parabolic curve is determined which gives β_0 as a function of X_1.

Loss coefficients and stalling incidences are predicted by using the methods of Ainley.[8] For the present method, the stalling incidence i_s is defined as that at which the loss coefficient is twice the value of the minimum loss coefficient. Following Ainley's methods, loss coefficients are computed as a function of the ratio of flow incidence to stalling incidence $\frac{i}{is}$. Loss coefficients are also a function of blade geometry or radius. Since the stator has zero incidence, its loss coefficient is a function of the radius only.

Stator and rotor loss coefficients and rotor stalling incidences are calculated for the hub, mean, and tip radial locations. Rotor loss coefficients ζ are determined for values of $\frac{i}{is}$ ranging from -2.0 to 1.6. Curves of ζ_R vs. $\frac{i}{is}$ are drawn for each of the three radial locations, and values of ζ_R, along with the corresponding quantities $\frac{i}{is}$, are used to determine fourth order polynomials which approximate these curves. A similar procedur is followed to obtain a fourth order polynomial representing stalling incidence i_s as a function of radius r_1. Sample calculations for the prediction of stator and rotor loss coefficients and stalling incidences are contained in Appendix B, Section 2.

---

[8] Ainley, op. cit., pp. 4-5.

Variation of loss coefficients with radial location is accounted for by assuming a linear variation of these quantities between the hub and the mean radius and between the mean and the tip. To demonstrate the procedure followed in computing rotor loss coefficients, the following example is given. For a particular incidence, the first step in the determination of $\bar{\omega}_R$ for the number 2 streamline would be to calculate i_s by using the radius r_1 of that streamline and the polynomial of the form $i_s = i_s(r_1)$. Loss coefficients for the hub and mean radius would then be computed using the resulting $\frac{i}{i_s}$ in the polynomials, for these radii, of the form $\bar{\omega}_R = \bar{\omega}_R\left(\frac{i}{i_s}\right)$. With the assumed linear variation $\bar{\omega}_R(2)$ would be

$$\bar{\omega}_R(2) = \bar{\omega}_R(1) + \left[\frac{r_1(2) - r_1(1)}{r_1^{**} - r_1(1)}\right]\left[\bar{\omega}_R^{**} - \bar{\omega}_R(1)\right] \tag{28}$$

The reason for using the superscript ** on the mean streamline values is the same as previously mentioned in connection with Eq. 27.

For the first approximation, the Mach number M_0 ahead of the stator is assumed, and the static properties and flowrate at station 0 are found by

$$T_0 = \frac{T_{t_0}}{1 + \frac{\gamma - 1}{2} M_0^2} \tag{29}$$

$$V_0 = \sqrt{\gamma g R T_0}\; M_0 \tag{30}$$

$$P_0 = \frac{P_{t_0}}{\left(1 + \frac{\gamma - 1}{2} M_0^2\right)^{\gamma/\gamma - 1}} \tag{31}$$

$$\rho_0 = \frac{P_0}{R T_0} \tag{32}$$

$$A_0 = \pi\left(r_T^2 - r_H^2\right) \tag{33}$$

$$\dot{w} = \rho_0 A_0 V_0 \tag{34}$$

$$\Phi A = \frac{\dot{w}}{P_{t_0}}\sqrt{\frac{R T_{t_0}}{g}} = W_{ref} \tag{35}$$

The reference flowrate W_{ref} will be used to check continuity at stations 1 and 2.

The next step is to determine axial velocities after the stator that satisfy the equation of motion. Total enthalpy after the stator is constant by assumption, and streamline curvature effects are neglected at this stage of the analysis. With these conditions, Eq. 8 simplifies to

$$\frac{d(\ln Y_1^2)}{dX_1} = 2\,\mathrm{TAN}\,\alpha_1 \frac{d\alpha_1}{dX_1} - \frac{2}{X_1}\,\mathrm{SIN}^2\alpha_1 + \left(1 - \frac{C_1 H \cos^2\alpha_1}{Y_1^2 V_{A_1 m}^2}\right)\frac{ds_1^*}{dX_1} = I \tag{36}$$

This equation can be integrated to give

$$\ln Y_1^2 = \int_{X_0}^{X} I\,dX + \ln C^2 \tag{37}$$

where X_o is arbitrary and $\ln C^2$ is the constant of integration. Using the boundary condition Y = 1.0 at X = 1.0, $\ln C^2$ can be found by

$$0 = \int_{X_0}^{1} I\,dX + \ln C^2 \quad \text{OR} \quad \ln C^2 = -\int_{X_0}^{1} I\,dX$$

then

$$\ln Y_1^2 = \int_{X_0}^{X} I\,dX - \int_{X_0}^{1} I\,dX = \int_{1}^{X} I\,dX \tag{38}$$

Equation 38 must be expressed in a form that can be utilized in the computer. Expansion by infinite series yields

$$Y = e^{\frac{1}{2}\int_1^X I\,dX} = 1 + n + \frac{n^2}{2} + \frac{n^3}{6} + \frac{n^4}{24} + \frac{n^5}{120} + \cdots\cdots; \quad n = \frac{1}{2}\int_1^X I\,dX \tag{39}$$

The quantities contained in I, Eq. 36, must be evaluated before proceeding with the solution. For the first approximation, assumptions are made for the values of Y_1, M_1, and V_{A_m}. The flow angles α_1 are then calculated by using Eqs. 26 and 27. After the value of α_1 has been determined for each streamline, $\frac{d\alpha_1}{dX_1}$ is computed. This derivative and all others needed in the analysis are found by finite difference methods.

Enthalpy is computed by

$$H = c_p T_{t_0} \tag{40}$$

and the entropy term is found by the method of Vavra.[9]

---

[9]Vavra, M. H., Aero-Thermodynamics and Flow in Turbomachines. New York, London: John Wiley and Sons, Inc., 1960. pp. 445-447.

$$s^* = \ln \left[\frac{1 - \dfrac{Y_1^2 V_{A_{1m}}^2}{C_1 H \cos^2 \alpha_1}}{1 - \dfrac{Y_1^2 V_{A_{1m}}^2}{C_1 H \cos^2 \alpha_1 (1 - \omega_s)}} \right] \tag{41}$$

The stator loss coefficients ω_s are determined by equations similar to Eq. 28.

Each time a solution to Eq. 36 is found, the new values of Y_1 are then used for the next iteration. After five iterations, α_1 and $\frac{d\alpha_1}{dX_1}$ are recalculated using the new stator exit Mach numbers. The Mach number for each streamline is found by

$$V_{A_1} = Y_1 V_{A_{1m}} \tag{42}$$

$$V_1 = \frac{V_{A_1}}{\cos \alpha_1} \tag{42a}$$

$$T_1 = T_{t_0} - \frac{V_1^2}{2 g J c_p} \tag{43}$$

$$M_1 = \frac{V_1}{\sqrt{\gamma g R T_1}} \tag{44}$$

With the new values for α_1 and $\frac{d\alpha_1}{dX_1}$, five more iterations are made to determine the corrected values of Y_1.

The quantities represented by Eqs. 42-44 are recomputed after satisfying the equation of motion and additional quantities determined by

$$V_{U_1} = V_{A_1} \tan \alpha_1 \tag{45}$$

$$T_{1is} = T_{t_0} - \frac{T_{t_0} - T_1}{1 - \omega_s} \tag{46}$$

$$P_1 = P_{t_0} \left(\frac{T_{1is}}{T_{t_0}} \right)^{\gamma/\gamma - 1} \tag{47}$$

The flowrate through the stator is computed next and compared with that required to satisfy continuity. Reference flowrate between the hub and each streamline is found from

$$SUM = a_m Z r_m \int_{X_H}^{X} \frac{a}{a_m} \xi \Phi \, dX = a_m Z r_m \int_{X_H}^{X} WI \; dX \tag{48}$$

where

$$\Phi = \left\{ \frac{2\gamma}{\gamma - 1} \left[\left(\frac{P}{P_{t_0}} \right)^{2/\gamma} - \left(\frac{P}{P_{t_0}} \right)^{\gamma + 1/\gamma} \right] \right\}^{\frac{1}{2}} \tag{49}$$

The "a" and "a_m" in Eq. 48 are found from the polynomial which represents throat opening as a function of radius.

Before Eq. 48 is solved, the pressure ratio is compared with the critical pressure ratio. If the critical pressure ratio has been exceeded, the flow is choked at that radial location and the critical pressure ratio is used in calculating Φ and Ξ.

The fraction of the total flowrate passing between the hub and each streamline is computed by

$$W_f = \frac{\int_{X_H}^{X} WI\, dX}{\int_{X_H}^{X_T} WI\, dX} \tag{50}$$

Total flowrate, as found by the denominator of Eq. 50 multiplied by $a_m \Xi r_m$, is then compared with the reference flowrate. Overall continuity is satisfied if the difference is less than 0.0002.

If required and computed flowrates are not within this tolerance, the axial velocity for the mean streamline is adjusted by

$$V_{A_m (NEW)} = V_{A_m (OLD)} + \frac{\dot{W}_{req.} - \dot{W}_{computed}}{0.00065} \tag{51}$$

$\dot{W}_{req}$ is the required reference flowrate divided by $a_m \Xi r_m$, and $\dot{W}_{computed}$ is the denominator of Eq. 50.

Solutions to the equation of motion and continuity are successively found until overall continuity is satisfied.

The fractions of the total flowrate determined for each streamline by Eq. 50 are then compared with the corresponding flowrate fractions ahead of the stator. Streamline continuity is satisfied if agreement is within 0.002 for each streamline. If streamline continuity has not been satisfied, the streamlines in error are adjusted by

$$X_{NEW} = X_{OLD} + \left[W_{f_{req.}} - W_{f_{computed}}\right] \frac{dX}{dW_f} \tag{52}$$

Equation 52 applies only to streamlines 2, 3, and 4 since $W_f = 0$ at the hub and $W_f = 1.0$ at the tip.

If streamline positions have been adjusted, new streamline radii are found by

$$r_{NEW} = X_{NEW}\, r_{m\,OLD} \tag{53}$$

and new values of X for each streamline are obtained by

$$X = \frac{r_{NEW}}{r_{m\,NEW}} \tag{54}$$

With the new streamline radii the equation of motion and overall continuity must be satisfied again.

The following values are determined after streamline continuity is satisfied:

$$U_1 = \frac{\pi\, RPM}{(30)(12)}\, r_1 \tag{55}$$

$$U_2 = \frac{r_2}{r_1} U_1 \tag{56}$$

$$W_{U_1} = V_{U_1} - U_1 \tag{57}$$

$$\beta_1 = TAN^{-1}\left(\frac{W_{U_1}}{V_{A_1}}\right) \tag{58}$$

$$W_1 = \frac{V_{A_1}}{\cos\beta_1} \tag{59}$$

$$T_{t_E} = T_1 + \frac{W_1^2}{2gJc_p} + \frac{U_2^2 - U_1^2}{2gJc_p} \tag{60}$$

$$H_E = T_{t_E}\, c_p \tag{61}$$

$$P_{t_E} = P_1\left(\frac{T_{t_E}}{T_1}\right)^{\gamma/\gamma-1} \tag{62}$$

Rotor blade inlet angles are determined for each streamline by means of the parabola which establishes β_0 as a function of X_1. Incidence is found by

$$i = \beta_1 - \beta_0 \tag{63}$$

Stalling incidences and rotor loss coefficients are then determined using the procdure described in connection with Eq. 28. If the incidence ratio $\frac{i}{i_s}$ is less than -2.0 or greater than 1.6, the value for $\frac{i}{i_s}$ is set equal to -2.0 or 1.6, respectively.

One of the quantities necessary for the equation of motion after the rotor is $\frac{ds_2^*}{dX_2}$. This quantity is separated into two parts,

$$\frac{ds_2^*}{dX_2} = \frac{ds_{10}^*}{dX_2} + \frac{ds_{21}^*}{dX_2} \tag{64}$$

$\frac{ds_{10}^*}{dX_2}$ represents the entropy gradient due to changes of entropy across the stator and referred to station 2. The term $\frac{ds_{21}^*}{dX_2}$ represents the entropy gradient due to the different entropy changes through the rotor. The entropy increase through the rotor is computed by using the corresponding values of the rotor in Eq. 41; for example, H_E would be used instead of H.

Neglecting streamline curvature and slope, Eq. 9 can be rewritten

$$\frac{d(\ln Y_1^2)}{dX_2} = -2\,\mathrm{TAN}\,\beta_2 \frac{d\beta_2}{dX_2}\,\mathrm{SIN}^2\beta_2 - \frac{4U_m \cos\beta_2 \sin\beta_2}{Y_2\,W_{A2m}}$$

$$- \frac{2U_m U_2 \cos^2\beta_2}{Y_2^2\,W_{A2m}^2} + \frac{C_1 \cos^2\beta_2}{Y_2^2\,W_{A2m}^2}\frac{dH_E}{dX_2} + \left(1 - \frac{C_1 H_E \cos^2\beta_2}{Y_2^2\,W_{A2m}^2}\right)\frac{ds_2^*}{dX_2} \tag{65}$$

The discharge angle β_2 and its derivative $\frac{d\beta_2}{dX_2}$ are found in the same manner as previously described for the stator discharge angles. The method for solving Eq. 65 is similar to that used for Eq. 36 with the exception that iterations are carried out until corresponding values of Y change by less than 0.005, or until 13 iterations have been completed. The extra iterations are necessary because there may be a slower convergence of the values of Y at station 2. After satisfying the equation of motion, values at station 2 corresponding to those represented by Eqs. 42-47, are computed. It should be noted that where absolute velocity terms are used in Eqs. 42-47, the corresponding equations for the rotor will employ relative velocities. Therefore M_2 is the Mach number of the flow relative to the rotating rotor blade.

Overall continuity is checked at the rotor discharge using the same procedure utilized for the stator; however, the reference flowrate is increased according to Eq. 25 to account for the flowrate between the blade tips and the surrounding shroud.

After overall continuity has been satisfied at station 2, streamline continuity is checked. In addition to the functions performed for the check after the stator, there are certain quantities that must be adjusted for streamline relocation. These are

$$\left(\frac{dH_E}{dX_2}\right)_{NEW} = \left(\frac{dH_E}{dX_2}\right)_{OLD} + \frac{d^2H_E}{dX_2^2}\left(X_{NEW} - X_{OLD}\right) \tag{66}$$

$$H_{E_{NEW}} = H_{E_{OLD}} + \frac{dH_E}{dX_2}\left(X_{NEW} - X_{OLD}\right) \tag{67}$$

$$\left(\frac{ds_{10}^*}{dX_2}\right)_{NEW} = \left(\frac{ds_{10}^*}{dX_2}\right)_{OLD} + \frac{d^2s_{10}^*}{dX_2^2}\left(X_{NEW} - X_{OLD}\right) \tag{68}$$

$$U_{2_{NEW}} = \left(U_{2_{OLD}}\right)\frac{X_{NEW}}{X_{OLD}} \tag{69}$$

A solution exists when the equations of motion, and overall and streamline continuity have been satisfied; however, this solution has neglected streamline curvature and streamline slope. To obtain a solution which accounts for streamline curvature effects, the terms in Eqs. 8 and 9 that contain δr or ΔR must be included when solving the equations of motion.

The streamline displacements δr and ΔR, shown in Fig. 2, are computed for each streamline by

$$\delta r = r_1 - \frac{r_0 + r_2}{2} \tag{70}$$

and

$$\Delta R = r_0 - r_2 \tag{71}$$

Equation 70 is based on the assumption that the radii of any streamline at stations 0 and 2 are not greatly different. Therefore the cosine of the angle between the line connecting these points and the axis of the machine is approximately equal to unity. The length L, also shown in Fig. 2, is taken to be half the distance from 0.1 inch ahead of the stator to 0.1 inch after the rotor.

After a solution is obtained which accounts for streamline curvature effects, the resultant pressure ratio $\frac{P_{t_0}}{P_2}$ is compared with the $\frac{P_{t_0}}{P_2}$ specif'ed initially. Ideally $\frac{P_{t_0}}{P_2}$ for each streamline will be the same. However, computer solutions for this quantity may vary slightly from streamline to streamline. Therefore a mass-flow-weighted value of $\frac{P_{t_0}}{P_2}$, called $\left(\frac{P_{t_0}}{P_2}\right)_{\dot{w}}$, is found by

$$\left(\frac{P_{t_0}}{P_2}\right)_{\dot{w}} = \sum_{i=1}^{4} \left(\frac{P_{t_0}}{P_2}_{(i+1)} + \frac{P_{t_0}}{P_2}_{i}\right)\left(\frac{W_{f_{(i+1)}} - W_{f_i}}{2}\right) \tag{72}$$

If the specified $\frac{P_{t_0}}{P_2}$ and $\left(\frac{P_{t_0}}{P_2}\right)_{\dot{w}}$ differ by more than 0.0003, the Mach number of the flow ahead of the stator is properly adjusted and another solution is found.

After the iterations for $\frac{P_{t_0}}{P_2}$ have been completed, additional quantities are determined for each streamline, using

$$\Delta H = H_1 - H_2 = (U_1 V_{U_1} - U_2 V_{U_2}) \frac{1}{gJ} \tag{73}$$

$$T_{t_2} = T_{t_0} - \frac{\Delta H}{c_p} \tag{74}$$

$$T_{2_{is}} = T_{t_0} \left(\frac{P_2}{P_{t_0}}\right)^{\frac{\gamma-1}{\gamma}} \tag{75}$$

Overall efficiency is then computed by

$$\eta = \frac{\Delta H}{\Delta h_{is}} = \frac{T_{t_0} - T_{t_2}}{T_{t_0} - T_{2_{is}}} \tag{76}$$

The ideal change in enthalpy Δh_{is} is the isentropic enthalpy drop from the total inlet pressure P_{t_0} to the static discharge pressure P_2. Equation 76 is used to compute the efficiency of a

single stage turbine because the kinetic energy leaving the rotor cannot be utilized. The efficiency defined by Eq. 76 will be referred to as total-static efficiency.

Theoretical degree of reaction r* and head coefficient k_{is} are given by

$$r^* = \frac{T_{1is} - T_{2is}}{T_{to} - T_{2is}} \tag{77}$$

and

$$k_{is} = \frac{\Delta h_{is}}{U_1^2/2gJ} = \frac{2c_p(T_{to} - T_{2is})gJ}{U_1^2} \tag{78}$$

For turbine performance curves it is desirable to obtain the mass-flow-weighted values of efficiency ( )$_{\dot{w}}$, head coefficient $(k_{is})_{\dot{w}}$, theoretical degree of reaction $(r^*)_{\dot{w}}$, horsepower $(HP)_{\dot{w}}$, and moment $(M_R)_{\dot{w}}$. The last two quantities are found from

$$(HP)_{\dot{w}} = \frac{(\Delta H)_{\dot{w}} J \dot{w}}{550} \tag{79}$$

and

$$(M_R)_{\dot{w}} = \frac{(HP)_{\dot{w}}(550)}{\omega} \tag{80}$$

The mass-flow-weighted ΔH, called $(\Delta H)_{\dot{w}}$, as well as $(\eta)_{\dot{w}}$, $(k_{is})_{\dot{w}}$, and $(r^*)_{\dot{w}}$ are computed using equations similar to Eq. 72.

Referred values are obtained, following NASA practice.
For $\gamma = 1.4$:

$$HP_{ref} = \frac{(HP)_{\dot{w}}}{\sqrt{\theta}\ \delta} \tag{81}$$

$$M_{R\,ref} = \frac{(M_R)_{\dot{w}}}{\delta} \tag{82}$$

$$RPM_{ref} = \frac{RPM}{\sqrt{\theta}} \tag{83}$$

$$\dot{W}_{ref} = \frac{\dot{w}\sqrt{\theta}}{\delta} \tag{84}$$

$$V_{ref} = \frac{V}{\sqrt{\theta}} \tag{84a}$$

where:

$$\theta = \frac{T_{to}}{T_{STD.}} = \frac{T_{to}}{518.4} \tag{85}$$

$$\delta = \frac{P_{to}}{P_{STD.}} = \frac{P_{to}}{14.7} \tag{86}$$

4. MOD I and MOD II Turbines

The method of analysis as presented was used to determine performance curves for the so-called MOD I and MOD II turbines. Both turbines are single stage axial-flow machines. Experimental tests were conducted on the MOD II turbine by Commons and Messegee and are described in Refs. 4 and 6. The test results are plotted with appropriate predicted performance curves.

The so-called MOD I turbine was designed for free-vortex flow and has highly twisted blades. Outer diameter of this turbine is 9.898 inches. The hub diameters of the stator inlet and rotor discharge are 6.930 and 5.970 inches, respectively. The stator contains 13 blades and the rotor 22 blades. Blades of the MOD I turbine are generally thin. The stator and rotor profiles used to predict outlet angles and loss coefficients are shown in Fig. 4.

The MOD II turbine is approximately the same size as the MOD I, but its blading is considerably different. The blades of the MOD II turbine are thick with blunt leading edges and constant profiles over the blade height. Outer diameters of the MOD II turbine stator and rotor are 9.701 and 9.836 inches, respectively. The stator has a hub diameter of 6.796 inches, and the hub diameter of the rotor is 6.598 inches. There are 19 stator blades and 18 rotor blades. Stator and rotor blade profiles for the MOD II turbine are shown in Fig. 5.

Throughout the remainder of this thesis the MOD I and MOD II turbines will be referred to simply as MOD I and MOD II.

The minimum throat opening "a" of the blade channels is a very critical dimension. Slight variations of this quantity have a considerable effect on turbine performance. Since this quantity is so sensitive, values of "a" measured from the actual hardware were used for the analysis rather than those obtained from the manufacturing

drawings. Then errors due to manufacturing will not be a factor in comparison of predicted and experimental results. Figure 6 shows the throat openings "a" as a function of radius for the stator and rotor blading of both turbines.

Predicted stator outlet angle α_1 as a function of radius r_1 for the MOD I is plotted in Fig. 7. The assumed linear variation of α_1 between the hub and the mean radius and between the mean and the tip is readily apparent in this figure. Figure 8 shows the predicted variations of α_1 with Mach number M_1 for the MOD I. Figures 9 and 10 are the corresponding plots for the MOD II.

Relative discharge angles β_2 were computed for two radial tip clearances k for each turbine; namely, 0.020 and 0.033 inches for the MOD I, and 0.015 and 0.033 inches for the MOD II. The predicted flow angles β_2 are plotted in the same manner as previously described for the flow angles α_1. Figures 11 and 12 show β_2 as a function of radius r_2 and as a function of Mach number M_2, respectively, for the MOD I, where M_2 refers to the Mach number of the flow relative to the rotor. Figures 13 and 14 show the corresponding plots for the MOD II. The predicted effect of radial tip clearance on the discharge angles β_2 can be seen in Figs. 11 - 14.

Stator loss coefficients ζ_s were computed for the radial locations corresponding to the hub, mean radius, and tip. Figure 15 shows ζ_s as a function of radius r_1 for both the MOD I and MOD II. The straight lines in this figure between the values of ζ_s at the hub and mean radius, and between the mean and the tip, reflect the assumed linear variation of ζ_s in these regions.

Variation of rotor blade inlet angle β_0 with radius r_1 is plotted for both turbines in Fig. 16. The difference between the untwisted and the free-vortex blades is easily noted in this plot. Also shown in this figure are curves representing the variation of stalling incidence i_s with r_1. The change of the MOD I rotor blade profiles with radius is reflected by a considerable variation of i_s whereas just the opposite is true for the MOD II.

Curves for the MOD I showing predicted rotor loss coefficients φ_R as a function of incidence ratio $\frac{i}{i_s}$ for the hub, mean radius, and tip are shown in Fig. 17. Since the loss coefficients between the mean radius and the tip are dependent on tip clearance, there are two curves for the tip. One curve holds for the tip clearance of 0.020 inches; the other is for the larger tip clearance of 0.033 inches. For negative incidence ratios between -0.5 and -2.0 the curves for the tip are estimations. This was necessary because the computations by the method shown in Appendix B, Section 2, gave unrealistically low values of φ_R as the flow inlet angle β_1 approached -90^o. The situation is more easily understood when it is noted that the blade inlet angle is -33.7^o and the stalling incidence is 37^o at the rotor blade tip. Figure 17 shows that the loss coefficients for the hub (r_1=3.300 in.) are relatively large. The loss coefficients at the hub are larger for most incidence ratios than those at the tip for a tip clearance of 0.020 inches. The larger value of at the hub reflects the higher losses that are associated with an impulse type blade. It can be seen in Fig. 4 that the blade shape varies from a reaction type profile at the tip to an impulse type profile at the hub.

Loss coefficients for the MOD II rotor are plotted in Fig. 18 for tip clearances of 0.015 and 0.033 inches. The predicted similarity of the curves for the hub and mean radius is to be expected since the blading differs only in solidity. Although the blade profile is the same at all radii, the losses due to tip clearance result in larger loss coefficients for the tip profile.

For convenience, the blade properties used for calculating the MOD II rotor loss coefficients were those at the hub, mean and tip radii of the rotor discharge. Since the annulus area at the rotor discharge is larger than the annulus area at the stator discharge and since the flow incidence is a significant parameter for the rotor loss coefficients, it would have been more appropriate to use the blade characteristics at the hub, mean, and tip radii of the rotor inlet. However, the error is insignificant because the blade profile does not change along the radius.

It may be noted from Fig. 4 that the minimum radius, for which a blade profile is given, is 3.597 inches whereas the radius at the hub of the MOD I stator exit is 3.300 inches. The outlet angle and loss coefficient for the hub were found by extrapolation, using the values computed for the radii of 4.125 and 3.597 inches and assuming a linear variation of these quantities with radius. The relative outlet angle for the hub of the MOD I rotor was found in a similar manner.

Performance curves for the two turbines were determined for the rotor tip clearances mentioned earlier. The total inlet to static discharge pressure ratios investigated were 1.30, 1.40, 1.50, and 1.60, with the exception that pressure ratios of 1.31 and 1.51 were used for the MOD II with 0.033 inch rotor tip clearance. These pressure ratios agree more closely with those experimentally investigated by Commons and Messegee.

The axial distances L used for the determination of the curvatures depend on the axial clearance between the stator and rotor as well as on the blade geometries. Axial clearances of 0.4 and 1.0 inches were used for the analyses of the MOD I and MOD II, respectively.

Curves representing the performance of the MOD I are plotted in Figs. 19 through 26. Performance values plotted are mass-flow-weighted values unless stated otherwise. Figure 19 shows referred flowrate as a function of referred RPM. The increase in flowrate due to an increase in rotor tip clearance can be seen in this figure. Although the flowrate is greater for the larger tip clearance, the torque developed is greater at the smaller tip clearance. The decrease in torque for the larger tip clearance results from the increased losses and decrease in turning angle of the flow through the rotor near the tip. The predicted effect of tip clearance on torque is shown in Fig. 20 where referred moment is plotted versus referred RPM.

The variation of total-static efficiency with referred RPM for the two tip clearances can be seen in Figs. 21 and 22. The referred RPM at which maximum efficiency occurs increases when the total inlet to static discharge pressure ratio is increased. Blade losses

and the kinetic energy of the flow leaving the rotor affect the total-static efficiency. As pressure ratio is increased the absolute velocity leaving the stator and the relative velocity leaving the rotor increase. Therefore the peripheral speed of the rotor must increase to obtain conditions where the absolute velocity leaving the rotor is in an axial direction and where the relative flow ahead of the rotor has zero incidence. The RPM where the flow has zero incidence on the rotor will not necessarily be that at which the absolute velocity leaving the rotor is axial. At any RPM,flow incidence and absolute discharge angles vary from streamline to streamline,and the above statements refer to mass-flow-weighted values.

It may be noted in Figs. 21 and 22 that the peak total-static efficiency decreases somewhat as the pressure ratio increases. At higher pressure ratios the ratio of kinetic energy leaving the rotor to the work done on the rotor increases. Since the kinetic energy leaving the rotor is lost energy for a single stage turbine, the total-static efficiency declines. The effects of pressure ratio and tip clearance on efficiency can be seen in Fig. 23 where total-static efficiency is plotted as a function of the isentropic head coefficient.

The variation of referred power with referred RPM can be seen in Fig. 24. Peak power does not occur at the same referred RPM at which peak efficiency occurs. The peak referred power occurs at the referred RPM where the product of total-static efficiency and referred flowrate is greatest.

Theoretical degree of reaction is plotted as a function of isentropic head coefficient in Fig. 25. It may be noted that the theoretical degree of reaction increases with increasing pressure ratio and decreases with increasing tip clearance for any given isentropic head coefficient. The predicted effects are considerably different from the results of the radial turbine tests conducted by Riley.[10] Riley found that theoretical degree of reaction was independent of pressure ratio and axial clearance for radial turbines.

[10] Riley, M. W., The Effect of Axial Clearance on the Performance of a Dual Discharge Radial Turbine (USNPG Thesis, December 1966), p. 70.

Performance values for each streamline are obtained from the computer solution. However, plots utilizing values for each streamline would be difficult to analyze. The deviation of the hub and tip values from that of the mass-flow-weighted average may be seen in Fig. 26. In this figure, hub, tip, and mass-flow-weighted values of theoretical degree of reaction are plotted as functions of referred RPM for a total inlet to static discharge pressure ratio of 1.40.

Performance curves for the MOD II corresponding to those presented for the MOD I are plotted in Figs. 27 through 39. Additional plots have been used for the MOD II because of the inclusion of experimental results. An axial clearance of 1.0 inches was used for the theoretical prediction. Therefore, only experimental data for that axial clearance are shown.

Comments made concerning the performance curves of the MOD I are applicable to the MOD II performance curves also. Differences in the performance of the two turbines will be discussed later.

Plots of the variation of referred flowrate with referred RPM are shown in Figs. 27 and 28 for two rotor tip clearances. The quantitative values as well as the curve shapes agree well with the experimental data. The maximum difference between predicted and experimental referred flowrates occurs at a pressure ratio of 1.51 for a tip clearance of 0.033 inches. There are two experimental points for this pressure ratio and tip clearance that differ from the predicted curve by about 2 per cent. The predicted and experimental values for all pressure ratios and tip clearances have an average difference of less than 1 per cent.

Figures 29 and 30 show curves of referred moment versus referred RPM. The trends expressed by the predicted curves are in excellent agreement with the experimental data. Although the quantitative agreement between theoretical and experimental values is very good for three of the curves, the experimental torque is generally lower than the predicted torque. The average difference between predicted and experimental values is about 3 per cent.

Figures 31 through 34 show total-static efficiency as a function of referred RPM. The shapes of the predicted curves generally agree well with the experimental results. However, there is an indication that experimental efficiencies decrease more rapidly at high RPM than is predicted by the theoretical curves. In the high RPM region the upper part of the rotor blade has a large negative flow incidence. In the prediction analysis when the incidence ratio $\frac{i}{i_s}$ had a value less than -2.0, the value of -2.0 was used for computing loss coefficients. This limitation may be the reason that the predicted efficiencies in the high RPM range do not decrease as rapidly as the test data indicate.

The quantitative agreement between predicted and experimental efficiencies varies considerably between different pressure ratios and tip clearances. There are two data points at a pressure ratio of 1.31 and tip clearance of 0.033 inches where the experimental efficiencies are over five points below the predicted values. At a pressure ratio of 1.50 and a tip clearance of 0.015 inches the average difference between predicted and experimental efficiencies is 1.5 points. Giving equal weight to all experimental values the average difference between experimental and predicted values is 2.6 points.

The calculations gave a decrease in efficiency by about two points as the tip clearance was increased from 0.015 to 0.033 inches. The decrease in experimental efficiencies for the increased tip clearance varied with the different pressure ratios. However, the average decrease in efficiency is close to the predicted decrease.

Total-static efficiency as a function of isentropic head coefficient k_{is} is shown in Fig. 35 for pressure ratios of 1.40 and 1.60. Figure 38 shows degree of reaction r* versus k_{is}. No experimental data are plotted in these figures because experimental values of mass-flow-weighted r* and k_{is} were not available.

Plots of referred power as a function of referred RPM are shown in Figs. 36 and 37. The comments made earlier concerning the referred moment plots apply to these curves also, since the turbine power is proportional to the product of torque and RPM.

Hub, tip, and mass-flow-weighted values of theoretical degree of reaction are plotted in Fig. 39 for a pressure ratio of 1.40. The experimental values for the hub and tip are also plotted in this figure. The trend of the experimental data is in close agreement with the predicted trend; however, the quantitative agreement is poor, especially at the hub. The decrease in degree of reaction, as the tip clearance is increased, is considerably greater than predicted. Both predicted and experimental results indicate that an axial flow turbine differs from a radial turbine inasmuch as the theoretical degree of reaction changes if rotor tip clearance is changed.

Figure 40 shows the absolute flow angles α_1 and α_2 as a function of radius for the stator and rotor outlets, respectively, of the MOD II. Experimental data were obtained for the same operating conditions; namely, $P_{t_o}/P_2=1.40$, $k=0.015$ inches, $RPM/\sqrt{\theta}=13{,}394$. The experimental and predicted stator outlet angles have an average difference of less than half a degree over the blade height. Predicted and experimental agreement for the absolute flow angles at the rotor outlet is not as close. If the experimental point near the hub is neglected, the average difference between predicted and experimental values of α_2 is about 3.5 degrees. The experimental flow angles α_2 are larger than the predicted angles over most of the blade height, which explains why the predicted torque was generally larger than the measured torque.

Velocity distributions at the stator and rotor exits of the MOD II are shown in Fig. 41 for the operating conditions listed in the preceding paragraph. The experimentally found stator discharge velocities varied only slightly more from hub to tip than predicted. The average difference between predicted and experimental stator exit velocities was about 1 1/2 per cent.

The experimentally determined absolute rotor exit velocities, which are shown in Fig. 41, are considerably larger than the predicted velocities except at the hub and tip. Although experimental points could be taken only at distances greater than 0.16 inches from the inner diameter of the shroud, the trend of the data points indicates that the experimental velocities are less than predicted at the tip.

Near the hub the experimental velocities were less than predicted. The decrease in experimental velocities near the hub and tip is the result of separated flow in these regions. The reader is referred to Ref. 6 for additional information concerning the experimental data and for photographs of the rotor showing indications of separation.

Experimental relative rotor discharge angles β_2 were determined for the known rotor speed from the measured values of absolute rotor outlet angles and velocities, which are plotted in Figs. 40 and 41, respectively. The experimental and predicted values of β_2 are shown in Fig. 42. The magnitudes of the experimental values of β_2 near the hub are larger than predicted. Over approximately the outer three fourths of the rotor blade height the magnitudes of the experimental values of β_2 are less than predicted. At a radius of 4.4 inches, for instance, the experimental value of β_2 is about -57 degrees whereas the predicted value is about -67 degrees. The average difference between experimental and predicted values of β_2 is about 6.5 degrees. The lower values of β_2 predicted near the hub,provide some compensation in the overall performance for the high values of β_2 predicted for the outer part of the blade.

The MOD II was not designed to achieve the highest possible efficiency. The objectives of the design were to investigate the effects of b unt untwisted bladings of constant profile. This type of blading has the following advantages:

1. Blade cooling passages are easily accommodated.

2. A wider operating RPM range is posible for a specified turbine efficiency variation.

3. Constant profile blades can be manufactured more economically than twisted blades, especially if exotic high strength materials are needed for elevated temperatures.

The following discussion concerning comparison of the MOD I and MOD II is based entirely on the predicted performance of these turbines using the methods described in this thesis. The reader should be aware that Ainley's methods for predicting loss coefficients were not developed for use with rotor blades having blunt leading edges.

Therefore the accuracy of the rotor loss coefficients predicted for the MOD II is probably not as good as for the MOD I.

Figure 43 shows the predicted axial velocity ratios as a function of radius ratio at the stator exit and at the rotor exit for the MOD I and the MOD II. The curves are for the conditions that occur at the maximum efficiency of each turbine. The axial velocities of the MOD I are nearly constant over the blade height at the stator exit and at the rotor exit. The blading of this turbine was originally designed for free-vortex flow by assuming uniform axial velocity components from hub to tip. From Fig. 43 it can be seen that this condition is only approximately satisfied since loss variations and curvature influences produce slight variations from the assumed distribution. Axial velocities for the MOD II decrease from the hub to the tip at the stator exit, and increase from the hub to the tip at the rotor exit, since the bladings of this turbine have constant profiles. The variation of axial velocities for the MOD II is more pronounced at the rotor exit than at the stator exit. At the rotor exit $\frac{W_{A2}}{W_{A2m}}$ varies from 0.735 at the hub to 1.195 at the tip.

The maximum predicted total-static efficiency of the MOD I at a tip clearance of 0.033 inches is about 84 per cent. The MOD II has a maximum predicted efficiency at that tip clearance of about 80 per cent. The difference in predicted peak efficiencies is due to different factors. The stator loss coefficients are higher for the MOD I than for the MOD II, whereas the loss coefficients for the MOD II rotor at zero incidence are somewhat larger than those for the MOD I at zero incidence. An accurate comparison of loss coefficients is more involved for the rotor than for the stator. Because of its twisted blades, the MOD I rotor has nearly zero incidence at all points along the blade height in the vicinity of the optimum efficiency. Only at one radius of the MOD II rotor blade, however, is the incidence zero. The incidence angles at larger radii are negative and at smaller radii they are positive. Therefore part of the blade is always operating at a loss coefficient larger than the minimum. Of probably even greater significance

for the efficiency decrease is the kinetic energy of the gas leaving the turbine. Minimum kinetic energy is lost when the flow is axial in direction. The design of the MOD I is such that at all points along the blade height the absolute velocity at the rotor exit is nearly axial in the vicinity of the optimum efficiency. The MOD II has only a small radial portion of the rotor blade where the discharge angle α_2 is zero. At radii greater than the radius where α_2 is zero, the absolute flow discharge angle is positive and at smaller radii it is negative. Therefore the kinetic energy leaving the rotor of the MOD II is greater than that of the MOD I when both turbines are operating at peak efficiency.

A comparison of the total-static efficiency versus isentropic head coefficient curves for the MOD I (Fig. 23) and MOD II (Fig. 35), shows a larger variation of efficiency with head coefficient for the MOD I. For example, at k=0.033 inches and $\frac{P_{to}}{P_2}=1.60$, the MOD I efficiency decreases about 11.5 points as the head coefficient increases from 3 to 7 whereas the MOD II efficiency decreases only about 7 points for the same change in head coefficient. This difference in efficiency variation results from the effects of blade twist mentioned earlier.

To investigate the influence of the streamline curvatures on the predicted performance of the MOD I and MOD II the presented flow equations were solved for an axial length of the bladings L of 9×10^5 inches. Increasing L to this value has the same effect as neglecting streamline curvature effects as can be seen from Eqs. 124 and 125. Differences between performance values neglecting streamline curvature, and those where curvature effects were accounted for, were less than 0.2 per cent for both turbines.

5. Conclusions and Recommendations

Effects of streamline curvature were found to be insignificant for the MOD I and MOD II. The small effect on predicted turbine performance due to streamline curvature indicates that the exact value assumed for the curvature factor K will not greatly affect predicted performance. The results of this analysis also indicate that Vavra's method of approximating streamline curvature is of sufficient accuracy for methods of analysis where the flow equations are satisfied at stations between blade rows.

It is recommended that the MOD I be tested. Results of that investigation would provide additional information concerning the general applicability and accuracy of the method of analysis proposed in this thesis.

Predicted and experimental flowrates for the MOD II were in close agreement. Since the restriction factor ξ is a significant factor in the predicted flowrates, the experimental results verify the validity of the theory used in the developement of ξ.

Experimental results for the MOD II showed that the predicted rotor torque and turbine efficiency were generally 2 to 3 per cent too high. The angles and velocities predicted for the flow at the stator outlet were in excellent agreement with the experimental results. Therefore the high values predicted for rotor torque and turbine efficiency must be tied to the rotor solution. The measured values of outlet angles and velocities for the rotor discharge also indicate that the predicted rotor solution is not completely correct.

Exactly what parameters are in error in the predicted rotor solution, and to what extent, cannot be stated without more experimental data. More traverses should be taken at the stator and rotor outlets using recently calibrated probes. With this information,loss coefficients and relative discharge angles for the rotor could be determined on a streamline basis. Based on the experimental results included in this thesis,it is suspected that the magnitudes of the predicted discharge angles β_2 are too large. If the predicted turning angles of the flow through the rotor were less, the predicted torque and efficiency would decrease. Also, the separated flow at the hub and tip at the discharge of the MOD II rotor indicates that predicted loss coefficients should be higher for the streamlines at these locations.

To accurately predict turbine performance at off-design as well as design conditions,a streamline analysis is necessary. The experimental verification obtained for the proposed method indicates that the method possesses much potential and that additional developement

is warranted. For future developement work on this type of analysis it is recommended that the following changes be considered:

1. Use seven streamlines instead of five.

2. Calculate discharge angles using the methods of this thesis but neglecting blade curvature effects. That would decrease the angles by 2 to 3 degrees and be in closer agreement with experimental results.

3. Introduce a multiplying factor for the rotor loss coefficients which would more accurately account for the separated flow at the hub and tip but would not greatly change the average rotor loss coefficient. For example, rotor loss coefficients would first be calculated using the methods of this thesis, and then the loss coefficients for streamlines 1, 2, 6, and 7 would be multiplied by, say, 1.4 and those for streamlines 3, 4, and 5 would be multiplied by 0.6 or 0.7.

4. Calculate rotor loss coefficients for an range of -3.0 to 2.0 instead of -2.0 to 1.6. The increased range would improve performance prediction for turbines with untwisted rotor blades at off-design conditions.

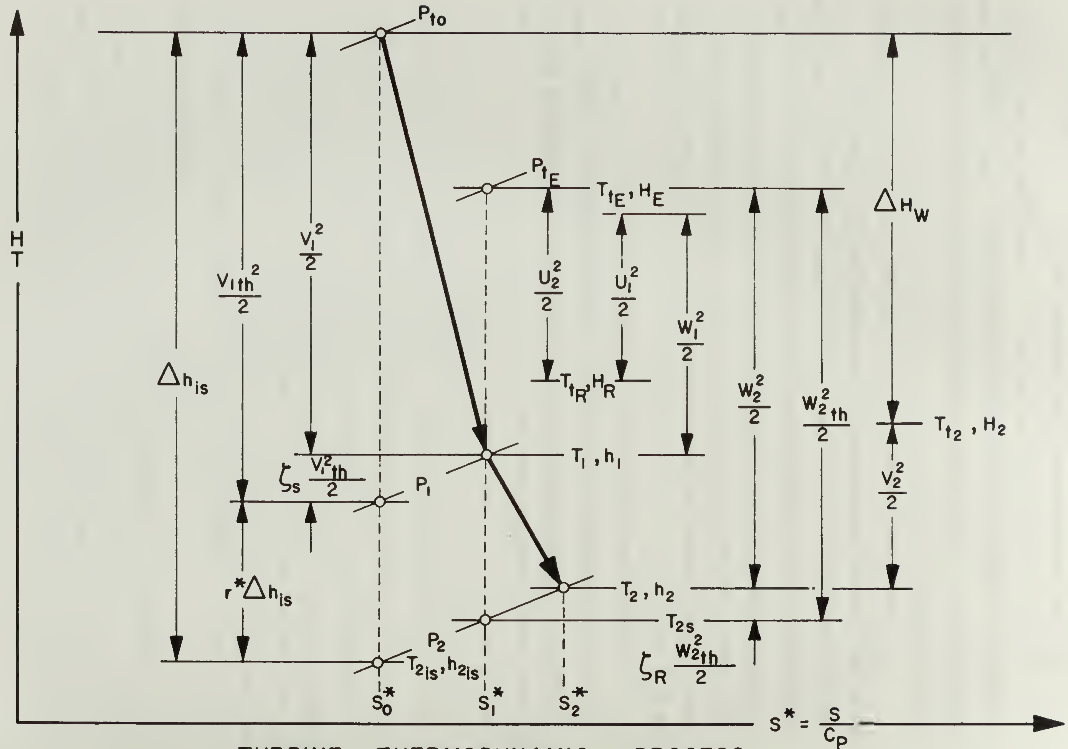

TURBINE THERMODYNAMIC PROCESS

FIG. 1

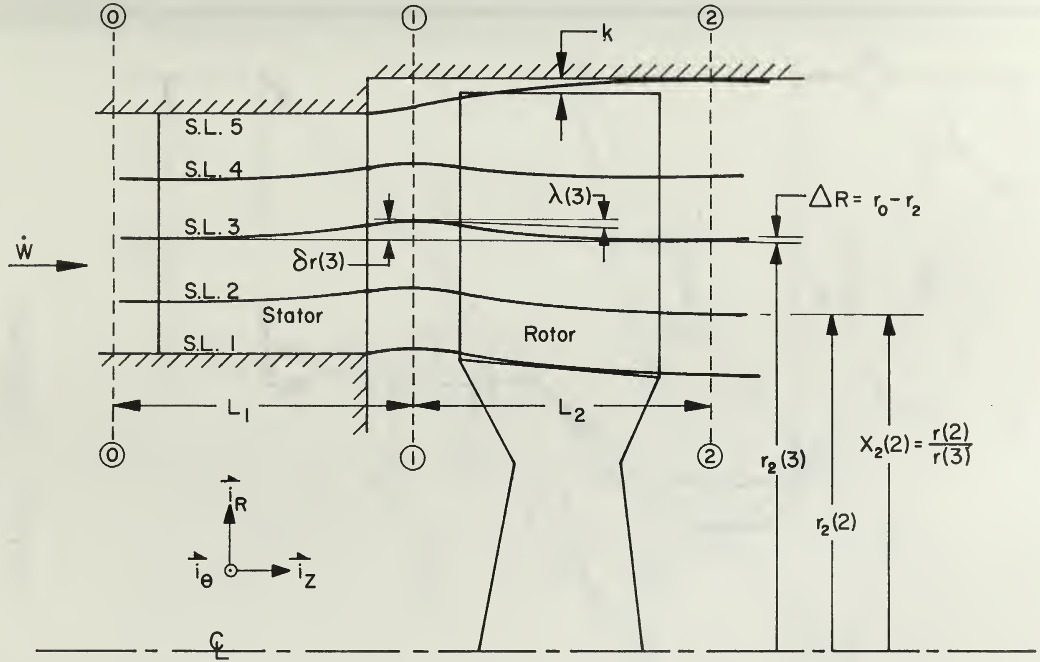

COORDINATES AND STREAMLINES

FIG. 2

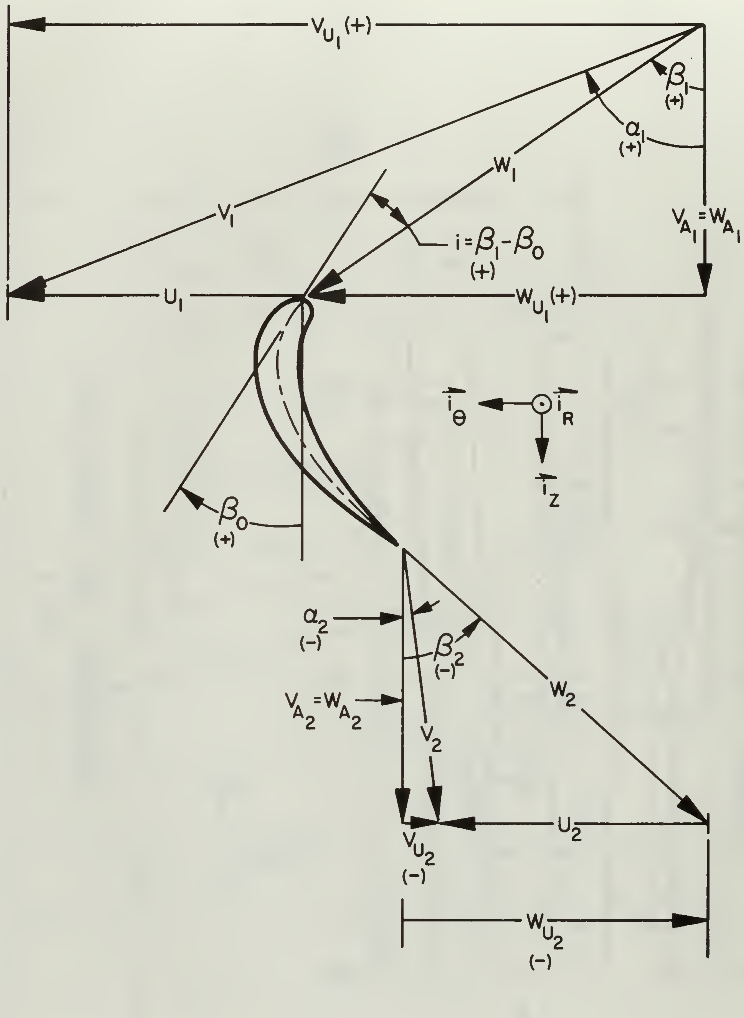

VELOCITY DIAGRAMS
FIG. 3

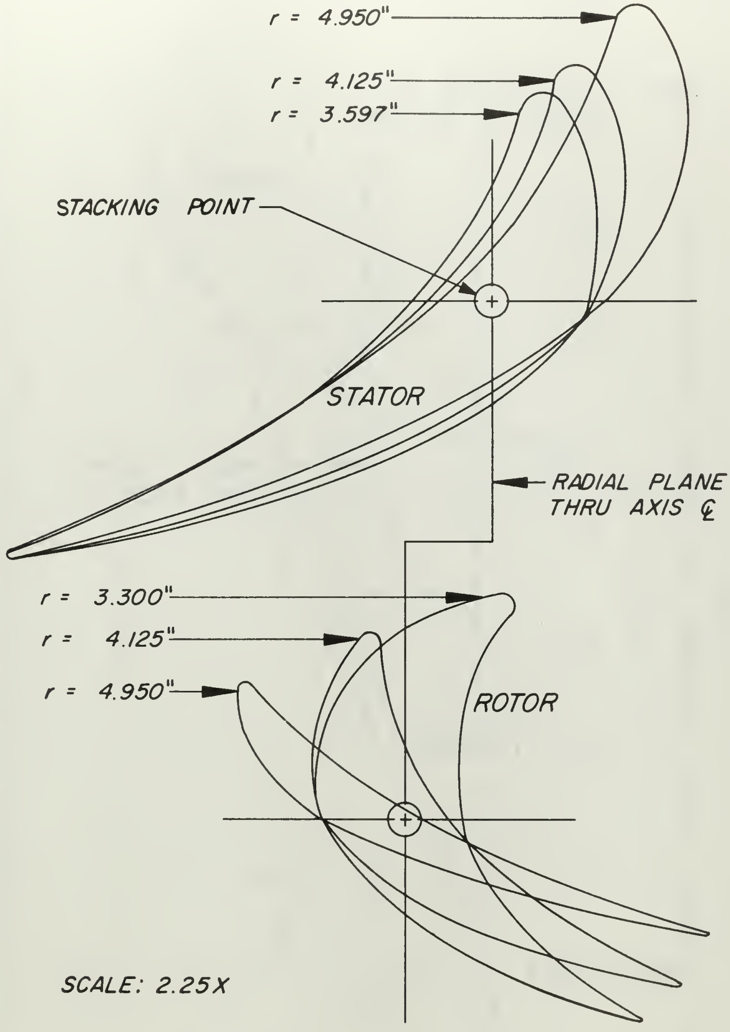

FIG. 4

STATOR & ROTOR BLADE PROFILES (MOD I).

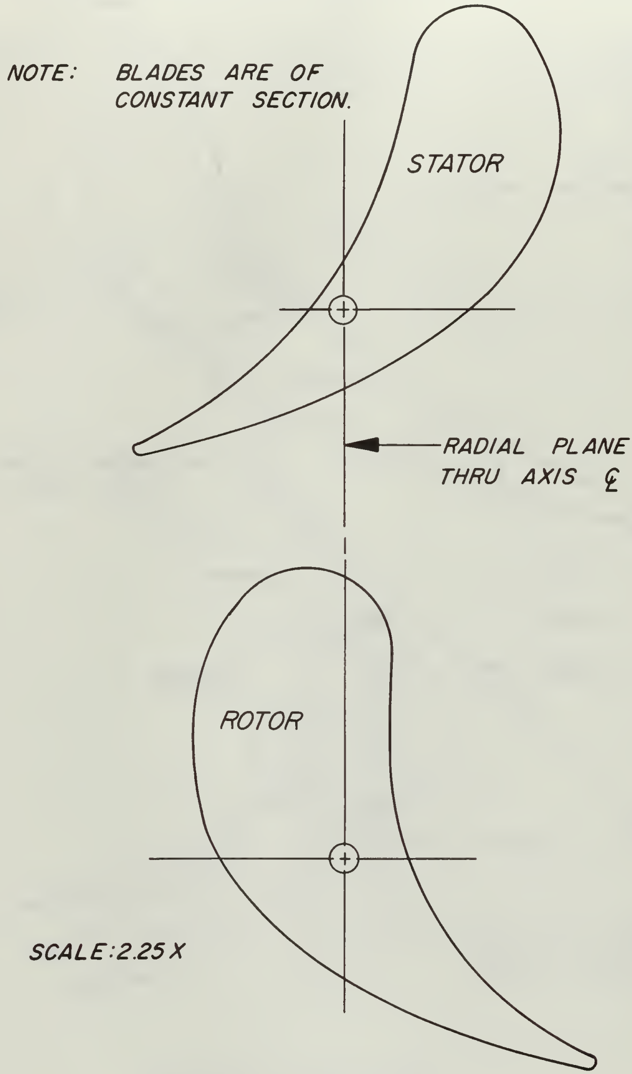

FIG. 5

STATOR & ROTOR BLADE PROFILES (MOD II).

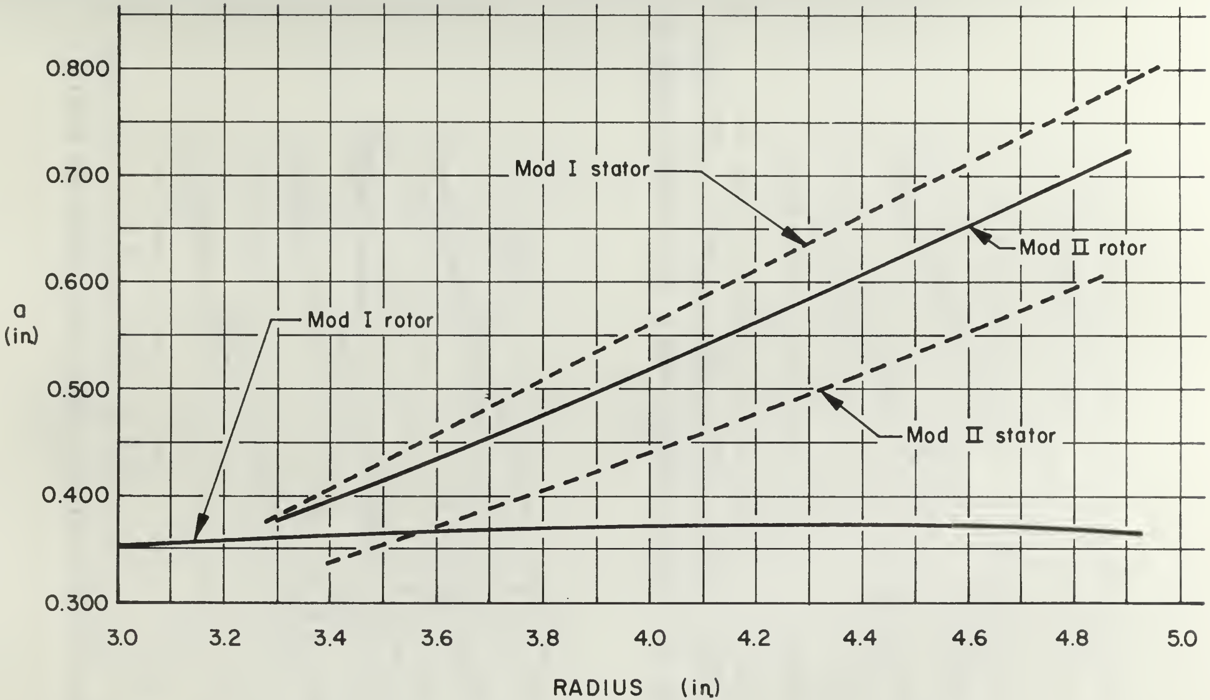

STATOR & ROTOR THROAT OPENINGS VS RADIAL POSITION (MOD I & MOD II)

FIG. 6

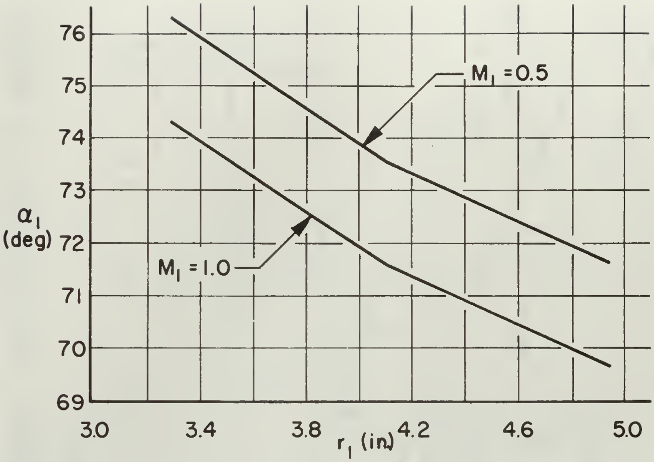

VARIATION OF STATOR OUTLET ANGLE WITH RADIUS (MOD I)
FIG. 7

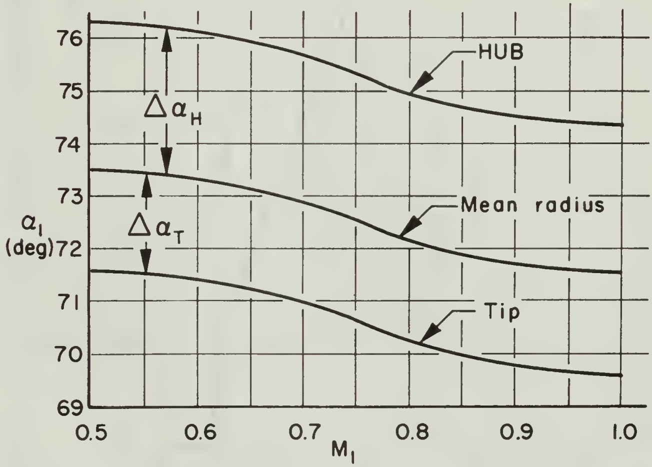

VARIATION OF STATOR OUTLET ANGLE WITH MACH NO. (MOD I)
FIG. 8

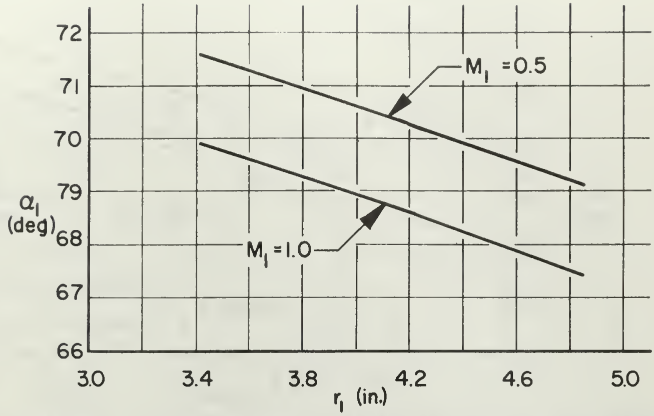

VARIATION OF STATOR OUTLET ANGLE WITH RADIUS (MOD II)

FIG. 9

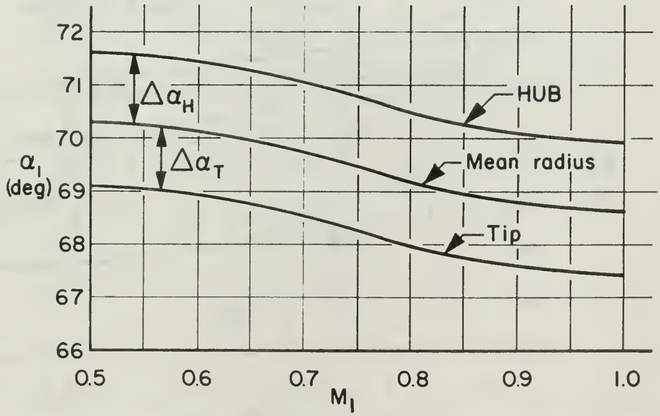

VARIATION OF STATOR OUTLET ANGLE WITH MACH NO. (MOD II)

FIG. 10

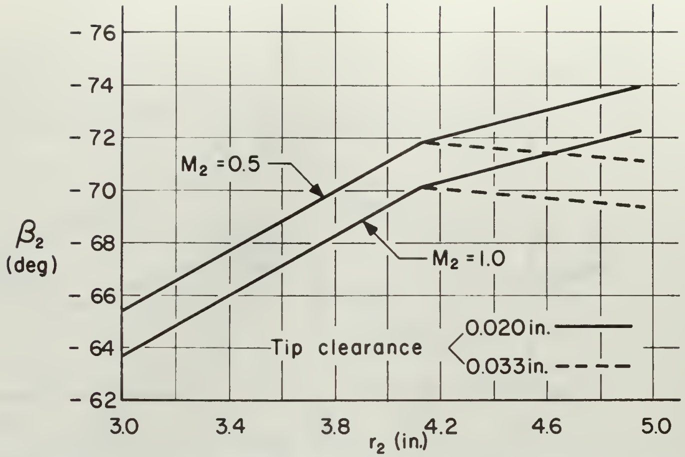

VARIATION OF ROTOR OUTLET ANGLE WITH RADIUS (MODI)

FIG. 11

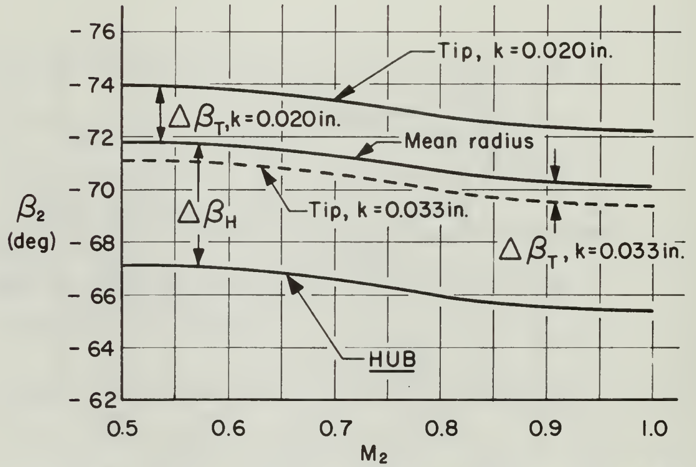

VARIATION OF ROTOR OUTLET ANGLE WITH MACH NO. (MODI)

FIG. 12

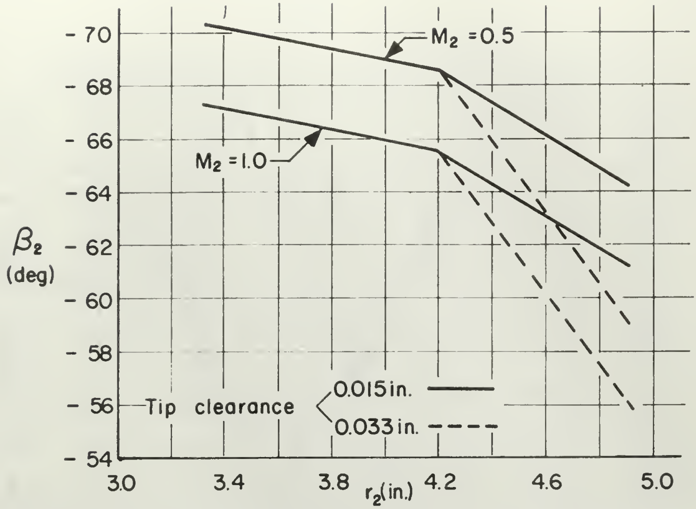

VARIATION OF ROTOR OUTLET ANGLE WITH RADIUS (MOD II)

FIG. 13

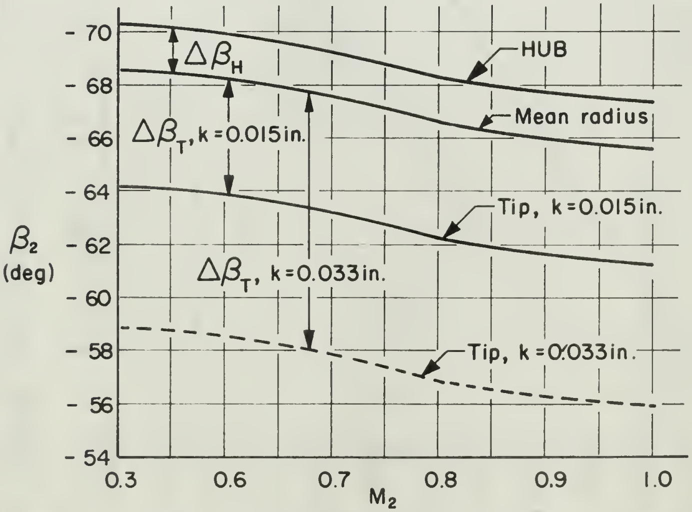

VARIATION OF ROTOR OUTLET ANGLE WITH MACH NO. (MOD II)

FIG. 14

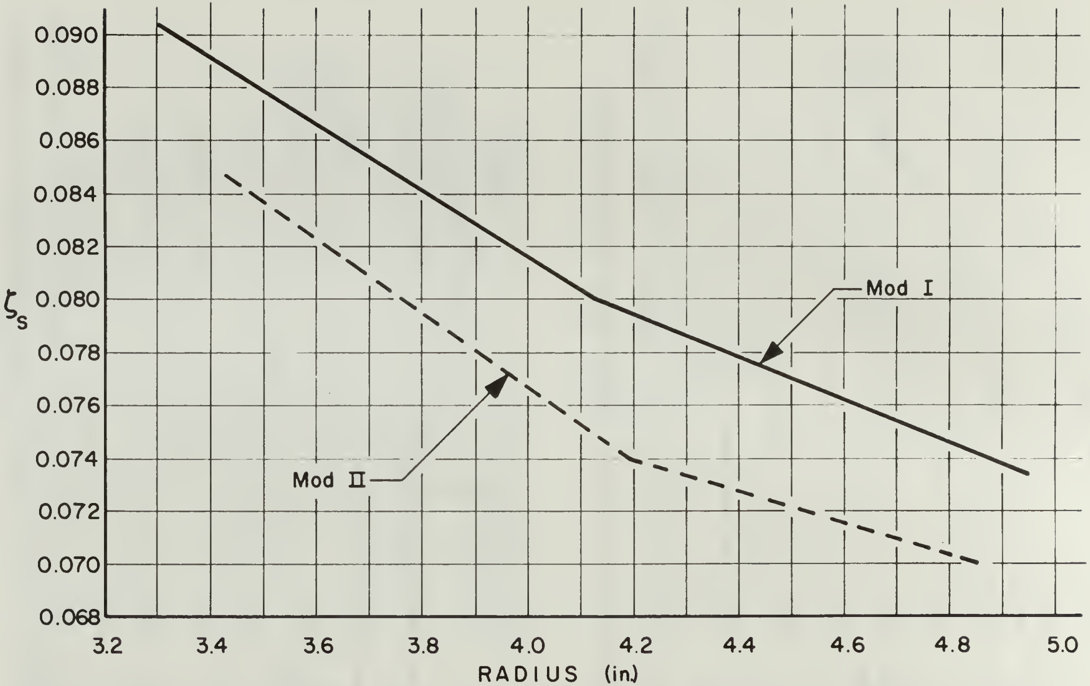

STATOR LOSS COEFFICIENTS AS FUNCTION OF RADIUS (MOD I & II)

FIG. 15

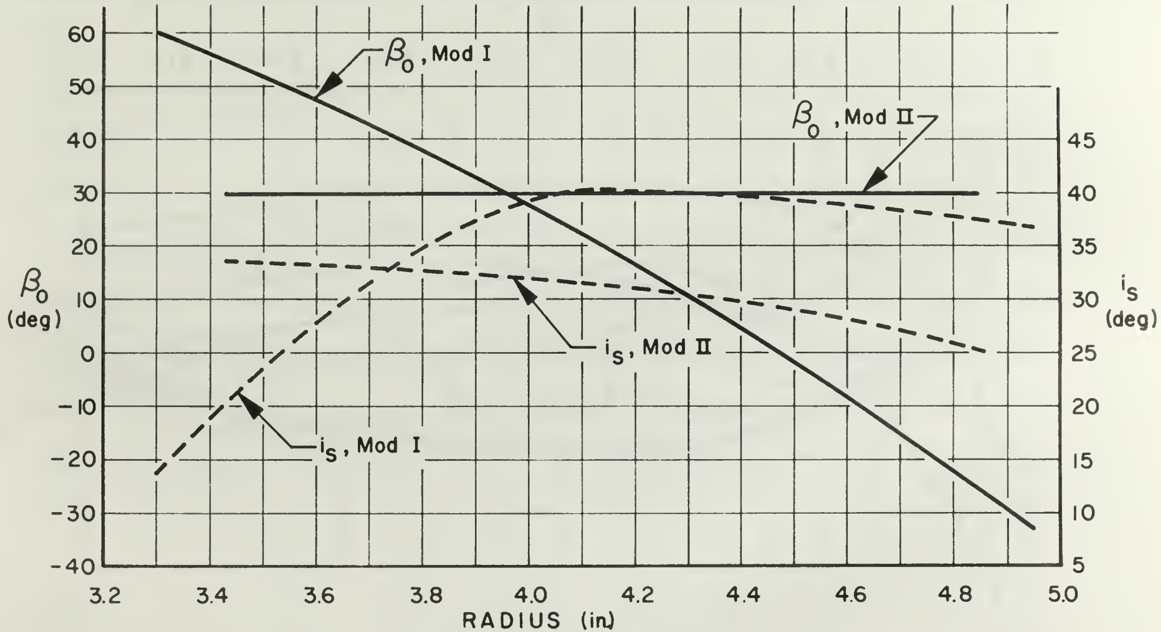

VARIATION OF BLADE INLET & STALL INCIDENCE ANGLES WITH RADIUS
(MOD I & MOD II)
FIG. 16

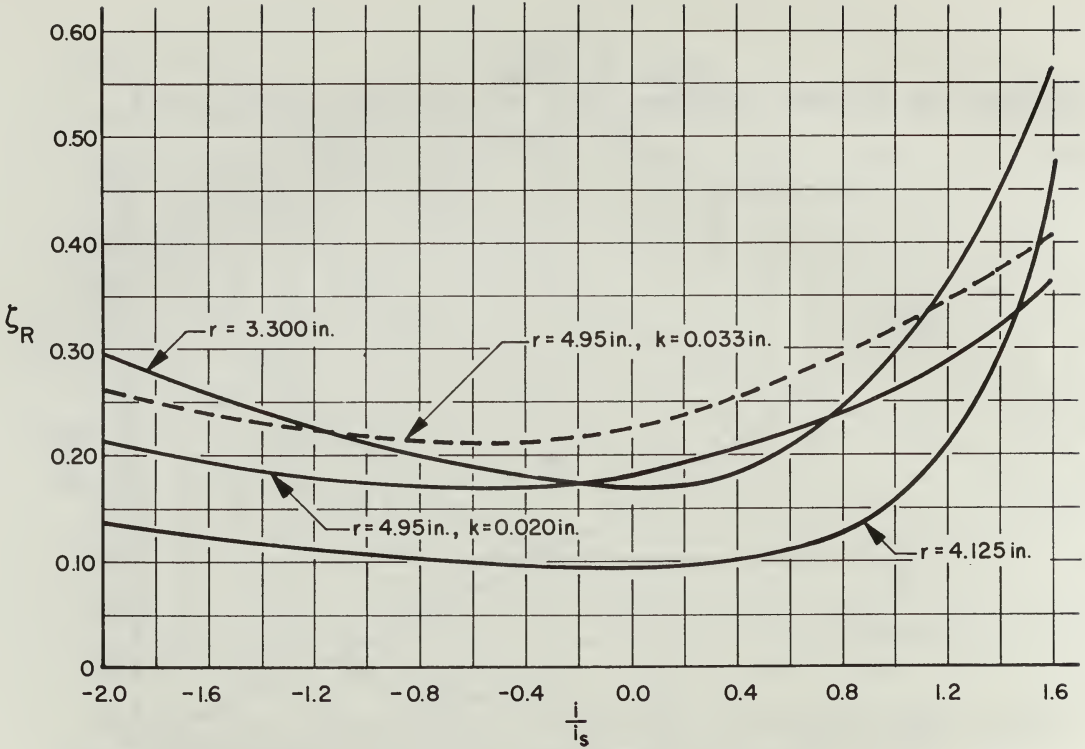

ROTOR LOSS COEFFICIENTS AS FUNCTION OF INCIDENCE RATIO (MOD I)
FIG. 17

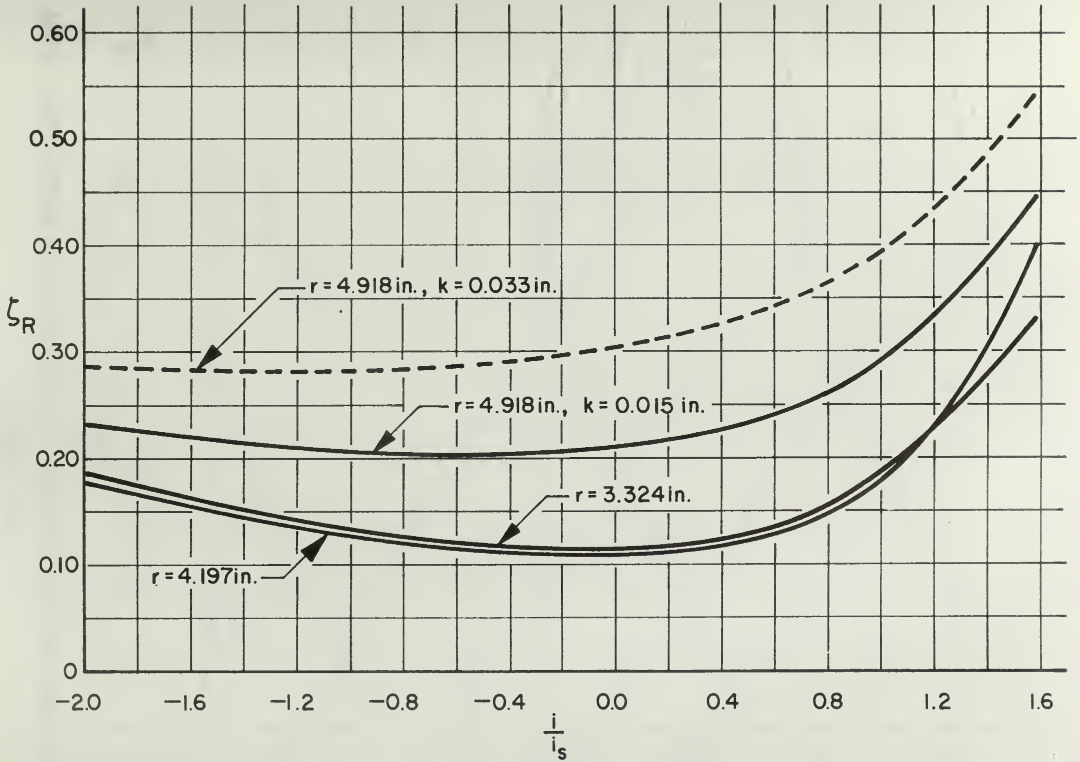

ROTOR LOSS COEFFICIENTS AS FUNCTION OF INCIDENCE RATIO (MOD II)
FIG. 18

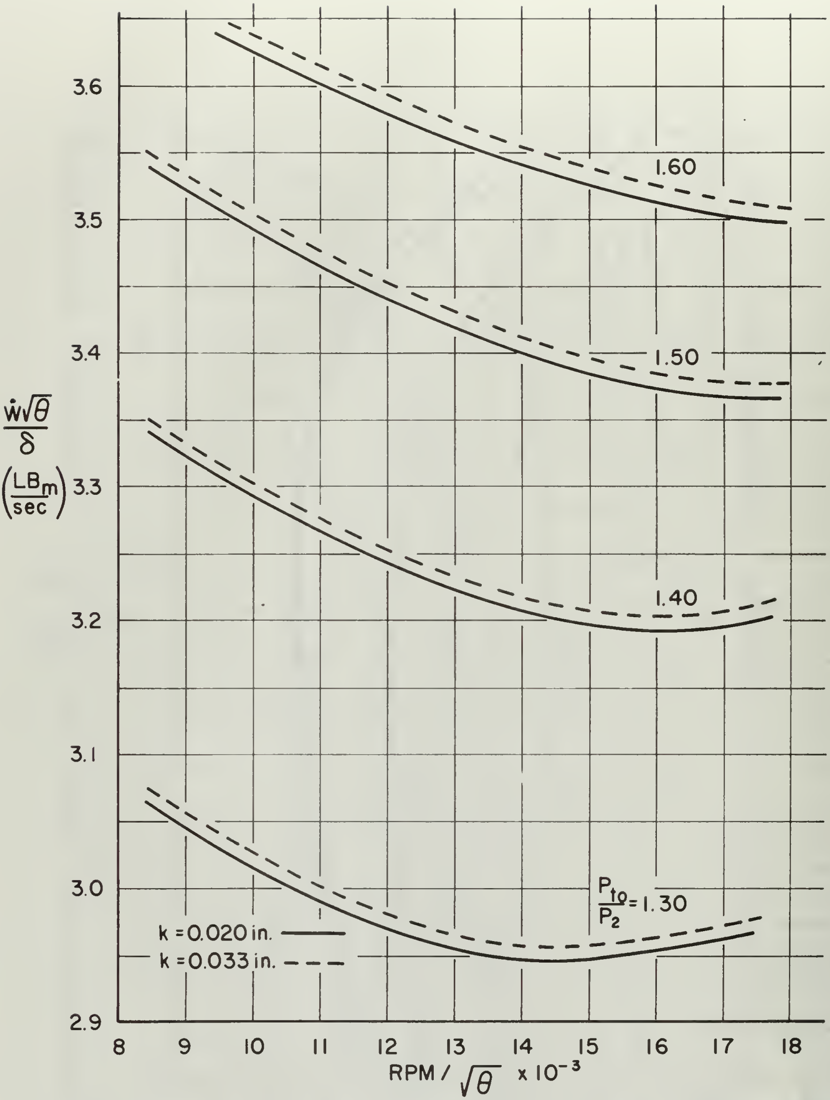

VARIATION OF REFERRED FLOWRATE WITH REFERRED RPM

(MOD I)

FIG. 19

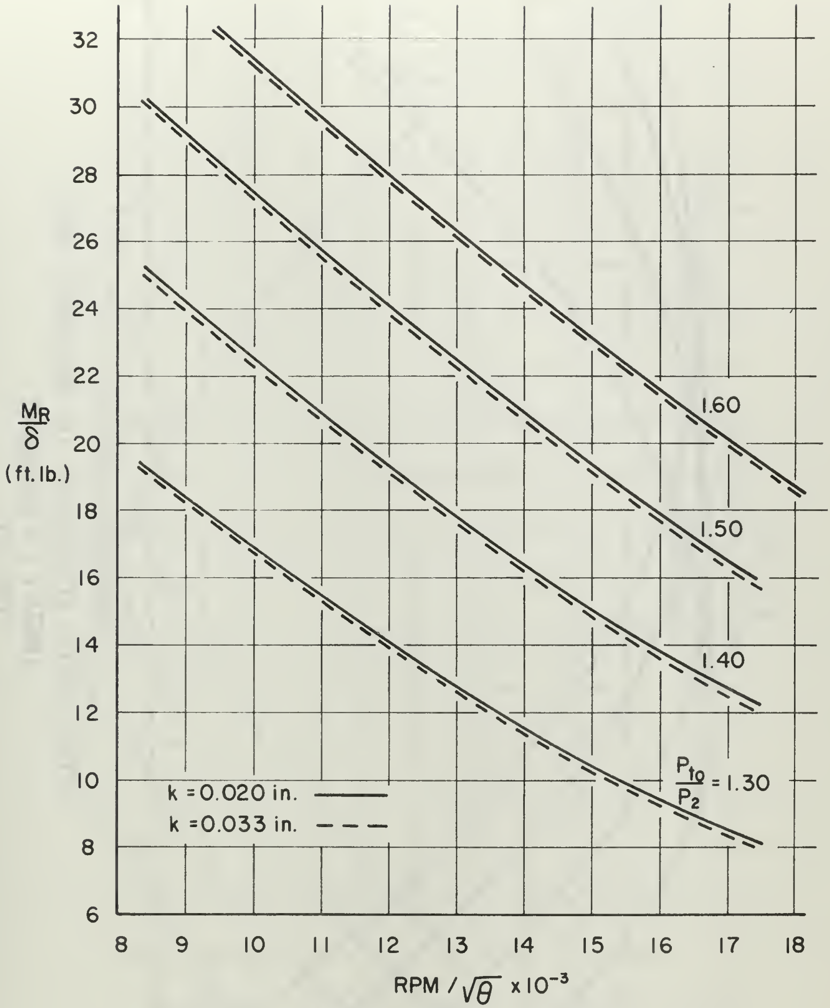

REFERRED MOMENT VS REFERRED RPM
(MOD I)

FIG. 20

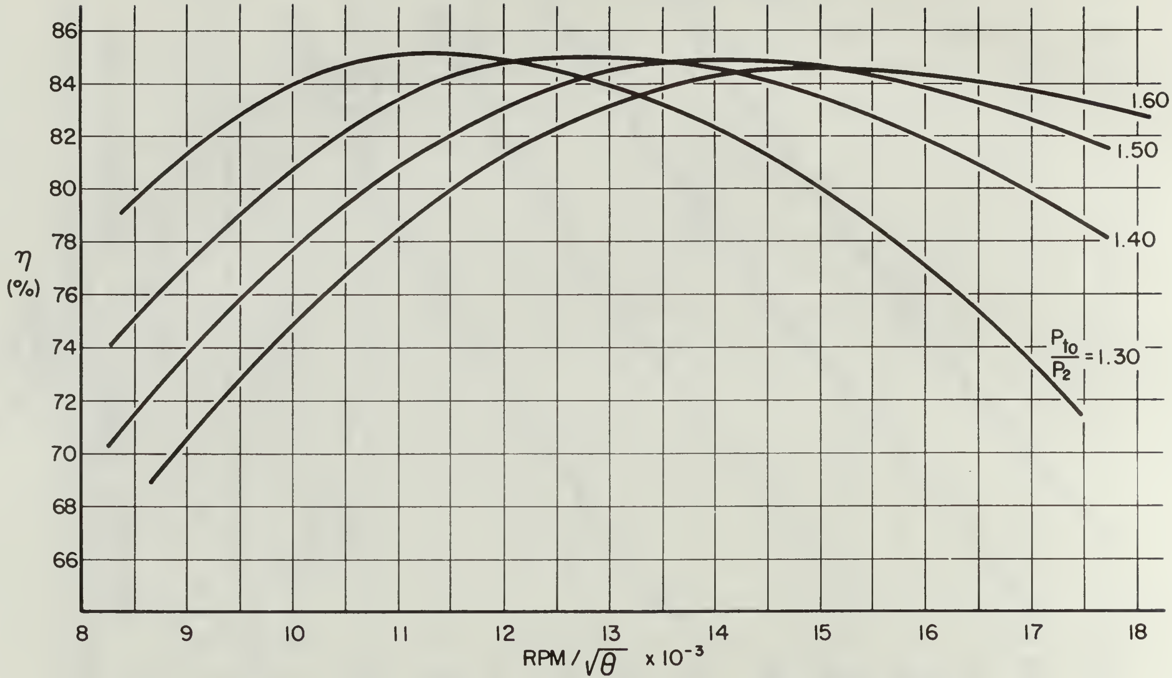

TOTAL-STATIC EFFICIENCY VS REFERRED RPM
(MOD I , k = 0.020 in.)
FIG. 21

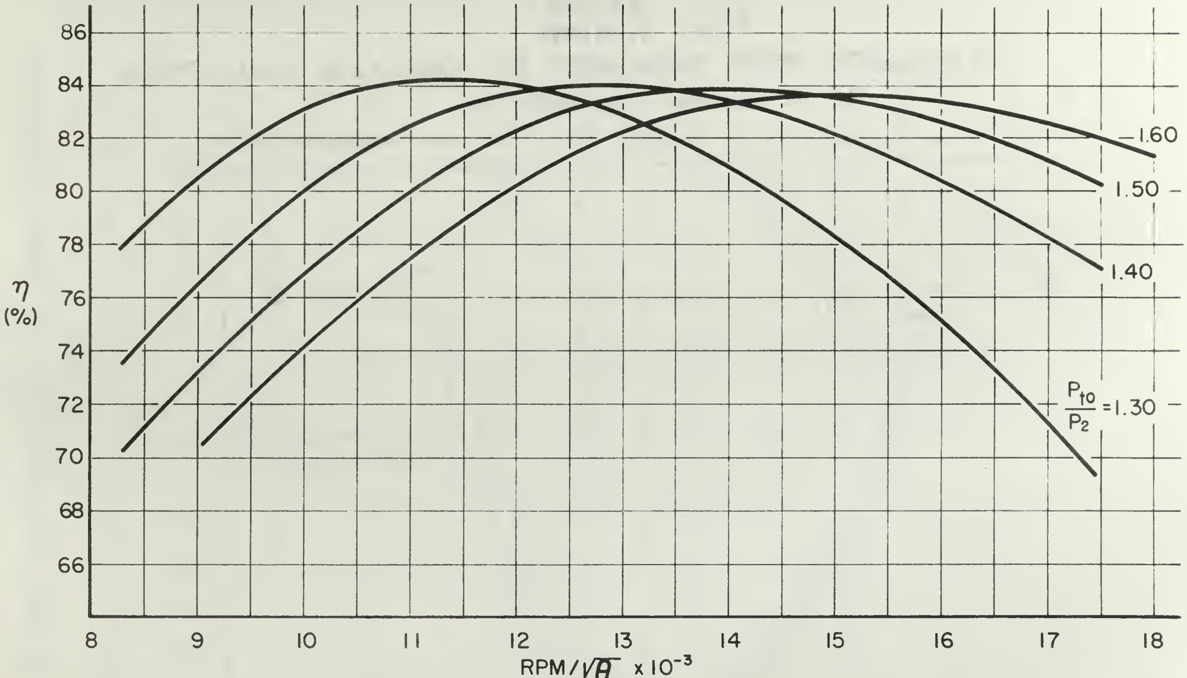

TOTAL-STATIC EFFICIENCY VS REFERRED RPM
(MOD I , k = 0.033 in.)
FIG. 22

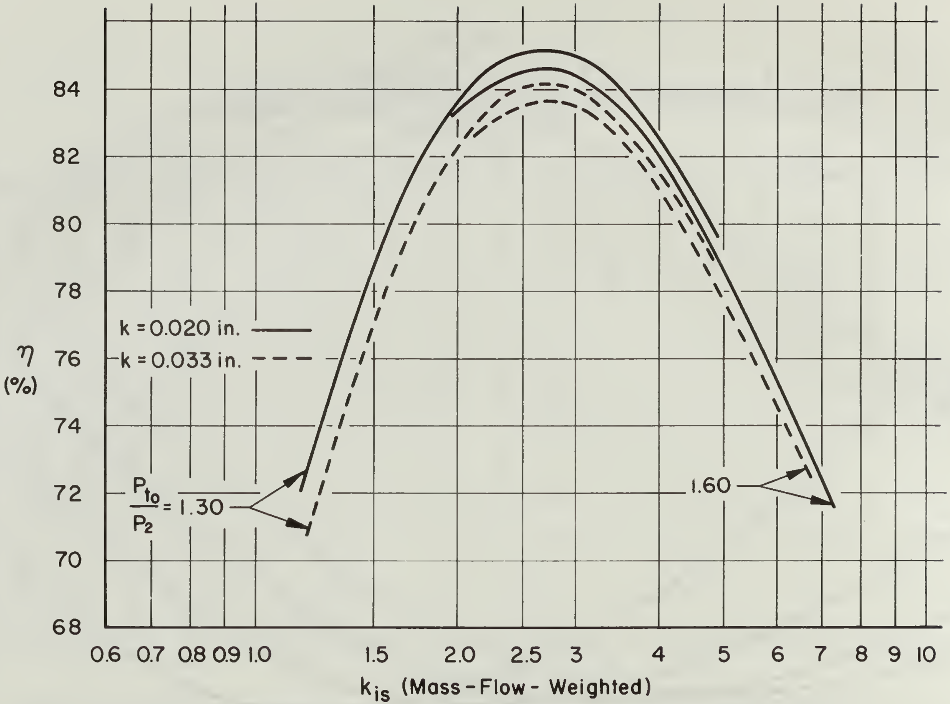

TOTAL-STATIC EFFICIENCY VS ISENTROPIC HEAD COEFFICIENT

(MOD I)

FIG. 23

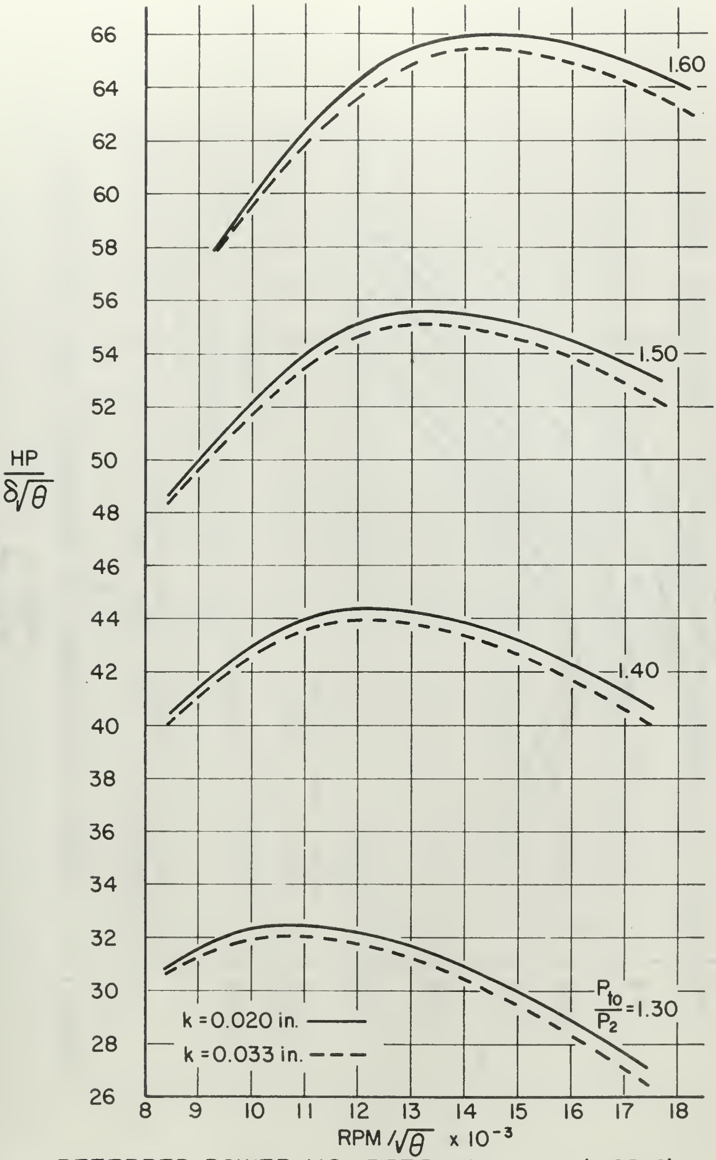

REFERRED POWER VS REFERRED RPM (MOD I)
FIG. 24

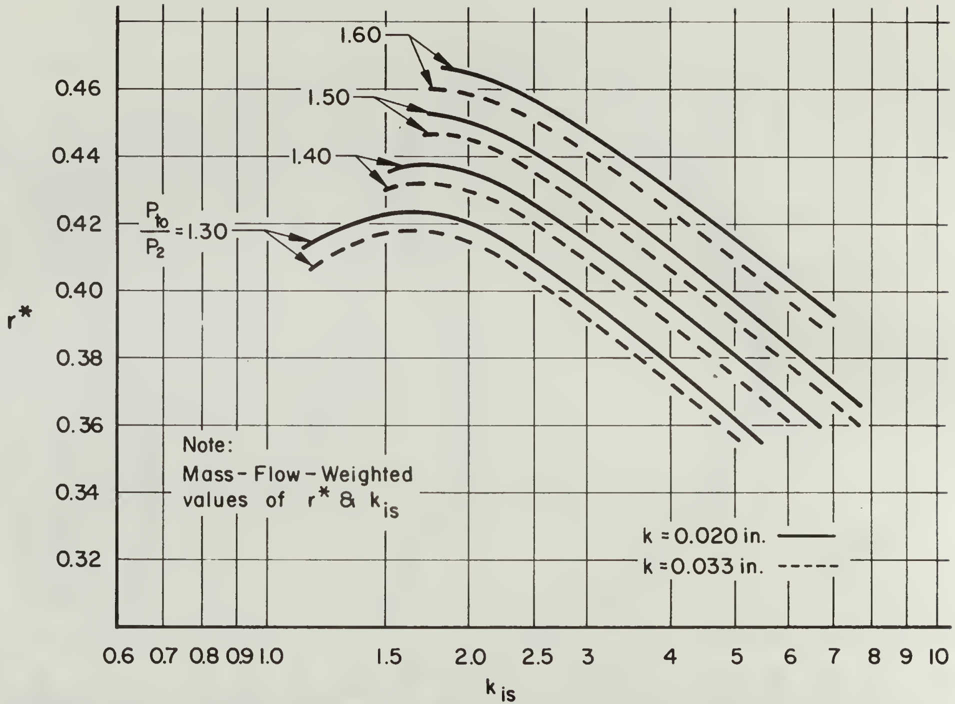

THEORETICAL DEGREE OF REACTION VS ISENTROPIC HEAD COEFFICIENT
(MOD I)
FIG. 25

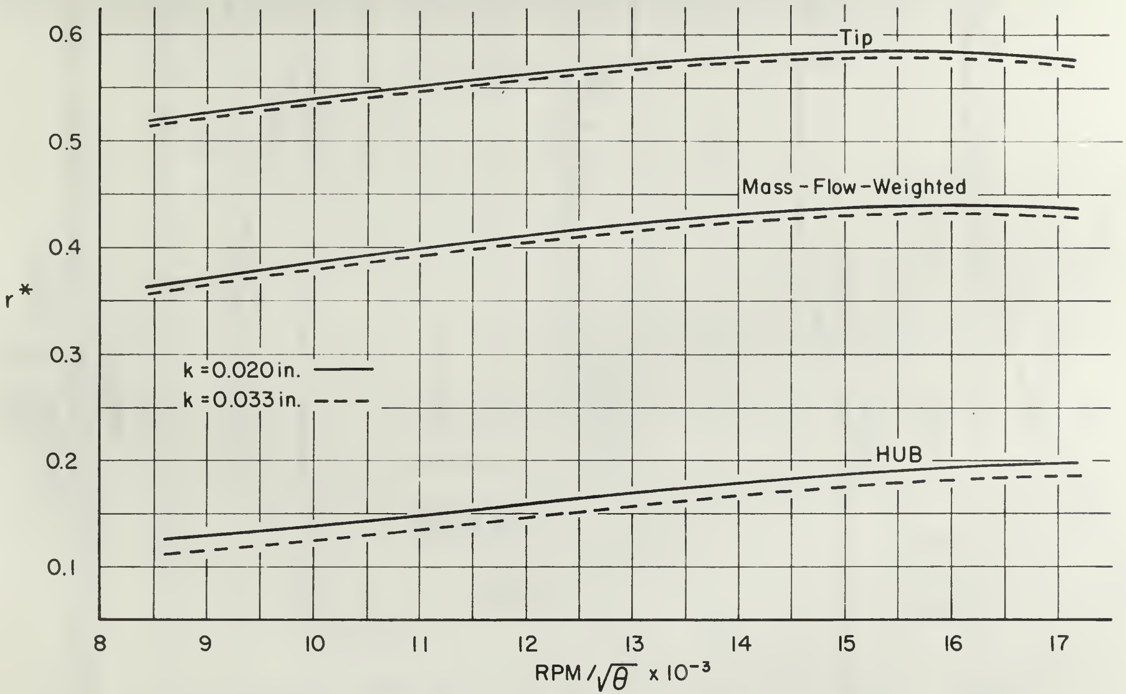

THEORETICAL DEGREE OF REACTION VS REFERRED RPM
(MOD I, $P_{to}/P_2 = 1.40$)
FIG. 26

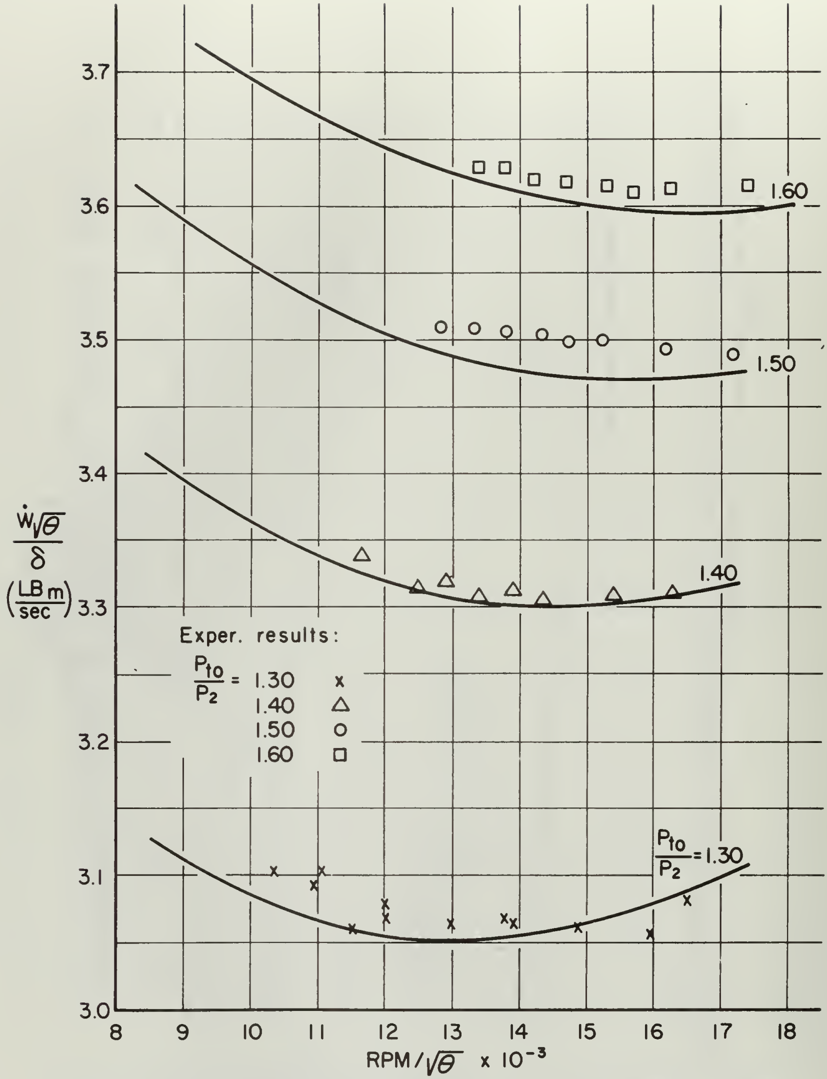

VARIATION OF REFERRED FLOWRATE WITH REFERRED RPM

(MOD II, k=0.015 in.)

FIG. 27

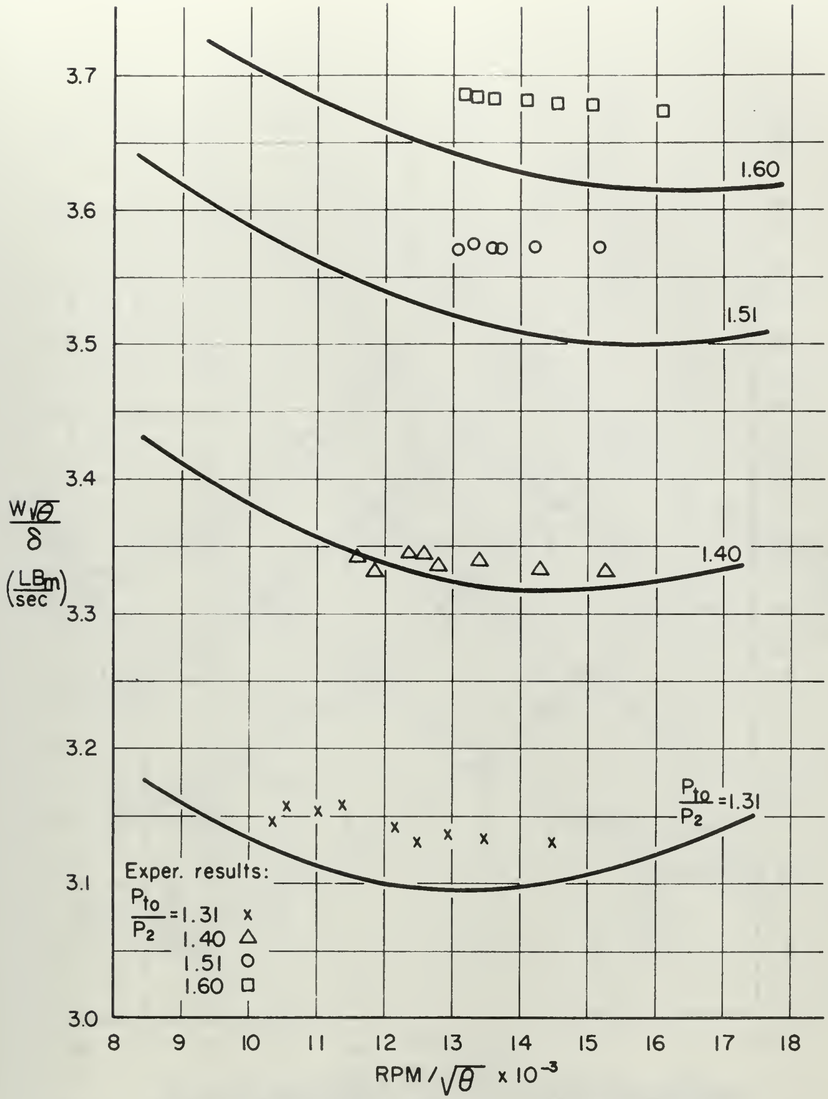

VARIATION OF REFERRED FLOWRATE WITH REFERRED RPM
(MOD II, k = 0.033 in.)
FIG. 28

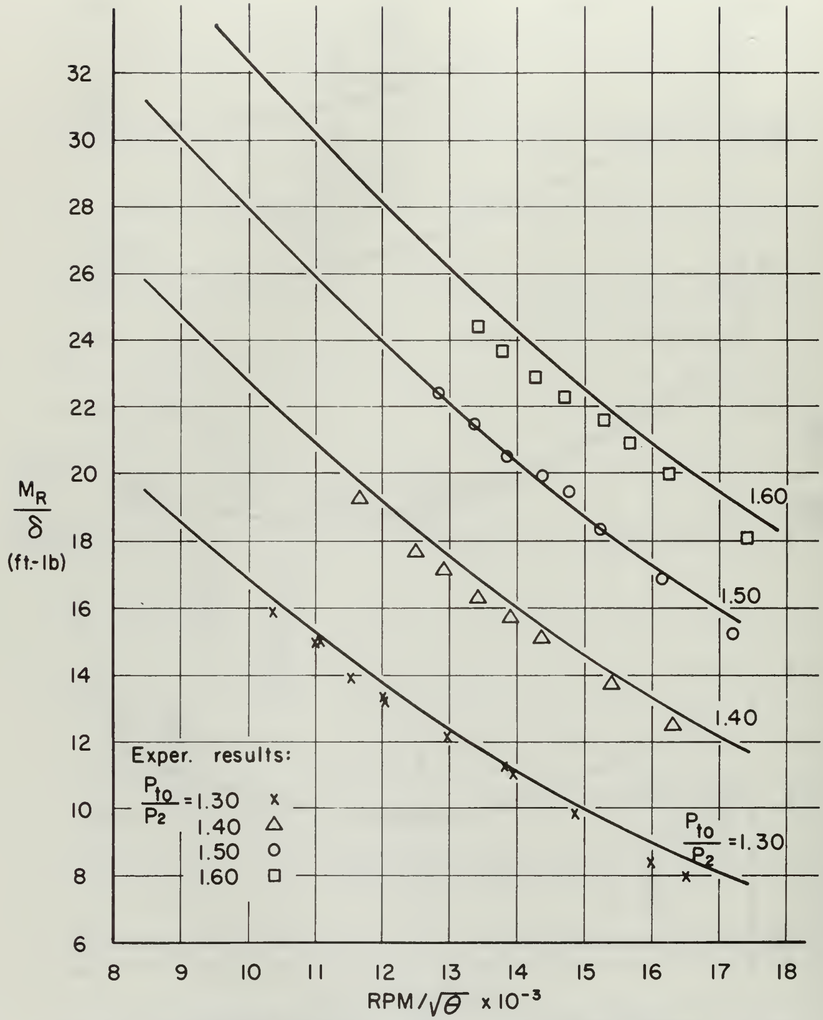

REFERRED MOMENT VS REFERRED RPM

(MOD II, k=0.015 in.)

FIG. 29

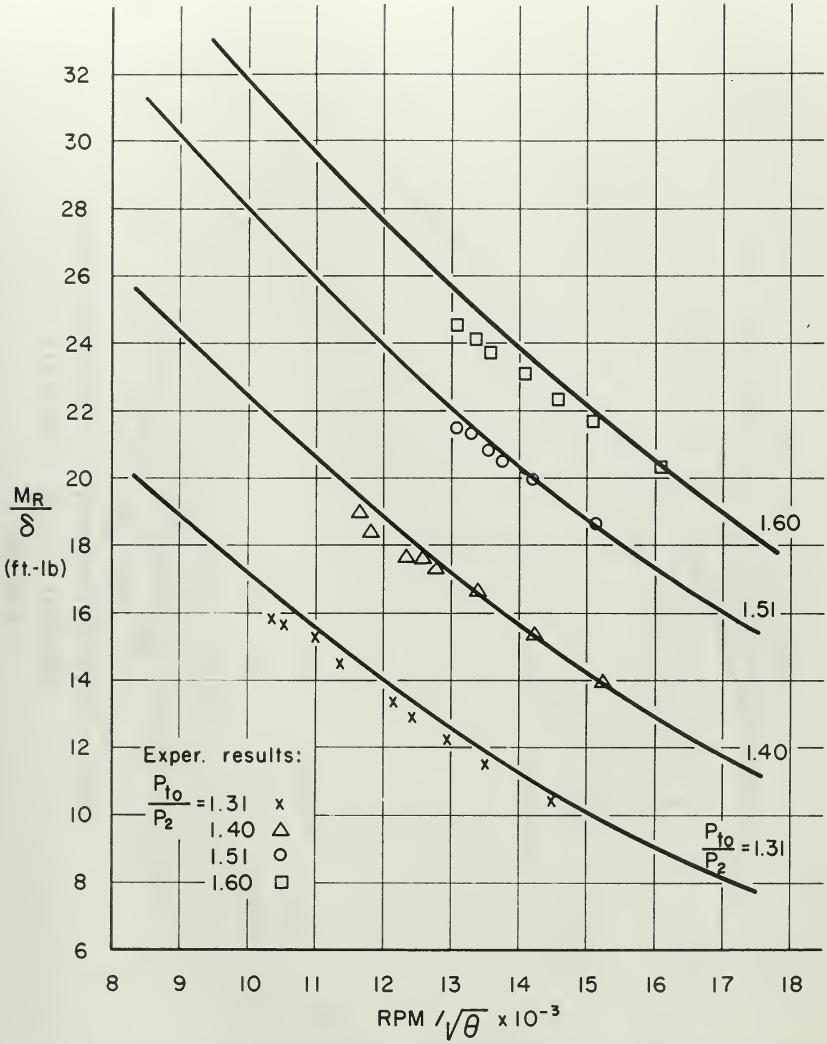

REFERRED MOMENT VS REFERRED RPM
(MOD II, k = 0.033 in.)
FIG. 30

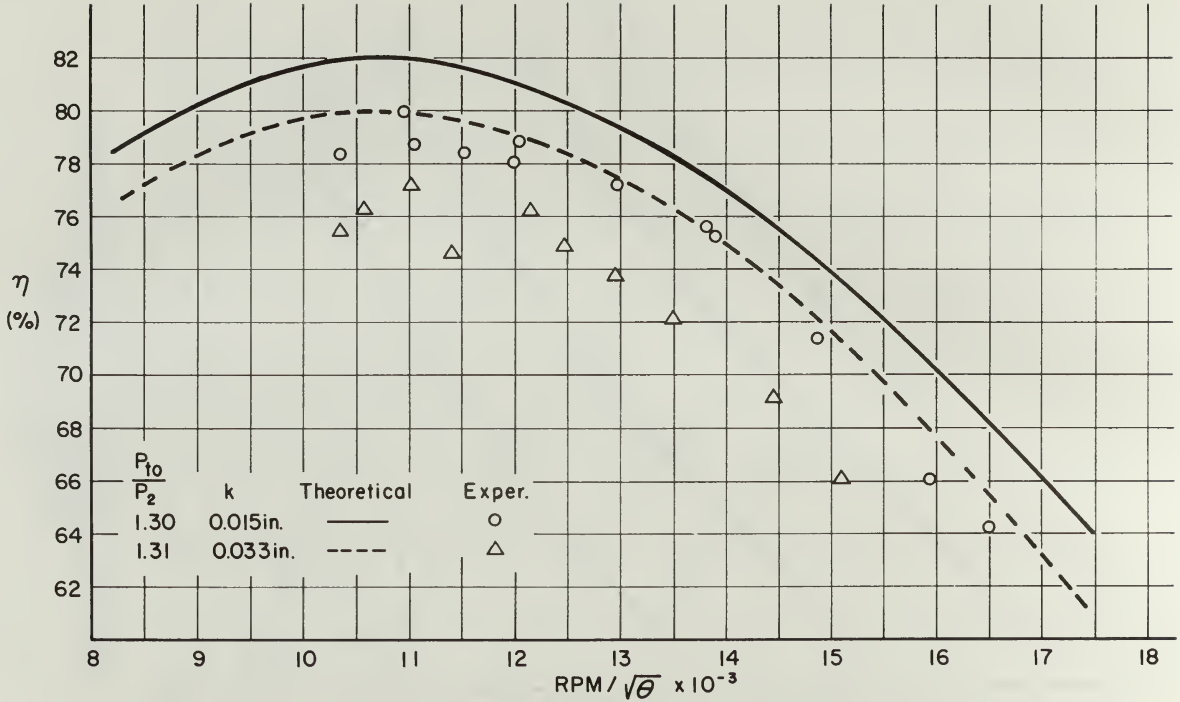

TOTAL-STATIC EFFICIENCY VS REFERRED RPM
(MOD II, P_{to}/P_2 = 1.30, 1.31)
FIG. 31

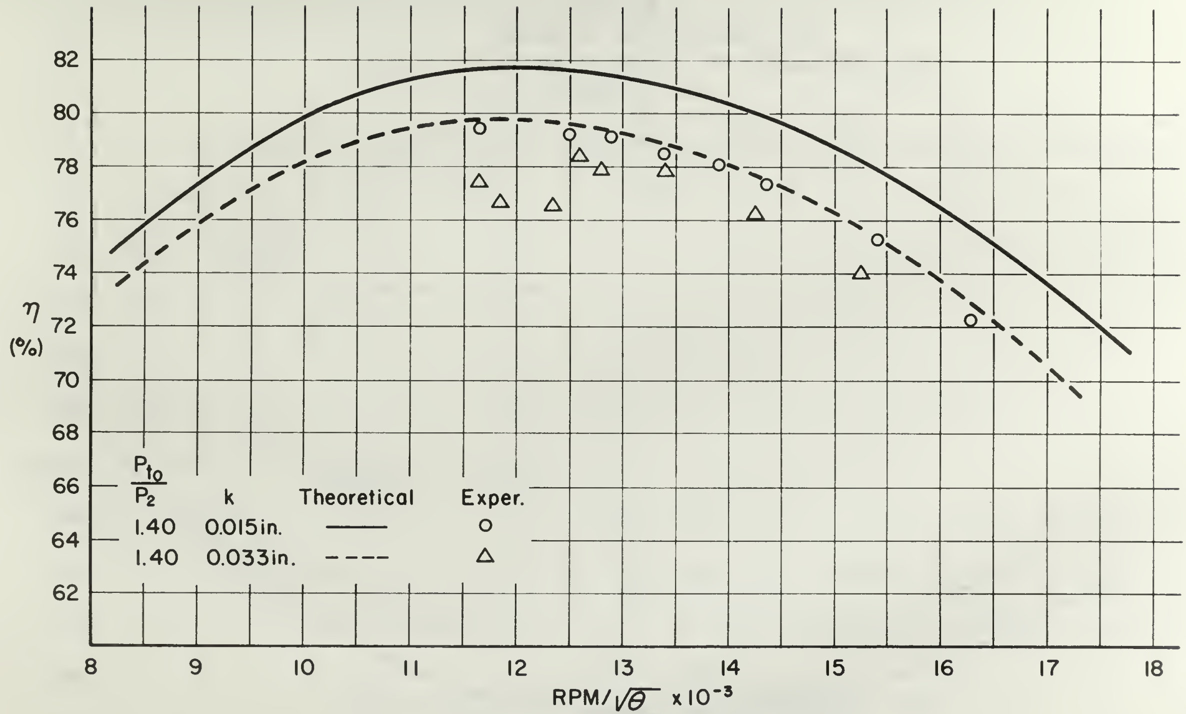

TOTAL-STATIC EFFICIENCY VS REFERRED RPM

(MOD II $P_{to}/P_2 = 1.40$)

FIG. 32

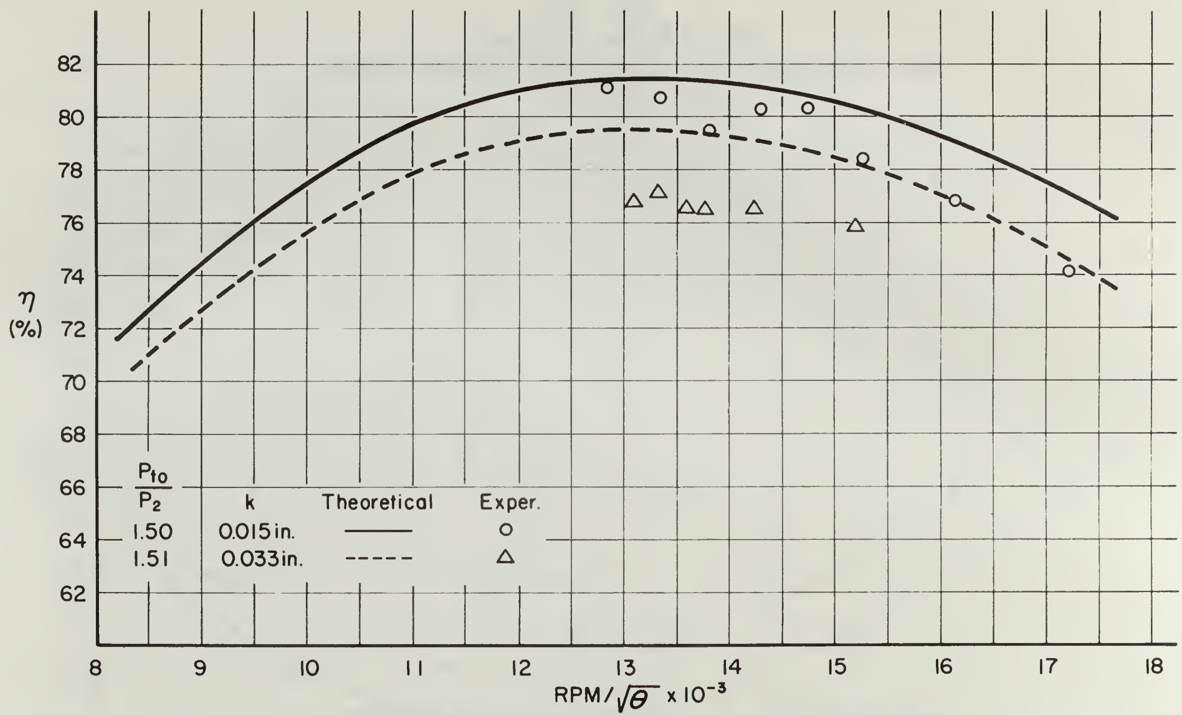

TOTAL-STATIC EFFICIENCY VS REFERRED RPM
(MOD II, P_{to}/P_2=1.50, 1.51)
FIG. 33

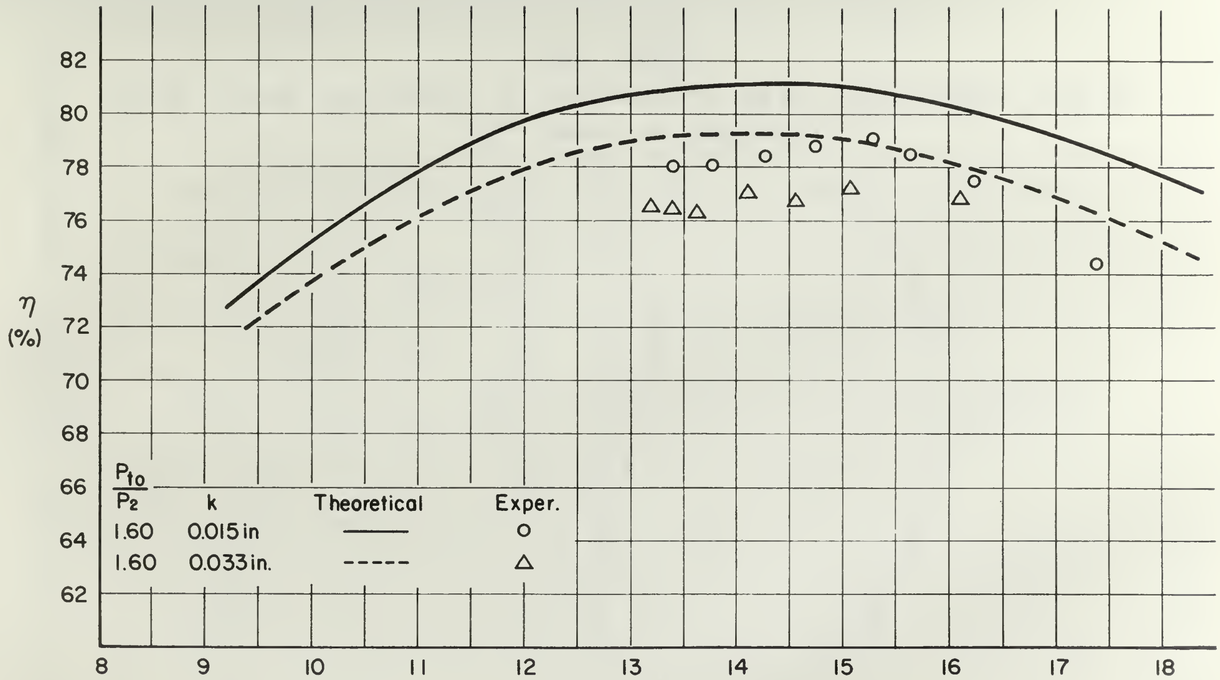

RPM / $\sqrt{\theta}$ x 10^{-3}

TOTAL-STATIC EFFICIENCY VS REFERRED RPM

(MOD II, P_{t0}/P_2 = 1.60)

FIG. 34

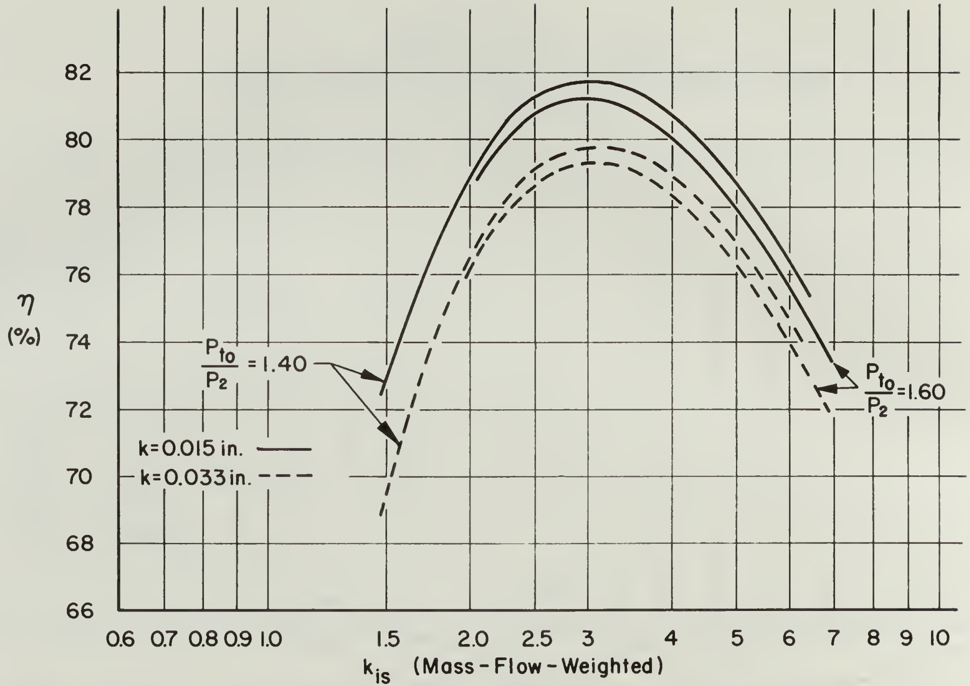

TOTAL-STATIC EFFICIENCY VS ISENTROPIC HEAD COEFFICIENT (MOD II)

FIG. 35

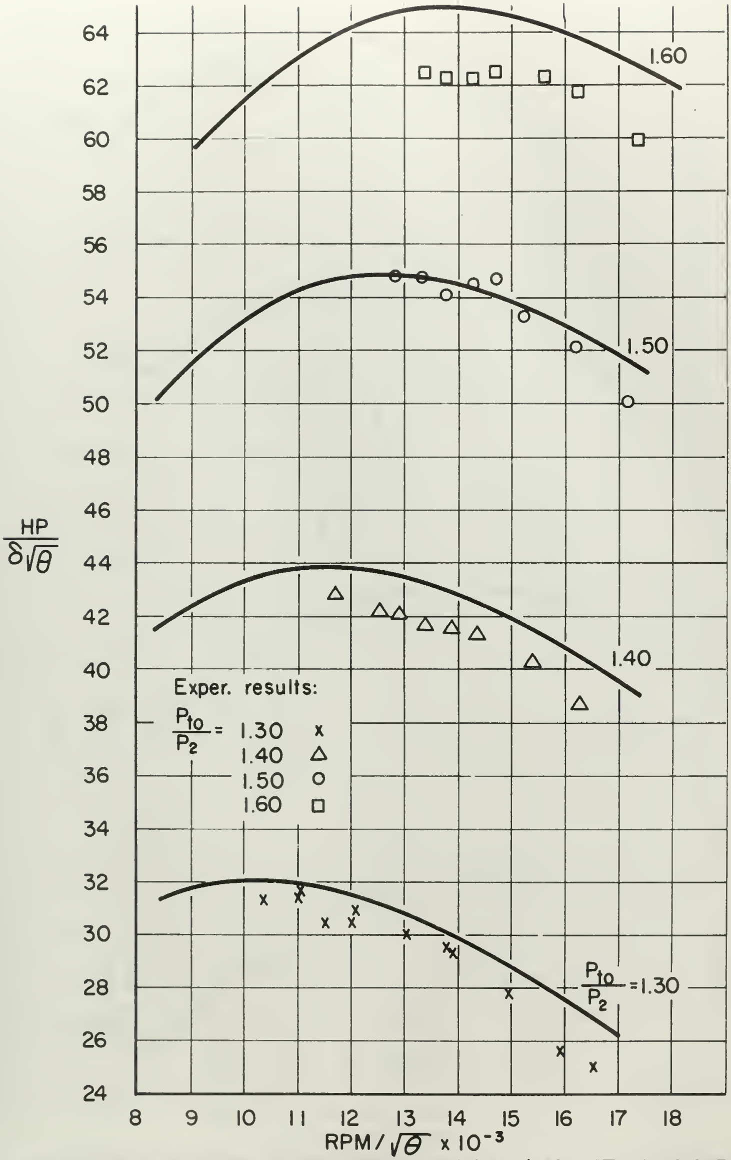

REFERRED POWER VS REFERRED RPM (MOD II, k=0.015in.)

FIG. 36

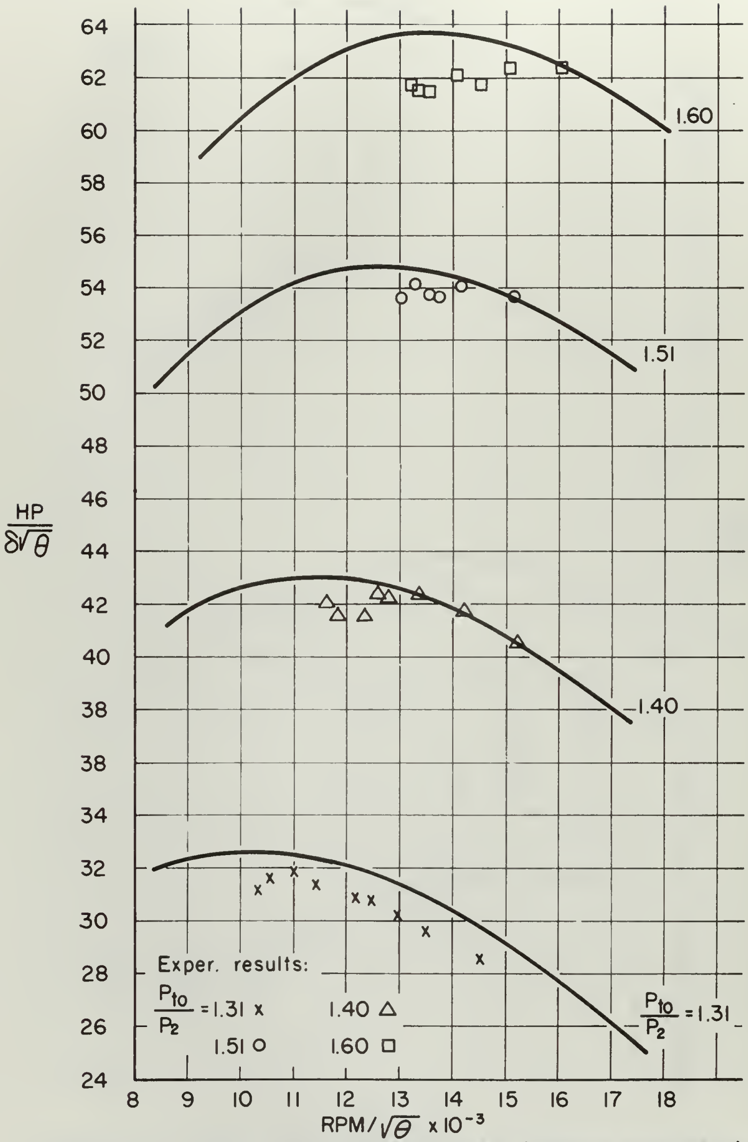

REFERRED POWER VS REFERRED RPM (MOD II, k=0.033in.)

FIG. 37

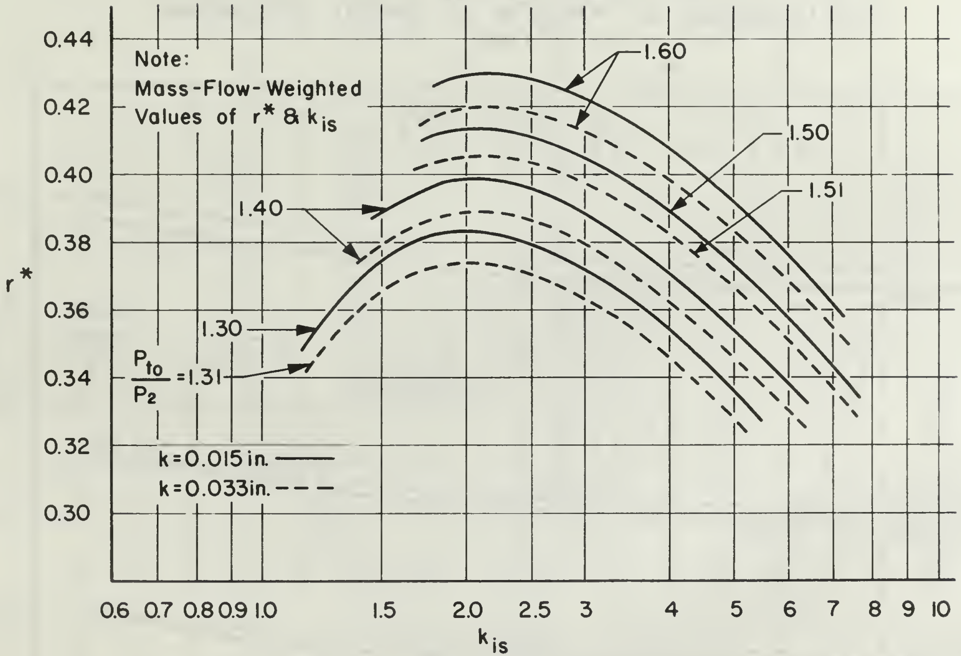

THEORETICAL DEGREE OF REACTION VS ISENTROPIC HEAD COEFFICIENT
(MOD II)
FIG. 38

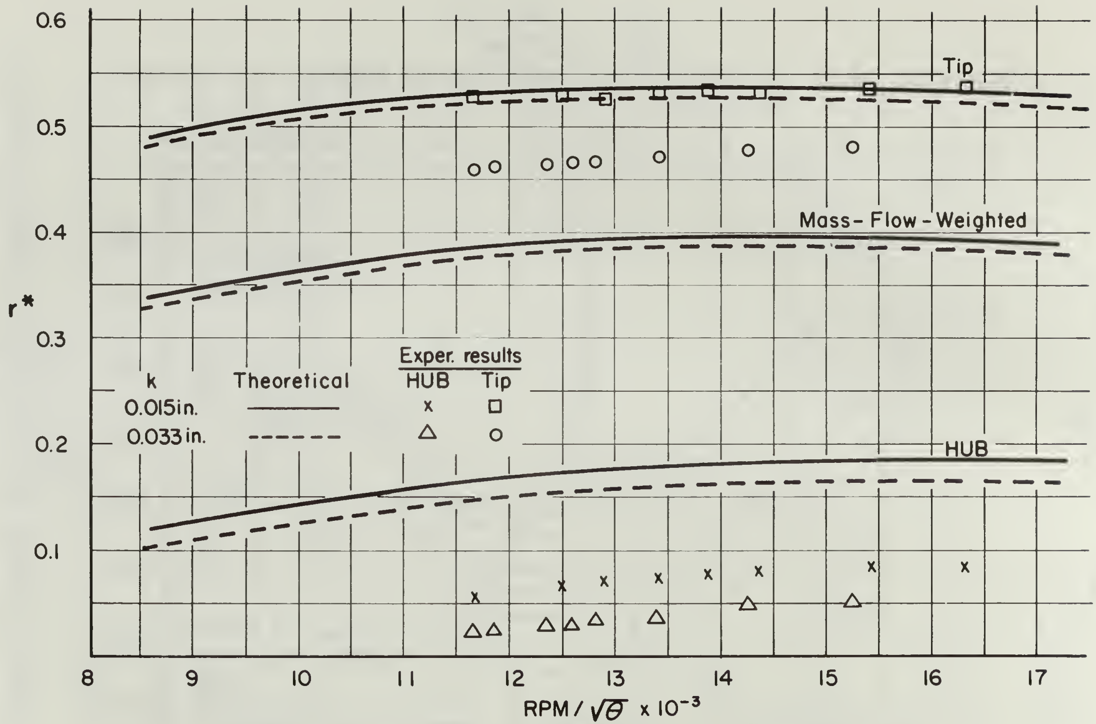

THEORETICAL DEGREE OF REACTION VS REFERRED RPM
(MOD II, $P_{10}/P_2 = 1.40$)

FIG. 39

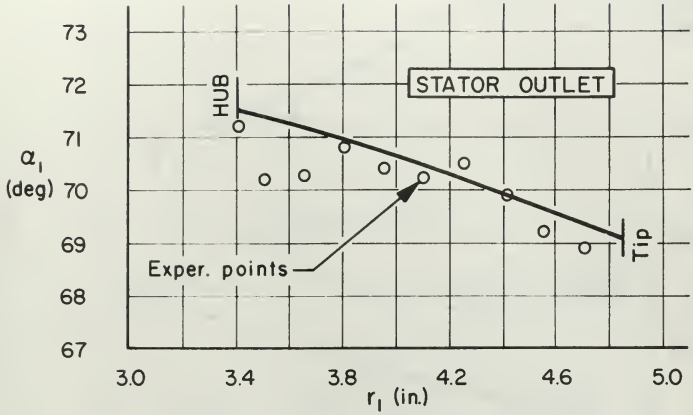

ABSOLUTE FLOW OUTLET ANGLES
AS FUNCTION OF RADIUS
(MOD II, k=0.015 in., P_{t0}/P_2=1.40, RPM/$\sqrt{\theta}$ = 13,934)

FIG. 40

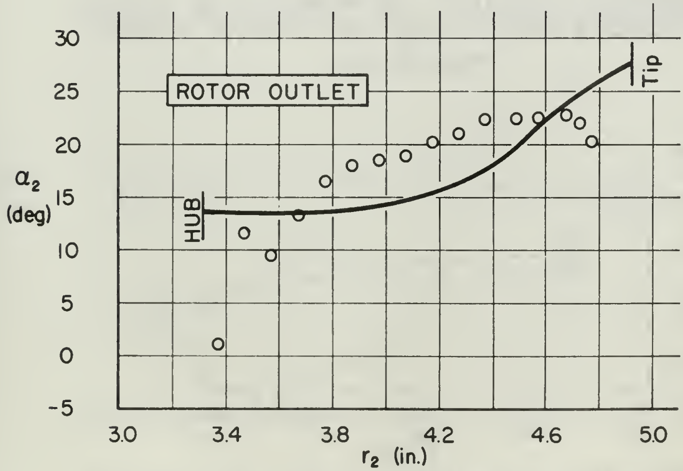

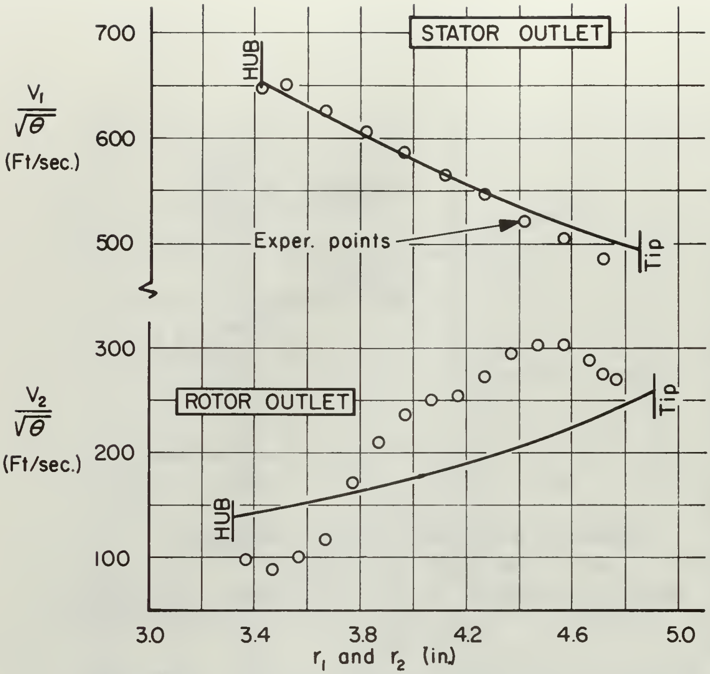

REFERRED VELOCITIES AS FUNCTION OF RADIUS
(MOD II, k=0.015 in. P_{t0}/P_2=1.40, RPM/$\sqrt{\theta}$ =13,934)
FIG. 41

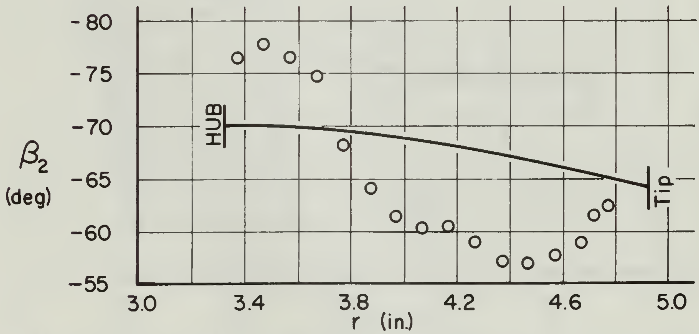

RELATIVE ROTOR FLOW OUTLET ANGLE AS FUNCTION OF RADIUS (MOD II, k=0.015in. P_{t0}/P_2=1.40, RPM/$\sqrt{\theta}$ =13,934)
FIG. 42

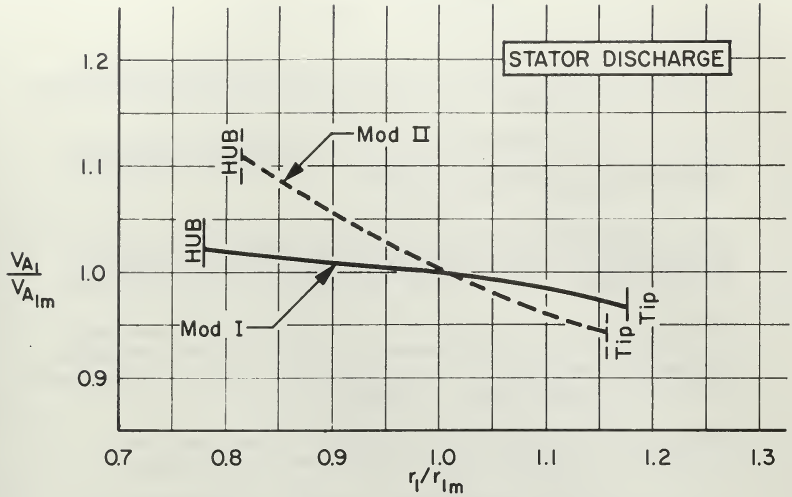

PLOTS OF AXIAL VELOCITY RATIOS VS RADIUS RATIOS AT PEAK EFFICIENCY (MOD I & II , P_{t_0}/P_2 =1.40)

FIG. 43

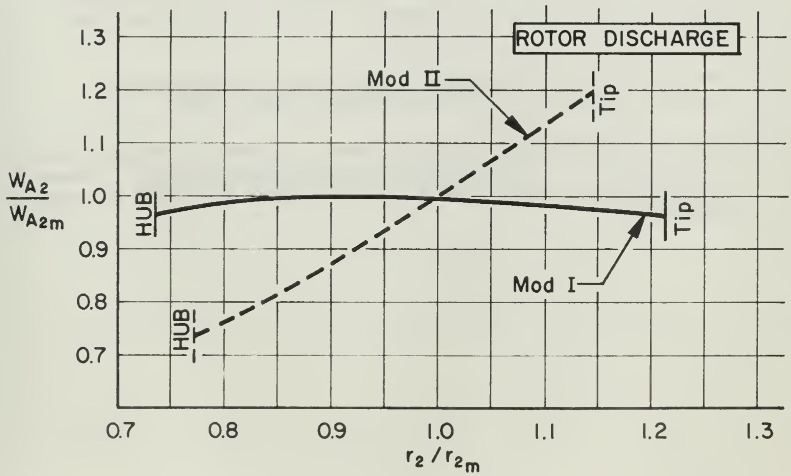

BIBLIOGRAPHY

1. Ainley, D. G. and Mathieson, G. C. R. An Examination of the Flow and Pressure Losses in Blade Rows of Axial-Flow Turbines. Aeronautical Research Council, R & M No. 2891, 1955.

2. Ainley, D. G. and Mathieson, G. C. R. A Method of Performance Estimation for Axial-Flow Turbines. Aeronautical Research Council, R & M No. 2974, 1967.

3. Beer, R. Aerodynamic Design and Estimated Performance of a Two-Stage Curtis Turbine for the Liquid Oxygen Turbopump of the M-1 Engine. NASA CR 54764 (AGC8800-12), Nov. 19, 1965.

4. Commons, P. M. Instrumentation of the Transonic Turbine Test Rig to Determine the Performance of Turbine Inlet Guide Vanes Through the Application of the Momentum and Moment of Momentum Equations. USNPGS Thesis, September 1967.

5. Eckert, H. E. Performance Analysis and Initial Tests of a Transonic Turbine Test Rig. USNPGS Thesis, May 1966.

6. Messegee, J. A. Influence of Axial and Radial Clearances on Performance of a Turbine Stage With Blunt Edge Non-Twisted Blades. USNPGS Thesis, September 1967.

7. Riley, M. W. The Effects of Axial Clearance on the Performance of a Dual Discharge Radial Turbine. USNPGS Thesis, December 1966.

8. Vavra, M. H. Aero-Thermodynamics and Flow in Turbomachines. New York, London: John Wiley and Sons, Inc., 1960.

9. Vavra, M. H. Problems of Fluid Mechanics in Radial Turbomachines, Pts. III and IV. Von Karman Institute Course Note 55b. Rhode-Saint-Genese, Belgium: Von Kármán Institute for Fluid Dynamics, March 1965.

APPENDIX A

DEVELOPEMENT OF EQUATIONS

1. Equation of Motion[11]

The equation of motion for relative flow is

$$\nabla H_R = \bar{W} \times (\nabla \times \bar{W} + 2\bar{\omega}) + T\nabla s \tag{2}$$

In cylindrical coordinates:

$$\nabla H_R = \frac{\bar{i}_\theta}{r}\frac{\partial H_R}{\partial \theta} + \bar{i}_z \frac{\partial H_R}{\partial z} + \bar{i}_r \frac{\partial H_R}{\partial r} \tag{87}$$

$$\begin{aligned}\bar{W} \times (\nabla \times \bar{W}) = {} & \bar{i}_\theta \left\{ W_A \frac{1}{r}\left[\frac{\partial W_A}{\partial \theta} - \frac{\partial (rW_U)}{\partial z}\right] - W_r \frac{1}{r}\left[\frac{\partial (rW_U)}{\partial r} - \frac{\partial W_r}{\partial \theta}\right]\right\} \\ & + \bar{i}_z \left\{ W_r \left[\frac{\partial W_r}{\partial z} - \frac{\partial W_A}{\partial r}\right] - W_U \frac{1}{r}\left[\frac{\partial W_A}{\partial \theta} - \frac{\partial (rW_U)}{\partial z}\right]\right\} \\ & + \bar{i}_r \left\{ W_U \frac{1}{r}\left[\frac{\partial (rW_U)}{\partial r} - \frac{\partial W_r}{\partial \theta}\right] - W_A \left[\frac{\partial W_r}{\partial z} - \frac{\partial W_A}{\partial r}\right]\right\}\end{aligned} \tag{88}$$

$$\bar{W} \times 2\bar{\omega} = \bar{i}_r (2\omega W_U) - \bar{i}_\theta (2\omega W_r) \tag{89}$$

$$T\nabla s = T\left(\bar{i}_\theta \frac{1}{r}\frac{\partial s}{\partial \theta} + \bar{i}_z \frac{\partial s}{\partial z} + \bar{i}_r \frac{\partial s}{\partial r}\right) \tag{90}$$

Equating Eq. 87 to the components in Eqs. 88-90,

$$\bar{i}_\theta : \frac{1}{r}\frac{\partial H_R}{\partial \theta} = \frac{W_A}{r}\left[\frac{\partial W_A}{\partial \theta} - \frac{\partial (rW_U)}{\partial z}\right] - \frac{W_r}{r}\left[\frac{\partial (rW_U)}{\partial r} - \frac{\partial W_r}{\partial \theta}\right] - 2\omega W_r + \frac{T}{r}\frac{\partial s}{\partial \theta} \tag{91}$$

$$\bar{i}_z : \frac{\partial H_R}{\partial z} = W_r \left[\frac{\partial W_r}{\partial z} - \frac{\partial W_A}{\partial r}\right] - \frac{W_U}{r}\left[\frac{\partial W_A}{\partial \theta} - \frac{\partial (rW_U)}{\partial z}\right] + T\frac{\partial s}{\partial z} \tag{92}$$

$$\bar{i}_r : \frac{\partial H_R}{\partial r} = \frac{W_U}{r}\left[\frac{\partial (rW_U)}{\partial r} - \frac{\partial W_r}{\partial \theta}\right] - W_A\left[\frac{\partial W_r}{\partial z} - \frac{\partial W_A}{\partial r}\right] + 2\omega W_U + T\frac{\partial s}{\partial r} \tag{93}$$

---

[11] Eckert, *op. cit.*, pp. 149-155.

For assumed axisymmetric flow, $\frac{\partial(\;\;)}{\partial\theta} = 0$,

$$\bar{i}_\theta:\; 0 = -\frac{W_A}{r}\frac{\partial(rW_u)}{\partial z} - \frac{W_r}{r}\frac{\partial(rW_u)}{\partial r} - 2\omega W_r \tag{94}$$

$$\bar{i}_z:\; \frac{\partial H_R}{\partial z} = W_r\frac{\partial W_r}{\partial z} - W_r\frac{\partial W_A}{\partial r} + \frac{W_u}{r}\frac{\partial(rW_u)}{\partial z} + T\frac{\partial s}{\partial z} \tag{95}$$

$$\bar{i}_r:\; \frac{\partial H_R}{\partial r} = \frac{W_u}{r}\frac{\partial(rW_u)}{\partial r} - W_A\frac{\partial W_r}{\partial z} + W_A\frac{\partial W_A}{\partial r} + 2\omega W_u + T\frac{\partial s}{\partial r} \tag{96}$$

Equation 94 can be written

$$\frac{\partial(rW_u)}{\partial z} = -\frac{W_r}{W_A}\frac{\partial(rW_u)}{\partial r} - 2\omega r\frac{W_r}{W_A} \tag{97}$$

Replacing $\frac{\partial(rW_u)}{\partial z}$ in Eq. 95 by its equivalent in Eq. 97,

$$\frac{\partial H_R}{\partial z} = W_r\frac{\partial W_r}{\partial z} - W_r\frac{\partial W_A}{\partial r} + \frac{W_u}{r}\left(-\frac{W_r}{W_A}\frac{\partial(rW_u)}{\partial r}\right) - 2\omega\frac{W_uW_r}{W_A} + T\frac{\partial s}{\partial z} \tag{98}$$

or

$$\frac{\partial H_R}{\partial z} = -\frac{W_uW_r}{rW_A}\frac{\partial(rW_u)}{\partial r} + W_r\frac{\partial W_r}{\partial z} - W_r\frac{\partial W_A}{\partial r} - 2\omega\frac{W_uW_r}{W_A} + T\frac{\partial s}{\partial z} \tag{99}$$

Multiplying Eq. 96 by W_r and Eq. 99 by W_a,

$$W_r\frac{\partial H_R}{\partial r} = \frac{W_uW_r}{r}\frac{\partial(rW_u)}{\partial r} - W_AW_r\frac{\partial W_r}{\partial z} + W_AW_r\frac{\partial W_A}{\partial r} + 2\omega W_uW_r + W_rT\frac{\partial s}{\partial r} \tag{100}$$

$$W_A\frac{\partial H_R}{\partial z} = -\frac{W_uW_r}{r}\frac{\partial(rW_u)}{\partial r} + W_AW_r\frac{\partial W_r}{\partial z} - W_AW_r\frac{\partial W_A}{\partial r} - 2\omega W_uW_r + W_AT\frac{\partial s}{\partial z} \tag{101}$$

Adding Eqs. 100 and 101,

$$W_r\frac{\partial H_R}{\partial r} + W_A\frac{\partial H_R}{\partial z} = T\left(W_r\frac{\partial s}{\partial r} + W_A\frac{\partial s}{\partial z}\right) \tag{102}$$

For adiabatic flow H_R is constant along a streamline, therefore,

$$\bar{W}\,dt\cdot\nabla H_R = 0 \tag{103}$$

For axisymmetric flow,

$$\bar{W}\,dt\cdot\nabla H_R = 0 = W_A\frac{\partial H_R}{\partial z} + W_r\frac{\partial H_R}{\partial r} \tag{104}$$

From Eq. 104,

$$\frac{\partial H_R}{\partial z} = -\frac{W_r}{W_A}\frac{\partial H_R}{\partial r} \tag{105}$$

Substituting Eq. 105 into Eq. 102,

$$W_r\frac{\partial H_R}{\partial r} + W_A\left(-\frac{W_r}{W_A}\frac{\partial H_R}{\partial r}\right) = T\left(W_r\frac{\partial s}{\partial r} + W_A\frac{\partial s}{\partial z}\right) \tag{106}$$

or

$$\frac{\partial s}{\partial z} = -\frac{W_r}{W_A}\frac{\partial s}{\partial r} \tag{107}$$

Using Eqs. 105 and 107, Eq. 99 becomes

$$-\frac{W_r}{W_A}\frac{\partial H_R}{\partial r} = -\frac{W_u W_r}{r W_A}\frac{\partial (rW_u)}{\partial r} - W_r\frac{\partial W_r}{\partial z} - W_r\frac{\partial W_A}{\partial r} - 2\omega\frac{W_u W_r}{W_A} - \frac{W_r}{W_A}T\frac{\partial s}{\partial r} \qquad (108)$$

Multiplying Eq. 108 by $\left(-\frac{W_A}{W_r}\right)$, gives

$$\frac{\partial H_R}{\partial r} = \frac{W_u}{r}\frac{\partial (rW_u)}{\partial r} - W_A\frac{\partial W_r}{\partial z} + W_A\frac{\partial W_A}{\partial r} + 2\omega W_u - T\frac{\partial s}{\partial r} \qquad (109)$$

Eq. 109 is identical with Eq. 96, therefore Eq. 109 is the equation that must be solved. With $\left[W_A\frac{\partial W_A}{\partial r} = \frac{1}{2}\frac{\partial (W_A^2)}{\partial r}\right]$, Eq. 109 becomes

$$\frac{\partial (W_A^2)}{\partial r} - 2W_A\frac{\partial W_r}{\partial z} + \frac{2W_u}{r}\frac{\partial (rW_u)}{\partial r} + 4\omega W_u - 2\frac{\partial H_R}{\partial r} + 2T\frac{\partial s}{\partial r} = 0 \qquad (110)$$

Rewriting Eq. 110 for the rotor discharge and using the substitutions $H_R = H_E - \frac{U_2^2}{2}$ and $T_2 = \frac{H_E}{c_p} - \frac{W_2^2}{2c_p}$,

$$\frac{\partial (W_{A_2}^2)}{\partial r_2} - 2W_{A_2}\frac{\partial W_{r_2}}{\partial z} + \frac{2W_{u_2}}{r_2}\frac{\partial (r_2 W_{u_2})}{\partial r_2} + 4\omega W_{u_2} - 2\frac{\partial}{\partial r_2}\left(H_E - \frac{U_2^2}{2}\right) + 2\left(\frac{H_E}{c_p} - \frac{W_2^2}{2c_p}\right)\frac{\partial s_2}{\partial r_2} = 0 \qquad (111)$$

The last term of Eq. 111 can be expressed by

$$\frac{1}{c_p}\left[2H_E - (W_{A_2}^2 + W_{u_2}^2 + W_{r_2}^2)\right] = \frac{1}{c_p}\left[2H_E - W_{u_2}^2 - W_{A_2}^2\left(1 + \frac{W_{r_2}^2}{W_{A_2}^2}\right)\right] \qquad (112)$$

With $\left(\frac{W_r^2}{W_A^2} = \tan^2\lambda\right)$ and $\left(1 + \tan^2\lambda = \frac{1}{\cos^2\lambda}\right)$ Eq. 112 becomes

$$\frac{1}{c_p}\left[2H_E - W_2^2\right] = \frac{1}{c_p}\left[2H_E - W_{u_2}^2\right] - \frac{W_{A_2}^2}{c_p\cos^2\lambda_2} \qquad (113)$$

Using Eq. 113, and after rearranging, Eq. 111 becomes

$$\frac{\partial (W_{A_2}^2)}{\partial r_2} - 2W_{A_2}\frac{\partial W_{r_2}}{\partial z} - \frac{W_{A_2}^2}{c_p\cos^2\lambda_2}\frac{\partial s_2}{\partial r_2} + 2\frac{W_{u_2}}{r_2}\frac{\partial (r_2 W_{u_2})}{\partial r_2}$$

$$+ 4\omega W_{u_2} - 2\frac{\partial H_E}{\partial r_2} + \frac{\partial (U_2^2)}{\partial r_2} + \frac{1}{c_p}\left[2H_E - W_{u_2}^2\right]\frac{\partial s_2}{\partial r_2} = 0 \qquad (114)$$

Noting that

$$\frac{\partial (U_2^2)}{\partial r_2} = \frac{\partial (\omega^2 r_2^2)}{\partial r_2} = 2\omega^2 r_2 \qquad (115)$$

Eq. 114 is

$$\frac{\partial (W_{A_2}^2)}{\partial r_2} - 2W_{A_2}\frac{\partial W_{r_2}}{\partial z} - \frac{W_{A_2}^2}{c_p\cos^2\lambda_2}\frac{\partial s_2}{\partial r_2} + 2\frac{W_{u_2}}{r_2}\frac{\partial (r_2 W_{u_2})}{\partial r_2} + 4\omega W_{u_2}$$

$$-2\frac{\partial H_E}{\partial r_2} + 2\omega^2 r_2 + \frac{1}{c_p}\left[2H_E - W_{u_2}^2\right]\frac{\partial s_2}{\partial r_2} = 0 \qquad (116)$$

This equation is made non-dimensional by multiplying by $\left(\frac{r_m}{W_{A_m}^2}\right)$, where the subscript m refers to the mean streamline. In the subsequent derivations the subscript 2 will be omitted. Then

$$\frac{r_m}{W_{A_m}^2}\frac{\partial(W_A^2)}{\partial r} - 2\frac{W_A}{W_{A_m}^2} r_m \frac{\partial W_r}{\partial z} - \frac{W_A^2}{W_{A_m}^2}\frac{r_m}{c_p \cos^2\lambda_2}\frac{\partial s}{\partial r} + \frac{W_U r_m}{W_{A_m} r}\frac{\partial\left(\frac{r}{r_m}\frac{W_U}{W_{A_m}}\right)}{\partial\left(\frac{r}{r_m}\right)}$$

$$+ 4\frac{\omega r_m W_U}{W_{A_m}^2} - 2\frac{r_m}{W_{A_m}^2}\frac{\partial H_E}{\partial r} - \frac{2\omega^2 r r_m}{W_{A_m}^2} + \frac{r_m}{c_p}\left[\frac{2H_E}{W_{A_m}^2} - \frac{W_U^2}{W_{A_m}^2}\right]\frac{\partial s}{\partial r} = 0 \qquad (117)$$

Now let

$$Y = \frac{W_A}{W_{A_m}} \qquad (118)$$

$$X = \frac{r}{r_m} \qquad (119)$$

$$s^* = \frac{s}{c_p} \qquad (120)$$

Equation 117 then becomes

$$\frac{\partial(Y^2)}{\partial X} - 2\frac{Y^2}{W_A} r_m \frac{\partial W_r}{\partial z} - \frac{Y^2}{\cos^2\lambda}\frac{\partial s^*}{\partial X} + 2Y\frac{\tan\beta}{X}\frac{\partial(XY\tan\beta)}{\partial X}$$

$$+ 4\frac{U_m Y\tan\beta}{W_{A_m}} - \frac{2}{W_{A_m}^2}\frac{\partial H_E}{\partial X} + 2\frac{U_m U}{W_{A_m}^2} + \left[\frac{2H_E}{W_{A_m}^2} - Y^2\tan^2\beta\right]\frac{\partial s^*}{\partial X} = 0 \qquad (121)$$

The fourth term in Eq. 121 can be expanded and rearranged as

$$2Y\frac{\tan\beta}{X}\left[\frac{\partial}{\partial X}(XY\tan\beta)\right] = 2Y\frac{\tan\beta}{X}\left[XY\frac{\partial\tan\beta}{\partial X} + X\tan\beta\frac{\partial Y}{\partial Y} + Y\tan\beta\right]$$

$$= 2Y^2\tan\beta\frac{\partial\tan\beta}{\partial X} + 2Y\tan^2\beta\frac{\partial Y}{\partial X} + \frac{2Y^2}{X}\tan^2\beta \qquad (122)$$

with

$$\frac{\partial\tan\beta}{\partial X} = \frac{1}{\cos^2\beta}\frac{\partial\beta}{\partial X}$$

and

$$2Y\tan^2\beta\frac{\partial Y}{\partial X} = \tan^2\beta\frac{\partial(Y^2)}{\partial X}$$

Equation 122 then is

$$\frac{\partial(Y^2)}{\partial X}\left(1+\mathrm{TAN}^2\beta\right)-2\frac{Y^2}{W_A}r_m\frac{\partial W_r}{\partial z}-\frac{Y^2}{\cos^2\lambda}\frac{\partial s^*}{\partial X}+2Y^2\frac{\mathrm{TAN}\beta}{\cos^2\beta}\frac{\partial\beta}{\partial X}+\frac{2Y^2}{X}\mathrm{TAN}^2\beta$$

$$+\frac{4U_mY\,\mathrm{TAN}\beta}{W_{A_m}}-\frac{2}{W_{A_m}^2}\frac{\partial H_E}{\partial X}+2\frac{U_mU}{W_{A_m}^2}+\left[\frac{2H_E}{W_{A_m}^2}-Y^2\mathrm{TAN}^2\beta\right]\frac{\partial s^*}{\partial X}=0 \qquad \text{(122a)}$$

Multiplying by $\left(-\cos^2\beta/Y^2\right)$, and with $1+\mathrm{TAN}^2\beta=\frac{1}{\cos^2\beta}$,

$$\frac{1}{Y^2}\frac{\partial(Y^2)}{\partial X}+\cos^2\beta\left(-\frac{2r_m}{W_A}\frac{\partial W_r}{\partial z}-\frac{1}{\cos^2\lambda}\frac{\partial s^*}{\partial X}\right)+2\,\mathrm{TAN}\beta\frac{\partial\beta}{\partial X}+\frac{2}{X}\mathrm{SIN}^2\beta$$

$$+\frac{4U_m\,\mathrm{SIN}\beta\cos\beta}{W_{A_m}Y}+\frac{2U_mU\cos^2\beta}{W_{A_m}^2Y^2}-\frac{2\cos^2\beta}{W_{A_m}^2Y^2}\frac{\partial H_E}{\partial X}+\left[\frac{2H_E\cos^2\beta}{W_{A_m}^2Y^2}-\mathrm{SIN}^2\beta\right]\frac{\partial s^*}{\partial X}=0 \qquad \text{(123)}$$

The terms $\cos^2\lambda$ and $\left(\frac{-2r_m}{W_A}\frac{\partial W_r}{\partial z}\right)$ represent the effects due to streamline curvature and can be approximated by

$$-\frac{1}{W_A}\frac{\partial W_r}{\partial z}=\pm K\frac{\delta r}{L^2}\quad ;\quad K\cong 5 \qquad \text{(124)}$$

$$\cos^2\lambda=\frac{L^2}{L^2+\left(\frac{\Delta R}{2}\right)^2} \qquad \text{(125)}$$

If the streamline curvature in meridional planes is zero, the terms represented by Eqs. 124 and 125 will take on values of zero and one, respectively. With δr positive as shown in Fig. 2, the plus sign is used for K at station 2 and the minus sign at station 1. The streamline slope as represented by Eq. 125 is the same at stations 1 and 2 since the streamline pattern is assumed to repeat itself after station 2.

Using Eqs. 124 and 125, Eq. 114 then becomes

$$\frac{d(\ln Y^2)}{dX}=-\cos^2\beta\left[\left(2Kr_m\frac{\delta r}{L^2}\right)-\left(\frac{L^2+\left(\frac{\Delta R}{2}\right)^2}{L^2}\right)\frac{ds^*}{dX}\right]-2\,\mathrm{TAN}\beta\frac{d\beta}{dX}-\frac{2}{X}\mathrm{SIN}^2\beta$$

$$-\frac{4U_m\,\mathrm{SIN}\beta\cos\beta}{W_{A_m}Y}-\frac{2U_mU\cos^2\beta}{W_{A_m}^2Y^2}+\frac{2\cos^2\beta}{W_{A_m}^2Y^2}\frac{dH_E}{dX}-\left[\frac{2H_E\cos^2\beta}{W_{A_m}^2Y^2}-\mathrm{SIN}^2\beta\right]\frac{ds^*}{dX} \qquad \text{(126)}$$

For the enthalpy terms to be in terms of BTU/lb_m, they must be divided by 2gJ to keep the equation dimensionless. With $C_1 = 2gJ$, Eq. 126 is

$$\frac{d(\ln Y^2)}{dX} = -\cos^2\beta\left[\left(2Kr_m\frac{\delta r}{L^2}\right)-\left(\frac{L^2+\left(\frac{\Delta R}{2}\right)^2}{L^2}\right)\frac{ds^*}{dX}\right]-2\tan\beta\frac{d\beta}{dX}-\frac{2}{X}\sin^2\beta$$

$$-\frac{4U_m\sin\beta\cos\beta}{W_{A_m}Y}-\frac{2U_mU\cos^2\beta}{W_{A_m}^2Y^2}+\frac{C_1\cos^2\beta}{W_{A_m}^2Y^2}\frac{dH_E}{dX}-\left[\frac{C_1H_E\cos^2\beta}{W_{A_m}^2Y^2}-\sin^2\beta\right]\frac{ds^*}{dX} \quad (127)$$

Noting the corresponding terms for the absolute flow of the stator, and with U=0, the equation for station 1 is

$$\frac{d(\ln Y^2)}{dX} = -\cos^2\alpha\left[\left(-K2r_m\frac{\delta r}{L^2}\right)-\left(\frac{L^2+\left(\frac{\Delta R}{2}\right)^2}{L^2}\right)\frac{ds^*}{dX}\right]-2\tan\alpha\frac{d\alpha}{dX}$$

$$-\frac{2}{X}\sin^2\alpha+\frac{C_1\cos^2\alpha}{Y^2V_{A_m}^2}\frac{dH}{dX}-\left[\frac{C_1H\cos^2\alpha}{Y^2V_{A_m}^2}-\sin^2\alpha\right]\frac{ds^*}{dX} \quad (128)$$

2. Flow Function Φ

Flowrate in lb_m/sec for the expansion process shown in Fig. 44 can be written

$$\dot{W} = \rho A V \quad (129)$$

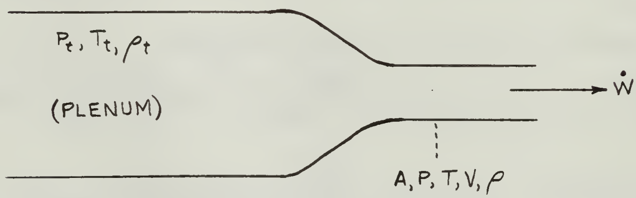

Expansion From Plenum

Fig. 44

Assuming an isentropic expansion,

$$\frac{T}{T_t} = \left(\frac{P}{P_t}\right)^{\frac{\gamma-1}{\gamma}} \tag{130}$$

and,

$$T_t - T = T_t\left(1 - \frac{T}{T_t}\right) = T_t\left[1 - \left(\frac{P}{P_t}\right)^{\frac{\gamma-1}{\gamma}}\right] \tag{131}$$

then using the thermodynamic relations

$$\frac{V^2}{2gJc_p} = T_t - T \qquad \text{and} \qquad c_p = \frac{R}{J}\,\frac{\gamma}{\gamma-1} \tag{132}$$

the discharge velocity can be expressed by

$$V = \left\{2gR\frac{\gamma}{\gamma-1}\,T_t\left[1 - \left(\frac{P}{P_t}\right)^{\frac{\gamma-1}{\gamma}}\right]\right\}^{\frac{1}{2}} \tag{133}$$

The density ρ is found with the isentropic assumption by

$$\frac{P_t}{\rho_t^{\gamma}} = \frac{P}{\rho^{\gamma}} \tag{134}$$

or

$$\rho = \left(\frac{P}{P_t}\right)^{\frac{1}{\gamma}}\rho_t = \left(\frac{P}{P_t}\right)^{\frac{1}{\gamma}}\frac{P_t}{RT_t} \tag{135}$$

Using Eqs. 133 and 135, Eq. 129 becomes

$$\dot{W} = A\frac{P_t}{RT_t}\left(\frac{P}{P_t}\right)^{\frac{1}{\gamma}}\left\{2gR\frac{\gamma}{\gamma-1}\,T_t\left[1 - \left(\frac{P}{P_t}\right)^{\frac{\gamma-1}{\gamma}}\right]\right\}^{\frac{1}{2}} \tag{136}$$

This can be rearranged to give

$$\dot{W} = \frac{AP_t}{\sqrt{\frac{R}{g}T_t}}\left\{\frac{2\gamma}{\gamma-1}\left[\left(\frac{P}{P_t}\right)^{\frac{2}{\gamma}} - \left(\frac{P}{P_t}\right)^{\frac{\gamma+1}{\gamma}}\right]\right\}^{\frac{1}{2}} \tag{137}$$

or

$$\frac{\dot{W}\sqrt{T_t}}{A\,P_t}\sqrt{\frac{R}{g}} = \left\{\frac{2\gamma}{\gamma-1}\left[\left(\frac{P}{P_t}\right)^{\frac{2}{\gamma}} - \left(\frac{P}{P_t}\right)^{\frac{\gamma+1}{\gamma}}\right]\right\}^{\frac{1}{2}} \equiv \Phi \tag{138}$$

3. Restriction Factor ξ [12]

The expansion process through a blade row is shown in Fig. 45 (a). The letter u represents the velocity at some point within the boundary layer and V_{th} represents the velocity for an isentropic expansion. The various dimensions, angles, and velocities for the throat location are shown in Fig. 45(b).

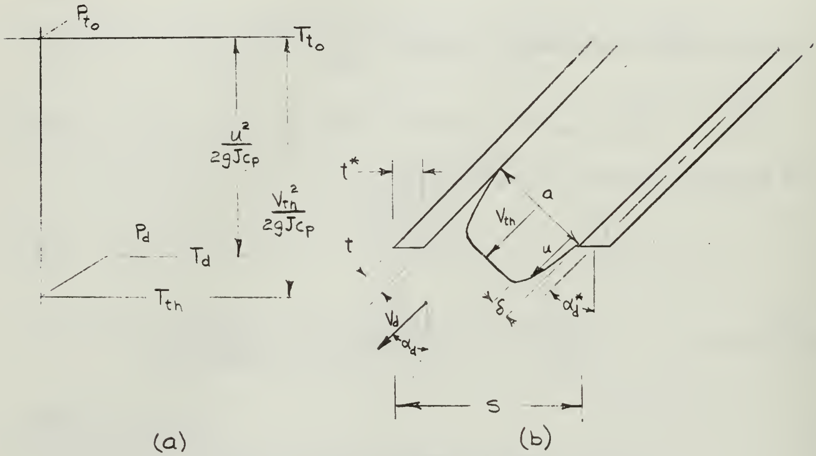

Conditions at Exit of Blade Row

Fig. 45

The mass flowrate per unit blade height can be written

$$\dot{m} = \rho_{th} V_{th} \cos\alpha_d \left[s - \frac{t}{\cos\alpha_d^*} - \frac{\Sigma\delta}{\cos\alpha_d} \right] + \Sigma \int_0^\delta u\rho \, dy \tag{139}$$

where:

ρ_{th} = density at P_d for isentropic expansion (slugs/ft^3)

ρ = density corresponding to the velocity u (slugs/ft^3)

α_d^* = blade angle

δ = boundary layer thickness

[12] Vavra, M. H., Problems of Fluid Mechanics in Radial Turbomachines (Rhode-Saint-Genese, Belgium: Von Kármán Institute for Fluid Dynamics, 1965) VKI Course Note 55b, pp. G46-50.

For Mach numbers of 0.8 or less, the discharge angle can be calculated quite accurately by

$$\alpha_d = \cos^{-1}\left[\frac{a}{s - \frac{t}{\cos\alpha_d^*}}\right] \tag{140}$$

where:

a = minimum throat width

t = blade thickness

then with $\eta = \frac{Y}{\delta}$ and using Eq. 140 in Eq. 139,

$$\dot{m} = \rho_{th} V_{th} \frac{a\cos\alpha_d^*}{s\cos\alpha_d^* - t}\left[\frac{s\cos\alpha_d^* - t}{\cos\alpha_d^*} - \Sigma\delta\left(\frac{s\cos\alpha_d^* - t}{a\cos\alpha_d^*}\right)\right] + \Sigma\rho_{th} V_{th}\delta\int_0^1 \frac{\rho}{\rho_{th}}\frac{u}{V_{th}}\,d\eta \tag{141}$$

which can be expressed as

$$\dot{m} = \rho_{th} V_{th}\, a\left\{1 - \Sigma\frac{\delta}{a}\left(1 - \int_0^1 \frac{\rho}{\rho_{th}}\frac{u}{V_{th}}\,d\eta\right)\right\} \tag{142}$$

Assuming constant pressure at the throat,

$$\rho = \frac{P_d}{RT}$$

and

$$\frac{\rho}{\rho_{th}} = \frac{T_{th}}{T} \tag{143}$$

where

$$\frac{T_{th}}{T} = \frac{T_{to} - \frac{V_{th}^2}{2gJc_p}}{T_{to} - \frac{u^2}{2gJc_p}} = \frac{T_{to} - \frac{V_{th}^2}{2gJc_p}}{T_{to} - \left(\frac{V_{th}^2}{2gJc_p}\right)\left(\frac{u}{V_{th}}\right)^2} = \frac{1 - X_e}{1 - X_e\left(\frac{u}{V_{th}}\right)^2} \tag{144}$$

In Eq. 144 the term X_e is

$$X_e = 1 - \frac{T_{th}}{T_{to}} = 1 - \left(\frac{P_d}{P_{to}}\right)^{\frac{\gamma-1}{\gamma}} \tag{145}$$

The boundary layer is assumed to be turbulent and the profile can therefore be expressed by

$$\frac{u}{V_{th}} = \left(\frac{Y}{\delta}\right)^m = \eta^m \tag{146}$$

Then with the displacement thickness of the boundary layer defined as

$$\delta^* \equiv \delta \left[1 - (1 - X_e) \int_0^1 \frac{\eta^m}{1 - X_e \eta^{2m}} d\eta \right] \tag{147}$$

Eq. 142 can be written

$$\dot{m} = \rho_{th} V_{th} a \left[1 - \frac{\Sigma \delta^*}{a} \right] \tag{148}$$

The loss coefficient to the throat is

$$\psi = 1 - \frac{V_d^2}{V_{th}^2} \tag{149}$$

The loss coefficient can also be expressed in terms of the kinetic energy lost, by

$$\psi = \frac{\Delta \dot{E}}{\dot{m} \frac{V_{th}^2}{2}} = 1 - \frac{\dot{E}}{\dot{m} \frac{V_{th}^2}{2}} \tag{150}$$

where $\dot{E}$ represents energy rate at the discharge due to the average velocity V_d, or

$$\dot{E} = \rho_{th} V_{th} \left[a - \Sigma \delta \right] \frac{V_{th}^2}{2} + \Sigma \int_0^\delta \left(u \rho \frac{u^2}{2} \right) dy \tag{151}$$

Equation 151 can be rewritten to give

$$\dot{E} = \rho_{th} \frac{V_{th}^3}{2} a \left\{ 1 - \Sigma \frac{\delta}{a} \left[1 - (1 - X_e) \int_0^1 \frac{\eta^{3m}}{(1 - X_e \eta^{2m})} d\eta \right] \right\} \tag{152}$$

Then using the energy thickness which is defined as

$$\delta^{***} \equiv \delta \left[1 - (1 - X_e) \int_0^1 \frac{\eta^{3m}}{(1 - X_e \eta^{2m})} d\eta \right] \tag{153}$$

the loss coefficient can be expressed by

$$\psi = 1 - \frac{\rho_{th} \frac{V_{th}^3}{2} a \left[1 - \Sigma \frac{\delta^{***}}{a} \right]}{\dot{m} \frac{V_{th}^2}{2}} = 1 - \frac{\rho_{th} \frac{V_{th}^3}{2} a \left[1 - \Sigma \frac{\delta^{***}}{a} \right]}{\rho \frac{V_{th}^3}{2} a \left[1 - \Sigma \frac{\delta^*}{a} \right]}$$

or

$$\psi = 1 - \frac{1 - \Sigma \frac{\delta^{***}}{a}}{1 - \Sigma \frac{\delta^*}{a}} \tag{154}$$

The restriction factor ξ represents that part of the throat opening in which would occur the uniform theoretical velocity, therefore

$$\xi = 1 - \Sigma \frac{\delta^*}{a} \tag{155}$$

Now defining an energy parameter H^{***} by

$$H^{***} \equiv \frac{\delta^{***}}{\delta^*} \tag{156}$$

Eq. 155 becomes

$$\xi = \frac{H^{***} - 1}{H^{***} - 1 + \psi} \tag{157}$$

The loss coefficient ψ in Eq. 157 accounts for the losses that occur from the inlet to the throat of the blade channel. No means exists for predicting this loss coefficient. Half the total loss coefficient for the blade row $\frac{\psi_t}{2}$ will be used to represent these losses. Eq. 157 then becomes

$$\xi = \frac{H^{***} - 1}{H^{***} - 1 + \frac{\psi_t}{2}} \tag{158}$$

4. Method of Evaluating H^{***}[13]

By use of the binomial theorem, the denominator of the integral part of Eqs. 147 and 153 can be expanded, yielding

$$\left(1 - X_e \eta^{2m}\right)^{-1} = 1 + X_e \eta^{2m} + X_e^2 \eta^{4m} + X_e^3 \eta^{6m} + X_e^4 \eta^{8m} + \cdots$$

The integral of Eq. 153 is then

$$\int_0^1 \left[\eta^{3m} + X_e \eta^{5m} + X_e^2 \eta^{7m} + X_e^3 \eta^{9m} + X_e^4 \eta^{11m} + \cdots\cdots\right] d\eta$$

Then, integrating and evaluating gives

$$\int_0^1 \frac{\eta^{3m}}{1 - X_e \eta^{2m}} d\eta = \frac{1}{3m+1} + \frac{X_e}{5m+1} + \frac{X_e^2}{7m+1} + \frac{X_e^3}{9m+1} + \frac{X_e^4}{11m+1} + \cdots$$

Equation 153 can now be expressed as

$$\frac{\delta^{***}}{\delta} = 1 - \left(\frac{1}{3m+1} + \frac{X_e}{5m+1} + \frac{X_e^2}{7m+1} + \frac{X_e^3}{9m+1} + \frac{X_e^4}{11m+1} + \cdots\right) + \frac{X_e}{3m+1} + \frac{X_e^2}{5m+1} + \frac{X_e^3}{7m+1} + \cdots$$

---

[13] Eckert, *op. cit.*, pp. 159-160.

or,

$$\frac{\delta^{***}}{\delta} = 1 + (X_e - 1)\left(\frac{1}{3m+1} + \frac{X_e}{5m+1} + \frac{X_e^2}{7m+1} + \frac{X_e^3}{9m+1} + \frac{X_e^4}{11m+1} + \cdots\right)$$

also,

$$\frac{\delta^{***}}{\delta} = (X_e - 1)\left(\frac{1}{X_e - 1} + \frac{1}{3m+1} + \frac{X_e}{5m+1} + \frac{X_e^2}{7m+1} + \frac{X_e^3}{9m+1} + \frac{X_e^4}{11m+1} + \cdots\right)$$

In a similar manner, the expression for Eq. 147 is

$$\frac{\delta^{*}}{\delta} = (X_e - 1)\left(\frac{1}{X_e - 1} + \frac{1}{m+1} + \frac{X_e}{3m+1} + \frac{X_e^2}{5m+1} + \frac{X_e^3}{7m+1} + \frac{X_e^4}{9m+1} + \cdots\right)$$

The energy parameter can now be expressed by

$$H^{***} = \frac{\dfrac{1}{X_e - 1} + \dfrac{1}{3m+1} + \dfrac{X_e}{5m+1} + \dfrac{X_e^2}{7m+1} + \dfrac{X_e^3}{9m+1} + \dfrac{X_e^4}{11m+1}}{\dfrac{1}{X_e - 1} + \dfrac{1}{m+1} + \dfrac{X_e}{3m+1} + \dfrac{X_e^2}{5m+1} + \dfrac{X_e^3}{7m+1} + \dfrac{X_e^4}{9m+1}} \tag{159}$$

The number of terms in the numerator and denominator of Eq. 159 is considered sufficient to give good convergence for H^{***}.

Although the exponent m for the turbulent boundary layer is dependent on Reynolds number, it is taken to be a constant for this analysis.

APPENDIX B

COMPUTATION OF OUTLET ANGLES AND LOSS COEFFICIENTS

1. Outlet Angles

The absolute discharge angles for the stator and the relative discharge angles for the rotor are computed by using the same methods. For these calculations, the assumption is made that the outlet angles are not influenced by the flow incidence angles. The factors which do affect the discharge angles are:

1. Blade geometry; this results in the angles being a function of the radius since spacing and possibly profiles change from hub to tip.

2. Radial tip clearance; the effects of tip clearance are assumed to influence the rotor flow from the mean streamline out to the tip, with the largest effect being near the tip.

3. Exit Mach number; in accordance with the experimental results surveyed by Ainley, the outlet angles are a function of Mach number. Values of the angles are calculated for Mach numbers M of 0.5 and 1.0. Then a smooth curve of outlet angle versus M is drawn between these points with an inflection point at M=0.75. Below M=0.5, the flow angles are assumed to be equal to the value computed for M=0.5.

Vavra's formula is used for the first approximation of the stator outlet angles for $M_1 \leq 0.5$.

$$\alpha^* = \cos^{-1}\left(\frac{a/s}{K_t}\right) \tag{160}$$

where

$$K_t = 1 - \frac{2.7}{10^3}\left(\frac{t}{s}100\right)^{3.3}\frac{a}{s} \tag{161}$$

The effects of blade curvature are next taken into account by using the method given by Ainley.[14]

$$\alpha = \alpha^* + 4\left(\frac{s}{e}\right) \tag{162}$$

---

[14] Ainley, op. cit., pp. 3-4.

In Eq. 162, "e" is the mean radius of curvature of the upper surface of the blade profile between the passage throat and the trailing edge. This quantity is approximated by

$$e = \frac{j^2}{8b} \qquad (163)$$

where j and b are shown in Fig. 46.

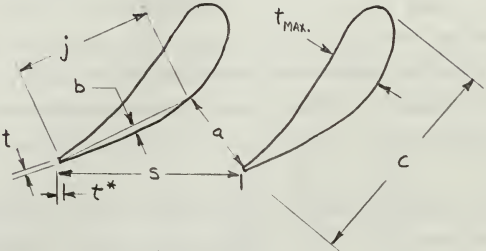

Blade Geometry

Fig. 46

The discharge angle for M=1.0 is found in a manner similar to that described by Ainley,

$$\alpha_{(M_1=1.0)} = \cos^{-1}\left(\frac{a}{s - t^*}\right) \qquad (164)$$

The change in α due to the increase in local Mach number from 0.5 to 1.0 is assumed to be constant along the blade height and equal to that computed for the mean radius.

$$\delta\alpha_T = \delta\alpha_H = \alpha_{m\,(M_1=0.5)} - \alpha_{m\,(M_1=1.0)} \qquad (165)$$

Relative discharge angles for the hub and mean radii of the rotor are found by the same method as used for the stator. The effects of tip clearance are accounted for in the computation of β_2 for the tip position. With Ainley's formula, the flow angle β_2 for the tip is

$$\beta_2 = \mathrm{TAN}^{-1}\left\{\left[1 - X\left(\frac{k}{h}\right)\left(\frac{\cos\beta_0}{\cos\beta_2'}\right)\right]\mathrm{TAN}\,\beta_2' + X\left(\frac{k}{h}\right)\left(\frac{\cos\beta_0}{\cos\beta_2'}\right)\mathrm{TAN}\,\beta_0\right\} \qquad (166)$$

The new terms in Eq. 166 are:

h - blade height

β_2' - discharge angle before tip clearance is accounted for

X - factor which depends on the type of shroud

Ainley suggests that X be set equal to 1.35 if no shroud is arranged at the rotor tips. However, Ainley's value has been determined with a mean streamline analysis. To localize the effects of tip clearance, X has been changed to 5.4, a value which gives about the same overall tip clearance effect as if the value of X=1.35 were used for the mean streamline. Fig. 47 shows that the areas under the two lines representing X as a function of radius are approximately equal. The slope of the solid line representing X for this method is obtained because of the assumed linear variation of outlet angle with radius between the mean radius and the tip.

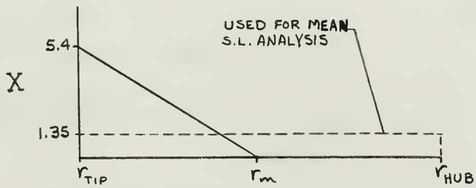

Tip Clearance Factor X as
Function of Radius

Fig. 47

Sample calculations for stator outlet angles are shown in Table I. A sample of rotor outlet angle computations can be seen in Table II.

TABLE I

SAMPLE CALCULATIONS FOR STATOR OUTLET ANGLES

MOD I turbine

$M_1 \leq 0.5$

radius - in.	3.597	4.125	4.950
spacing (s) - in.	1.738	1.994	2.392
throat opening (a) - in.	0.455	0.590	0.804
trailing edge thickness (t) - in.	--------	0.044	-------
$\frac{a}{s}$	0.2619	0.2960	0.3360
$\left(\frac{t}{s}100\right)^{3.3} = A$	21.4	13.6	7.48
$K_t = 1-(0.0027)\ (A)\ (\frac{a}{s})$	0.9849	0.9891	0.9932
$\frac{a}{sK_t}$	0.2658	0.2991	0.3384
$\alpha^* = \cos^{-1}(\frac{a}{sK_t})$	74.6°	72.6°	70.2°
$4\ (\frac{s}{e})$	0.703	0.9106	1.37
$\alpha = \alpha^* + 4(\frac{s}{e})$	75.3°	73.5°	71.6°

$M_1 = 1.0$

Use 4.125 in. from centerline as representative radius.

Projected trailing edge thickness (t*)-in. 0.13

$\alpha_{1m} = \cos^{-1}(\frac{a}{s-t^*})$ - deg. 71.5°

$\delta\alpha = 73.5 - 71.5 = 2.0$

α	73.3°	71.5°	69.6°

TABLE II

SAMPLE CALCULATIONS FOR ROTOR OUTLET ANGLES

MOD II turbine   tip clearance = 0.033 in.

$M \leq 0.5$

radius - in.	3.3235	4.197	4.918
spacing (s) - in.	1.595	1.4643	1.7158
throat opening (a) - in.	0.382	0.560	0.721
trailing edge thickness (t) - in.	-------	0.048	-------
$\frac{a}{s}$	0.3295	0.3824	0.4202
$\left(\frac{t}{s}\right)(100)$	4.1397	3.278	2.7975
$\left(\frac{t}{s}100\right)^{3.3} = A$	109.0	50.3	29.8
$K_t = 1-(0.0027)(A)\left(\frac{a}{s}\right)$	0.9030	0.9481	0.9662
$\frac{a}{s K_t}$	0.3649	0.4033	0.4349
$\beta^* = \cos^{-1}\left(\frac{a}{s K_t}\right)$	-68.5°	-66.2°	-64.2°
$4\left(\frac{s}{e}\right)$	1.75	2.37	3.04
$\beta = \beta^* - 4\left(\frac{s}{e}\right)$	$\underline{-70.3^\circ}$	$\underline{-68.6^\circ}$	-67.2°
k - in.			0.033
k/h			0.0207
X=(4) (1.35)=type shroud factor			5.4
$\cos\beta_o$, $\beta_o = 30^\circ$			0.86603
$\cos\beta_2'$, $\beta_2' = -67.2^\circ$			0.38268
$(X)\left(\frac{k}{h}\right)\frac{\cos\beta_o}{\cos\beta_2'} = B$			0.25297
$\tan\beta_2'$			-2.4142
$(1-B)\tan\beta_2'$			-1.8035
$\tan\beta_o$			0.57735
$(1-B)\tan\beta_2' + B\,\tan\beta_o = C$			-1.6574
$\beta_2 = \tan^{-1}(C)$			$\underline{-58.9^\circ}$

TABLE II (continued)

SAMPLE CALCULATIONS FOR ROTOR ANGLE

$M_2 = 1.0$

Use radius = 4.197 in. as representative radius.

Projected trailing edge thickness (t*)-in.	0.108
$\beta_{2m} = \cos^{-1}\left(\frac{a}{s-t^*}\right)$	-65.6°
$\delta\beta = -68.6 + 65.6 = -3.0$	

radius - in.	3.3235	4.197	4.918
β_2	-67.3°	-65.6°	-62.6°

2. Loss Coefficients

Loss coefficients were predicted using Ainley's methods. The techniques used are completely described in Refs. 1 and 2. The assumptions, definitions, and equations which are necessary for a basic understanding of the method are described below.

It is assumed that loss coefficients are independent of Mach number and, for a given glade geometry, are a function of the flow incidence on the blade. Losses are divided into profile losses, secondary losses, and losses due to tip clearance. Mixing losses are not accounted for separately but are included in profile and secondary losses.

A parameter Y is defined by

$$Y = \frac{\text{Loss in total pressure}}{\text{Total pressure at outlet - outlet static pressure}} \tag{167}$$

For incompressible flow, which is assumed for these calculations, the loss coefficient is

$$y = \frac{\Sigma Y_j}{1 + \Sigma Y_j} \tag{168}$$

The subscript j on Y in Eq. 168 indicates the type loss represented; i.e., Y_p would be the profile loss.

For zero incidence, the Y for profile losses is

$$Y_{P(i=0)} = \left\{ Y_{P(\beta_o=0)} + \left(\frac{\beta_o}{\beta_d'}\right)^2 \left[Y_{P(\beta_o=-\beta_d')} - Y_{P(\beta_o=0)} \right] \right\} \left(\frac{t_m/c}{0.2}\right)^{-\beta_o/\beta_d'} \tag{169}$$

where:

β_d' - blade discharge angle not accounting for tip clearance

t_m - maximum blade thickness

c - blade chord

Equation 169 is applicable to both the stator and rotor. However, for stator use the blade inlet angle β_o is zero. The quantities $Y_{P(\beta_o=-\beta_d')}$ and $Y_{P(\beta_o=0)}$ are taken from Fig. 4 in Ref. 2 where these quantities are plotted as a function of blade solidity. The maximum value of $t_{m/c}$ is set equal to 0.25 for thick blades.

To determine profile losses for incidences other than zero, Fig. 6 in Ref. 2 shows $\frac{Y_P}{Y_{P(i=0)}}$ versus $\frac{i}{i_s}$ where i_s is defined as that incidence where the losses are twice the minimum losses.

Secondary and tip clearance losses are computed by

$$Y_S + Y_K = \left[\lambda + B\,\frac{k}{h}\right]\left[\frac{C_L}{s/c}\right]^2 \frac{\cos^2\beta_d'}{\cos^3\beta_m} \tag{170}$$

where:

β_m - the mean of the gas inlet and exit angles of the blade row

B - factor representing type shroud, similar to X

$$\frac{C_L}{s/c} = 2\left(\mathrm{TAN}\,\beta_o - \mathrm{TAN}\,\beta_d'\right)\cos\beta_m = f(i)$$
$$\lambda = f\left[\left(A_d/A_i\right)^2 / \left(1 + \frac{\mathrm{I.D.}}{\mathrm{O.D.}}\right)\right] \tag{171}$$

in Eq. 171:

A_d = (annulus area at discharge) ($\cos\beta_d'$)

A_i = (annulus area at inlet) ($\cos\beta_o$)

I.D. and O.D. - inner and outer diameters, respectively, at the blade exit

Values of λ are obtained from Fig. 8 in Ref. 2. Ainley suggests a value of 0.5 for B for the type shroud used. With the same reasoning as previously used for the effect of tip clearance on discharge angles, B is set equal to 2.0 for the losses at the tip and zero for the mean radius and hub locations.

Sample calculations for the prediction of stator loss coefficients are shown in Table III. Sample calculations for prediction of stalling incidence and rotor loss coefficients are shown in Table IV.

TABLE III

SAMPLE CALCULATIONS FOR STATOR LOSS COEFFICIENT

MOD I turbine — inlet angle (α_0) = 0

radius = 3.597 in. — outlet angle (α_1) = 75.3°

pitch (s) = 1.738 in. — chord (c) = 2.691 in.

All figures referred to are in Ref. 2.

$$Y_{P(i=0)} = \left\{ Y_{P(\alpha_1=0)} + \left(\frac{\alpha_0}{\alpha_1}\right)^2 \left[Y_{P(\alpha_0=-\alpha_1)} - Y_{P(\alpha_0=0)} \right] \right\} \left(\frac{t/c}{0.2}\right)^{-\alpha_0/\alpha_1}$$

$$\alpha_0 = 0 \qquad \frac{\text{PITCH}}{\text{CHORD}} = \frac{1.738}{2.691} = 0.6459$$

$$Y_{P(i=0)} = 0.047$$

$$Y_S = \left[\lambda + B\frac{k}{h}\right]\left[C_L/s/c\right]^2\left[\frac{\cos^2\alpha_1}{\cos^3\alpha_m}\right] \qquad k=0$$

$$\lambda = f\left[\left(A_2/A_1\right)^2 \Big/ \left(1+\frac{I.D.}{O.D.}\right)\right] = f\left\{\left(\cos 75.3^\circ\right)^2 \Big/ \left(1+\frac{6.6}{9.898}\right)\right\} \qquad I.D. = 6.6 \text{ in.} \quad O.D. = 9.898 \text{ in.}$$

$$\lambda = f(0.0386) \qquad \lambda = 0.0056 \qquad (\text{Fig. } 8)$$

$$\alpha_m = \tan^{-1}\left(\frac{\tan 75.3^\circ}{2}\right) = \tan^{-1}(1.906) = 62.3^\circ$$

$$\frac{C_L}{s/c} = 2\left[\tan\alpha_0 - \tan\alpha_1\right]\cos\alpha_m = 2\left[-\left(\tan -75.3^\circ\right)\right]\cos 62.3^\circ$$

$$\frac{C_L}{s/c} = 3.5438$$

$$Y_S = [0.0056][3.5438]^2\left[\frac{\cos^2 75.3^\circ}{\cos^3 62.3^\circ}\right] = 0.0451$$

$$Y_S + Y_P = 0.0929$$

CORRECTION FACTOR FOR TRAILING EDGE THICKNESS , F = 1.03 (Fig. 9)

$$(1.03)(0.0929) = 0.0949$$

$$y = \frac{0.0949}{1+0.0949} = \underline{0.0866}$$

TABLE IV

SAMPLE CALCULATIONS FOR STALLING INCIDENCE AND ROTOR LOSS COEFFICIENTS

MOD II turbine	s = 1.7158 in.	$\beta_o = 30^o$
radius = 4.918	k = 0.033 in.	$\beta_2' = -67.2^o$
t_{max} = 0.728 in.	c = 1.967 in.	blade height(h) = 1.595 in.

Figures referred to are in Ref. 2.

$$Y_{P(i=0)} = \left\{ Y_{P(\beta_o=0)} + \left(\frac{\beta_o}{\beta_2'}\right)^2 \left[Y_{P(\beta_o=-\beta_2')} - Y_{P(\beta_o=0)} \right] \right\} \left(\frac{t/c}{0.2} \right)^{-\beta_o/\beta_2'}$$

$$\frac{t}{c} = \frac{0.728}{1.967} \text{ (USE 0.25)}, \quad -\frac{\beta_o}{\beta_2'} = 0.446, \quad \left(\frac{\beta_o}{\beta_2'}\right)^2 = 0.1993$$

$$\frac{s}{c} = \frac{1.7158}{1.967} = 0.8723, \quad Y_{P(\beta_o=0)} = 0.0365, \quad Y_{P(\beta_o=-\beta_2')} = 0.154 \quad \text{(Fig. 4)}$$

$$Y_{P(i=0)} = \{0.0365 + (0.1993)(0.154 - 0.0365)\}(1.25)^{0.446} = 0.0662$$

$$\frac{\beta_2'}{\beta_{2\left(\frac{s}{c}=0.75\right)}} = 0.955 \text{ (Fig. 7)}, \quad \beta_{2\left(\frac{s}{c}=0.75\right)} = -70.4^\circ, \quad \frac{\beta_o}{\beta_{2\left(\frac{s}{c}=0.75\right)}} = 0.426$$

$$i_{s\left(\frac{s}{c}=0.75\right)} = 32.5^\circ, \quad \Delta i_s = -7^\circ \text{ (Fig. 7)}, \quad i_s = 32.5^\circ - 7^\circ = \underline{\underline{25.5^\circ}}$$

$$Y_s + Y_K = \left[\lambda + B\left(\frac{k}{h}\right)\right]\left[C_L/s/c\right]^2 \left[\frac{\cos^2\beta_2'}{\cos^3\beta_m}\right] \qquad B = 2.0 \qquad B\frac{k}{h} = 0.01881$$

$$\cos\beta_2' = 0.38752 \qquad \cos^2\beta_2' = 0.15017$$

$$\lambda = f\left[\left(A_2/A_1\right)^2 \Big/ \left(1 + \frac{\text{I.D.}}{\text{O.D.}}\right)\right]$$

I.D. OUTLET = 3.3235 in. O.D. OUTLET = 4.918 in.

I.D. INLET = 3.3245 in. O.D. INLET = 4.8505 in.

$$\beta_{2m}' = 70.3^\circ$$

$$\frac{A_2}{A_1} = \frac{\pi(4.918^2 - 3.3235^2)}{\pi(4.8505^2 - 3.3245^2)} \; \frac{\cos 70.3^\circ}{\cos 30^\circ}$$

$$\lambda = f(0.148), \qquad \lambda = 0.0072 \qquad \text{(Fig. 8)}$$

$$Y_s + Y_K = \left[0.0072 + 0.01881\right]\left[C_L/s/c\right]^2 \left[\frac{0.15017}{\cos^3\beta_m}\right]$$

$$Y_s + Y_K = (0.003906)\left[C_L/s/c\right]^2 \frac{1}{\cos^3\beta_m}$$

TABLE IV (continued)

SAMPLE CALCULATIONS FOR ROTOR LOSS COEFFICIENT

i/i_s	-1.5	0.0	1.5
$i = (i/i_s)\, i_s$	-38.25	0	38.25
$\beta_1 = i + \beta_0$	-8.25	30	68.25
$\tan\beta_1$	-0.1450	0.5774	2.5065
$\frac{\tan\beta_1 + \tan\beta_2'}{2} = A$	-1.2619	-0.9008	0.0638
$\beta_m = \tan^{-1}(A)$	-51.6	-42.0	3.6
$\cos\beta_m$	0.6212	0.7430	0.9980
$\tan\beta_1 - \tan\beta_2' = B$	2.2339	2.9563	4.8854
$C_L/s/c = 2(B)\cos\beta_m$	2.7752	4.3928	9.7510
$\left[C_L/s/c\right]^2$	7.7016	19.2964	95.0813
$1/\cos^3\beta_m$	4.1726	2.4385	1.0061
$Y_s + Y_K = (0.003906)\left[\frac{C_L}{s/c}\right]^2 \frac{1}{\cos^3\beta_m}$	0.2345	0.3434	0.6980
$Y_P/Y_{P(i=0)}$ (Fig. 6)	2.1	1.0	4.5
$Y_P = \left[Y_P/Y_{P(i=0)}\right] Y_{P(i=0)}$	0.1390	0.0662	0.2979
$Y_P + Y_s + Y_K$	0.3735	0.4096	0.9959
(CORRECTION FACTOR)$(\Sigma Y) = C$ (Fig. 9)	0.3922	0.4301	1.0457
$\omega = \frac{C}{1+C}$	0.2817	0.3007	0.5112

APPENDIX C

COMPUTER PROGRAM

A computer program using Fortran IV was written for use with the performance analysis. The program was used to predict performance values for the MOD I and MOD II turbines. However, an attempt was made to keep the program general. If the methods of this thesis are utilized for expressing turbine characteristics, this program can be used for other single stage axial turbines.

Input for the program consists of information representing the turbine characteristics, an indicator specifying the detail of output desired, and the conditions for which performance values are to be obtained.

Twenty input cards are used to introduce the turbine characteristics. The information contained on each of these cards, with required dimensions, is listed below.

1. Stator mean streamline gas outlet angles (ALFAM-radians) for mean streamline exit Mach numbers of 0.5, 0.7, 0.75, 0.8 and 1.0.

2. Relative rotor mean streamline gas outlet angles (BETAM-radians) for the same Mach numbers listed in (1.).

3. Radii ahead of the stator (RC-in.) for the five streamlines, such that the flow area is divided into four equal parts.

4. Assumed radii of the five streamlines at the stator exit (RS-in.).

5. Same as (4.), only for the rotor exit plane (RR-in.).

6. The predicted stator loss coefficients (ZETAS) for the hub, mean radius, and tip.

7. Ten values of incidence ratio (RINC) ranging from -2.0 to 1.6, in increments of 0.4.

8. Ten values of rotor loss coefficients (ZETAR1) for the hub corresponding to the incidence ratios of (7.).

9. Same as (8.), only for the mean radius (ZETAR3).

10. Same as (8.), only for the tip (ZETAR5).

11. Length L shown in Fig. 2 (CL-in.) and the curvature factor K (CK).

12. Differences in stator gas outlet angles (DALF-radians) from the angle for the mean streamline, for streamlines 1, 3, and 5.

13. Same as (12.), only for the relative rotor outlet angles (DBET).

14. Ten radii for the stator exit plane, equally spaced or approximately equally spaced, ranging from the radius of the hub to the radius of the tip (R1-in.).

15. Ten values of stator throat opening (A1-in.) corresponding to the radii of (14.).

16. Same as (14.), only for the rotor exit plane (R2-in.).

17. Ten values of rotor throat opening (A2-in.) corresponding to the radii of (16.).

18. Inlet blade angles for the rotor (BETO-degrees) for the hub, mean radius, and tip.

19. Ten stall incidence angles (STALI-degrees) corresponding to the radii in (14.).

20. The radial tip clearance of the rotor (TIPC-in.), the number of stator blades (ZS), and the number of rotor blades (ZR).

Input card number 21 specifies the output to be printed, and its use will be described later. The remaining input specifies the conditions for which performance values are to be found,and enters the estimations of the flow Mach numbers used for the first approximations in the iteration process. Input card number 22 specifies the number of sets (NSETS) of operating conditions for which solutions are to be found. A card containing the following information is used for each point specified by NSETS:

a. Estimated Mach number of the flow ahead of the stator (AMC).

b. Estimated Mach number of the mean streamline flow after the stator (AMS).

c. Total inlet pressure (PTO-psi.).

d. Total inlet temperature (TTO-^{o}R).

e. Estimated relative Mach number of the mean streamline flow at the rotor exit (AMR).

f. The rotor speed (RPM).

g. The ratio of total inlet to static discharge pressure (PR).

There are eight subroutines in addition to the main or executive part of the program. The subroutines and their main functions are listed below:

1. Subroutine PARAB is used to determine the coefficients of the parabolic equations used to approximate curves.

2. Subroutine LSQPOL determines by the method of least squares the coefficients of the fourth order polynomials used to approximate curves.

3. Subroutine CHAN computes the flowrate and the reference flowrate from conditions ahead of the stator.

4. Subroutine STATOR determines the axial velocity ratios that satisfy the equation of motion at station 1.

5. Subroutine FLOWREF computes the reference flowrate at the stator exit and the rotor exit, and adjusts the axial velocity of the mean streamline flow at these locations to satisfy overall continuity.

6. Subroutine SLINE checks streamline continuity for the stator exit and the rotor exit, and determines new streamline radii to satisfy streamline continuity.

7. Subroutine ROTOR1 converts the absolute flow properties ahead of the rotor to relative flow properties.

8. Subroutine ROTOR2 determines the axial velocity ratios at station 2 that satisfy the equation of motion.

The main program computes the mass-flow-weighted value of total inlet to static discharge pressure ratio, and adjusts the Mach number of the flow ahead of the stator to obtain the pressure ratio specified. The overall turbine performance values of η, M_R, H.P., r^*, and k_{is} are also computed in the main program.

Computer output representing the solution for each set of conditions is printed on two pages. The flow properties at the stator exit plane are printed on one page. A sample of this output can

be seen in Table V. The second page contains the flow properties for the rotor as well as the overall turbine performance values. A sample of the second page of output is in Table VI. Most of the output quantities are self-explanatory. However, the following symbols may not be readily recognized and are defined as:

SLINE - streamline

ZETAP - one-half the total loss coefficient, used for calculating ξ

A - throat opening of the blade channel

W-FRAC - fraction of the flowrate $\dot{w}$ between the hub and the indicated streamline

BO - rotor blade inlet angle

INCID - rotor flow incidence angle

PSIR - relative flow velocity coefficient $\frac{W_2}{W_{2th}}$

In addition to the main output there are additional WRITE statements in the program. The additional output allows the user to follow more closely the intermediate steps of the solution process. This output is also helpful when program changes are made which require debugging. The extra output is not desirable for production runs because of the large amounts of computer running time and printout that result. When the additional output is wanted, 1 is read into the computer on input card number 21 for the indicator IND. If 0 is read into the computer for IND, only the main output representing the final solution will be printed.

The statements of the program are listed on the following pages.

```
0001        REAL*8 RINC,ZETAR1,Y3,B3,T10,C10,A10,R1,A1,Y1,B1,R2,A2,Y2,B2,
           1ZETAR3,Y4,B4,ZETAR5,Y5,B5,STALI,Y6,B6
0002        0DIMENSION ALFAM(10),BETAM(10),RS(10),RR(10),ZETAR(10),ZETAPR(10),
           1DALF(10),DBET(10),AS(10),AR(10),X1(10),X2(10),ALFA1(10),BETA2(10),
           2T1(10),P1(10),V1(10),VA1(10),SI1(10),SI2(10),YS(10),SL(10),
           3DSDX1(10),VU1(10),PRAT1(10),ZETAPS(10),WI1(10),VA2(10),WPER1(10),
           4U(10),BETA1(10),HE(10),TTE(10),PTE(10),W1(10),WU1(10),DHEDX(10),
           5DSDX2(10),WU2(10),W2(10),VU2(10),V2(10),YR(10),RI1(10),RI2(10),
           6RI3(10),RI4(10),RI(10),SR1(10),SR2(10),YOLD(10),AA(10),SR(10),
           7P2(10),T2(10),PRAT2(10),WPER2(10),DWDX(10),U2(10),T1IS(10),
           8 T2IS(10),PRAT3(10),SS(10),ALFA2(10)
0003        0DIMENSION DELH(10),TT2(10),PT2(10),PT1(10),T2S(10),
           1ETAI(10),ETAS(10),PSIR(10),RSTAR(10),AKIS(10),ETAR(10),
           2ALFA(10),BETA(10),AMS1(10),RC(10),DELR(10),WPERO(10),ZETAS(10),
           3ZETAR1(20),ZETAR3(20),ZETAR5(20),BETAO(10),STALI(10)
0004        DIMENSION R1(20),A1(20),WGT(20),Y1(20),DELY1(20),B1(20),SB(20),
           1T10(20),ST1(20),C10(20),CT1(20),A10(30,30),R2(20),A2(20),Y2(20),
           2DELY2(20),B2(20),Y3(20),DELY3(20),B3(20),Y4(20),DELY4(20),B4(20),
           3Y5(20),DELY5(20),B5(20),Y6(20),DELY6(20),B6(20),RINC(20),DR(10)
           4,BETO(10),STALII(10),RINCI(10),AMR2(10),ALFA22(10),BETA22(10),
           5ALFA11(10),BETA11(10),ZETA1(10),AREA1(10),AREA2(10)
0005        COMMON IND
0006        G=32.174
0007        CJ=778.16
0008        CP=0.24
0009        GAM=1.4
0010        EXP1=GAM/(GAM-1.)
0011        EXP2=1./EXP1
0012        READ (5,1) (ALFAM(I),I=1,5)
0013      1 FORMAT(5F8.4)
0014        READ (5,1) (BETAM(I),I=1,5)
0015        READ (5,1) (RC(I),I=1,5)
0016        READ (5,1) (RS(I),I=1,5)
0017        READ (5,1) (RR(I),I=1,5)
0018        READ (5,2) (ZETAS(I),I=1,5,2)
0019    783 FORMAT (2F8.4)
0020        READ(5,784)(RINC(I),I=1,10)
0021      3 FORMAT(5D8.4)
0022        READ(5,3)(ZETAR1(I),I=1,5)
0023        READ(5,3)(ZETAR1(I),I=6,10)
0024        READ(5,3)(ZETAR3(I),I=1,5)
0025        READ(5,3)(ZETAR3(I),I=6,10)
0026        READ(5,3)(ZETAR5(I),I=1,5)
0027        READ(5,3)(ZETAR5(I),I=6,10)
0028        READ (5,783) CL,CK
0029        READ (5,2) (DALF(I),I=1,5,2)
0030      2 FORMAT(3F8.4)
0031        READ (5,2) (DBET(I),I=1,5,2)
```

```
0032          READ(5,784)(F1(I),I=1,10)
0033          READ(5,3)(A1(I),I=1,5)
0034          READ(5,3)(A1(I),I=6,10)
0035          READ(5,784)(R2(I),I=1,10)
0036          READ(5,3)(A2(I),I=1,5)
0037          READ(5,3)(A2(I),I=6,10)
0038      784 FORMAT(10D5.2)
0039          READ (5,2) (BETAO(I),I=1,5,2)
0040          READ(5,784)(STALI(I),I=1,10)
0041          READ(5,2)TIPC,ZS,ZR
0042          READ (5,4) IND
0043          CALL PARAB (ALFAM,1,2,3,AA1,BA1,CA1,0.5,0.7,0.75)
0044          CALL PARAB(ALFAM,3,4,5,AA2,BA2,CA2,0.75,0.8,1.0)
0045          CALL PARAB (BETAM,1,2,3,AB1,BB1,CB1,0.5,0.7,0.75)
0046          CALL PARAB (BETAM,3,4,5,AB2,BB2,CB2,0.75,0.8,1.0)
0047          DO 10 I=1,5
0048          X1(I)=RS(I)/RS(3)
0049       10 X2(I)=RR(I)/RR(3)
0050          RROLD2=RR(2)
0051          RROLD3=RR(3)
0052          RROLD4=RR(4)
0053          RSOLD2=RS(2)
0054          RSOLD3=RS(3)
0055          RSOLD4=RS(4)
0056          RS1=RS(1)
0057          RS3=RS(3)
0058          RS5=RS(5)
0059          RR1=RR(1)
0060          RR3=RR(3)
0061          RR5=RR(5)
0062          CALL LSQPOL(10,4,0,0,0,SIGMA,R1,A1,WGT,Y1,DELY1,B1,SB,T10,ST1,
             1C10,CT1,A10)
0063          CALL LSQPOL(10,4,0,0,0,SIGMA,R2,A2,WGT,Y2,DELY2,B2,SB,T10,ST1,
             1C10,CT1,A10)
0064          ASF=B1(1)+B1(2)*RS(3)+B1(3)*RS(3)**2+B1(4)*RS(3)**3+B1(5)*RS(3)**4
0065          ARF=B2(1)+B2(2)*RR(3)+B2(3)*RR(3)**2+B2(4)*RR(3)**3+B2(5)*RR(3)**4
0066          RSF=RS(3)
0067          ASFO=ASF
0068          RSFO=RSF
0069          RRF=RR(3)
0070          RRFO=RRF
0071          ARFO=ARF
0072          XS1=X1(1)
0073          XS3=X1(3)
0074          XS5=X1(5)
0075          XR1=X2(1)
0076          XR3=X2(3)
0077          XR5=X2(5)
```

```
      CALL PARAB(BETA0,1,3,5,BR1,BR2,BR3,XS1,XS3,XS5)
      CALL LSQPOL(10,4,0,0,0,SIGMA,RINC,ZETAR1,WGT,Y3,DELY3,B3,SB,T10,
     1ST1,C10,CT1,A10)
      CALL LSQPOL(10,4,0,0,0,SIGMA,RINC,ZETAR3,WGT,Y4,DELY4,B4,SB,T10,
     1ST1,C10,CT1,A10)
      CALL LSQPOL(10,4,0,0,0,SIGMA,RINC,ZETAR5,WGT,Y5,DELY5,B5,SB,T10,
     1ST1,C10,CT1,A10)
      CALL LSQPOL(10,4,0,0,0,SIGMA,R1,STALI,WGT,Y6,DELY6,B6,SB,T10,ST1,
     1C10,CT1,A10)
      READ (5,4) NSETS
    4 FORMAT(I5)
      DO 400 J=1,NSETS
      READ (5,5) AMC,AMS,PTO,TTO,AMR,RPM,PR
    5 FORMAT (7F8.4)
      N9=0
  750 N5=0
      N9=N9+1
      IF(N9-10)290,290,223
  290 IF(AMS-0.75) 30,40,50
   30 ALFA1(3)=AA1+BA1*AMS+CA1*AMS**2
      GO TO 60
   40 ALFA1(3)=ALFAM(3)
      GO TO 60
   50 IF (AMS-1.) 280,270,270
  270 ALFA1(3)=ALFAM(5)
      GO TO 60
  280 ALFA1(3)=AA2+BA2*AMS+CA2*AMS**2
   60 IF(AMR-0.75) 70,80,90
   70 BETA2(3)=AB1+BB1*AMR+CB1*AMR**2
      GO TO 100
   80 BETA2(3)=BETAM(3)
      GO TO 100
   90 BETA2(3)=AB2+BB2*AMR+CB2*AMR**2
  100 RS(2)=RSOLD2
      RS(3)=RSOLD3
      RS(4)=RSOLD4
      DO 530 I=1,5
  530 X1(I)=RS(I)/RS(3)
      ASF=ASFO
      RSF=RSFO
      FS1=1.0
      FS2=1.0
      VA1(3)=185.0
      YS(1)=1.08
      YS(2)=1.035
      YS(3)=1.
      YS(4)=.973
      YS(5)=.95
```

```
      CALL CHAN (TTO,AMC,PTO,RC,WLBM,WCHAN,WPERO)
      NS=0
  810 DO 801 K=1,15
      CALL STATOR(ALFA1,X1,TTO,PTO,AMS,T1,P1,V1,VA1,SI1,SI2,YS,S1,
     1DSDX1,VU1,PRAT1,T1IS,SS,DALF,AA1,BA1,CA1,AA2,BA2,CA2,ALFAM,RSF,
     2DELR,CL,CK,ZETAPS,RS,RS1,RS3,RS5,ZETAS,DR,ZETA1,NS)
      DO 120 I=1,5
      PTE(I)=PTO
  120 TTE(I)=TTO
      CALL FLOWR(PRAT1,ZETAPS,X1,WI1,PTE,PTO,TTE,TTO,ASF,ZS,RSF,ASF,
     1ZR,RSF,1,WCHAN,VA1,WPER1,CODE,WLBM,B1,RS,TIPC,AREA1)
      IF (CODE-20.)801,802,801
  801 CONTINUE
  802 CALL SLINE (RS,X1,DWDX,WPER1,WPERO,HE,U2,DHEDX,S1,DSDX1,ASF,PSF,
     1FS1,FS2,CODE,1,B1)
      IF (CODE-40.)810,300,810
  300 VA2(3)=185.
      YR(1)=1.0
      YR(2)=1.0
      YR(3)=1.0
      YR(4)=1.0
      YR(5)=1.0
      FC1=1.
      FC2=FC1**2
      ARF=ARFO
      RRF=RROLD3
      RR(2)=RROLD2
      RR(3)=RRF
      RR(4)=RROLD4
      DO 71 I=1,5
      AMS1(I)=V1(I)/(49.01*SQRT(T1(I)))
      X2(I)=RR(I)/RR(3)
   71 CONTINUE
     0CALL ROTOR1(VU1,VA1,RPM,U,BETA1,HF,TTE,PTE,X2,P1,T1,W1,WU1,X1,
     1RS,ZETAR,ZETAPR,RR,DHEDX,DSDX1,S1,U2,OMEG,BR1,BR2,BR3,FS1,FS2,
     2B3,B4,B5,B6,RS1,RS3,RS5,BETO,STALII,RINCI)
      CODE=1.
  201 DO 200 K=1,14
      CALL ROTOR2 (BETA2,HF,DHEDX,DSDX1,DSDX2,VA2,WJ2,W2,VU2,V2,X2,U2,
     1YR,ZETAR,RI1,RI2,RI3,RI4,RI,SR1,SR2,AA,SR,TTE,PTE,T2,P2,PRAT2,
     2T2S,INDS,DBET,BETAM,AB1,BB1,CB1,AB2,BB2,CB2,RRF,DELR,CL,CK,DR,RR,
     3RR1,RR3,RR5,NS)
      IF (INDS-1) 310,320,310
  320 WRITE (6,36) (AA(I),I=1,5)
   36 FORMAT (/35H ENTROPY INDETERMINATE,PRINT AA 1-5, 5F8.3)
      GO TO 400
  310 CALL FLOWR(PRAT2,ZETAPR,X2,WI1,PTE,PTO,TTE,TTO,ASF,ZS,RSF,ARF,ZR,
     1RRF,2,WCHAN,VA2,WPER2,CODE,WLBM,B2,RR,TIPC,AREA2)
```

```
      IF (CODE-20.) 20C,13C,200
  200 CONTINUE
  130 CALL SLINE (RR,X2,DWDX,WPER2,WPERO,HE,U2,DHEDX,S1,DSDX1,
     1ARF,RRF,FC1,FC2,CODE,2,B2)
      IF (CODE-40.) 201,220,201
  220 DO 221 I=1,5
      DELR(I)=RS(I)-(RC(I)+RR(I))/2.
  221 DR(I)=RC(I)-RR(I)
      NS=1
  880 DO 881 K=1,15
      CALL STATOR(ALFA1,X1,TTO,PTO,AMS,T1,P1,V1,VA1,SI1,SI2,YS,S1,
     1DSDX1,VU1,PRAT1,T1IS,SS,DALF,AA1,BA1,CA1,AA2,BA2,CA2,ALFAM,RSF,
     2DELR,CL,CK,ZETAPS,RS,RS1,RS3,RS5,ZETAS,DR,ZETA1,NS)
      DO 860 I=1,5
      PTE(I)=PTO
  860 TTE(I)=TTO
      CALL FLOWR(PRAT1,ZETAPS,X1,WI1,PTE,PTO,TTE,TTO,ASF,ZS,RSF,ASF,
     1ZR,RSF,1,WCHAN,VA1,WPER1,CODE,WLBM,B1,RS,TIPC,AREA1)
      IF (CODE-20.)881,822,881
  881 CONTINUE
  822 CALL SLINE (RS,X1,DWDX,WPER1,WPERO,HE,U2,DHEDX,S1,DSDX1,ASF,RSF,
     1FS1,FS2,CODE,1,B1)
      IF (CODE-40.) 880,861,880
  861 CALL ROTOR1(VU1,VA1,RPM,U,BETA1,HE,TTE,PTE,X2,P1,T1,W1,WU1,X1,
     1RS,ZETAR,ZETAPR,RR,DHEDX,DSDX1,S1,U2,OMEG,BR1,BR2,BR3,FS1,FS2,
     2B3,B4,B5,B6,RS1,RS3,RS5,BETO,STALII,RINCI)
      CODE=1.
  894 DO 896 K=1,10
      CALL ROTOR2 (BETA2,HE,DHEDX,DSDX1,DSDX2,VA2,WJ2,W2,VU2,V2,X2,U2,
     1YR,ZETAR,RI1,RI2,RI3,RI4,RI,SR1,SR2,AA,SR,TTF,PTE,T2,P2,PRAT2,
     2T2S,INDS,DBET,BETAM,AB1,BB1,CB1,AB2,BB2,CB2,RRF,DELR,CL,CK,DR,RR,
     3RR1,RR3,RR5,NS)
      IF(INDS-1)895,32C,895
  895 CALL FLOWR(PRAT2,ZETAPR,X2,WI1,PTE,PTO,TTE,TTO,ASF,ZS,RSF,ARF,ZR,
     1RRF,2,WCHAN,VA2,WPER2,CODE,WLBM,B2,RR,TIPC,AREA2)
      IF(CODE-20.)896,897,896
  896 CONTINUE
  897 CALL SLINE (RR,X2,DWDX,WPER2,WPERO,HE,U2,DHEDX,S1,DSDX1,
     1ARF,RRF,FC1,FC2,CODE,2,B2)
      IF (CODE-40.)894,226,894
  226 DO 227 I=1,5
  227 PRAT3(I)=PTO/P2(I)
      PRAT5=(PRAT3(1)+2.*(PRAT3(2)+PRAT3(3)+PRAT3(4))+PRAT3(5))/8.
      DIFF=ABS(PR-PRAT5)
      IF(.0003-DIFF)91C,920,920
  910 N11=0
      GO TO 710
  920 N11=1
```

```
      GO TO 223
  710 IF(PR-PRAT5)712,712,714
  712 AMC=AMC-DIFF/18.
      IF(IND-1)750,223,223
  714 AMC=AMC+DIFF/18.
      IF(IND-1)750,223,223
  223 WRITE (6,999)
  999 FORMAT (1H1)
      WRITE (6,9)
    9 FORMAT (43H                                    STATOR SOLUTION)
      WRITE (6,7)
    7 FORMAT(/52H                        SET NO.   PTO      TTO      RPM  ,   PR)
      WRITE (6,8) J,PTO,TTO,RPM,PR
    8 FORMAT (16X,I5,F9.2,F8.2,F9.0,F6.2)
      WRITE (6,11)
   11 FORMAT (/47H SLINE    R1       X1     ZETAS   ZETAPS     Y      A)
      DO 500 I=1,5
  500 WRITE(6,12)I,RS(I),X1(I),ZETA1(I),ZETAPS(I),YS(I),AREA1(I)
   12 FORMAT(I4,2F8.3,3F8.5,F8.4)
      WRITE (6,13)
  130FORMAT (/60H SLINE    T1       P1     ALFA1    BETA1     U1     W-FRAC
     1PTO/P1)
      DO 510 I=1,5
      AMS1(I)=V1(I)/(49.01*SQRT(T1(I)))
      PRAT1(I)=1./PRAT1(I)
      RINCI(I)=RINCI(I)*57.3
      ALFA11(I)=ALFA1(I)*57.3
      BETA11(I)=BETA1(I)*57.3
  510 WRITE(6,14)I,T1(I),P1(I),ALFA11(I),BETA11(I),U(I),WPER1(I),PRAT1(
     1I)
   14 FORMAT(I4,F9.2,F7.2,2F8.2,F8.2,2F8.4)
      WRITE (6,15)
   15 FORMAT(/51H SLINE  VA1      VU1      V1       WU1      W1       M1)
      DO 520 I=1,5
  520 WRITE (6,16) I,VA1(I),VU1(I),V1(I),WU1(I),W1(I),AMS1(I)
   16 FORMAT(I4,5F8.1,F8.3)
      WRITE (6,999)
      WRITE (6,17)
   17 FORMAT (43H                                    ROTOR SOLUTION)
      WRITE (6,7)
      WRITE (6,8) J,PTO,TTO,RPM,PR
      WRITE (6,18)
  180FORMAT (/68H SLINE    R2       X2     TTE       PTE    ZETAR    ZETAPR
     1  Y        VA2 )
      DO 170 I=1,5
      AMR2(I)=W2(I)/(49.01*SQRT(T2(I)))
   19 FORMAT(I4,2F8.3,2F8.2,2F8.5,F8.4,F8.1)
  170 WRITE (6,19) I,RR(I),X2(I),TTE(I),PTE(I),ZETAR(I),ZETAPR(I),
```

```
      1YR(I),VA2(I)
      WRITE (6,23)
   23 FORMAT (/66H SLINE    T2        P2    PTO/P2    ALFA2    BETA2     U2
     1W-FRAC      A)
      DO 190 I=1,5
      ALFA2(I)=ATAN(VU2(I)/VA2(I))
      V2(I)=VA2(I)/COS(ALFA2(I))
      ALFA22(I)=ALFA2(I)*57.3
      BETA22(I)=BETA2(I)*57.3
   24 FORMAT(I4,F9.2,F7.2,3F8.3,F8.2,F8.5,F8.4)
  190 WRITE(6,24)I,T2(I),P2(I),PRAT3(I),ALFA22(I),BETA22(I),U2(I),
     1WPER2(I),AREA2(I)
      WRITE (6,25)
   25 FORMAT (/68H SLINE    M2      VU2      V2       WU2      W2        BO
     1STALI     INCID)
      DO 210 I=1,5
   26 FORMAT(I4,F8.3,4F8.1,3F8.2)
  210 WRITE(6,26)I,AMR2(I),VU2(I),V2(I),WU2(I),W2(I),BETO(I),STALII(I),
     1RINCI(I)
      DO 230 I=1,5
      DELH(I)=(U(I)*VU1(I)-U2(I)*VU2(I))/(G*CJ)
      TT2(I)=TTO-DELH(I)/CP
      PT2(I)=P2(I)*(TT2(I)/T2(I))**EXP1
      PT1(I)=P1(I)*(TTO/T1(I))**EXP1
      T2IS(I)=TTO*(P2(I)/PTO)**EXP2
      T2S(I)=TTE(I)*(P2(I)/PTE(I))**EXP2
      ETAI(I)=(TTO-TT2(I))/(TTO-T2IS(I))
      ETAS(I)=(TTO-T1(I))/(TTO-T1IS(I))
      ETAR(I)=(TTE(I)-T2(I))/(TTE(I)-T2S(I))
      RSTAR(I)=(T1IS(I)-T2IS(I))/(TTO-T2IS(I))
      AKIS(I)=2.*G*CJ*CP*(TTO-T2IS(I))/U(I)**2
  230 PSIR(I)=SQRT(ETAR(I))
      DELH(10)=0.
      DO 240 I=1,4
      L=I+1
  240 DELH(10)=DELH(10)+.5*(WPER2(L)-WPER2(I))*(DELH(L)+DELH(I))
      HP=DELH(10)*CJ*WLBM/550.
      AMOM=HP*550./OMEG
      THETA=SQRT(TTO/518.4)
      DELTA=PTO/14.7
      HP1=HP/(THETA*DELTA)
      AMOM1=AMOM/DELTA
      RPM1=RPM/THETA
      WLBM1=WLBM*THETA/DELTA
      WRITE (6,27)
   27 FORMAT (/51H SLINE  DELH     PT1      TT2      PT2      T2IS      T2S)
      DO 250 I=1,5
   28 FORMAT(I4,6F8.2)
```

```
  250 WRITE (6,28) I,DELH(I),PT1(I),TT2(I),PT2(I),T2IS(I),T2S(I)
      WRITE (6,29)
   29 FORMAT (/59H SLINE    ETAI    ETAS     ETAR     PSIR    RSTAR     AKIS
     1 DELR)
      DO 260 I=1,5
   31 FORMAT (I4,F9.4,F7.4,2F8.4,F8.5,F8.3,F8.5)
  260 WRITE (6,31) I,ETAI(I),ETAS(I),ETAR(I),PSIR(I),RSTAR(I),AKIS(I),
     1DELR(I)
      WRITE (6,32)
   32 FORMAT (/71H  HORSE    MOMENT    FLORATE  REF HORSE  REF MOMENT
     1      REF FLORATE)
      WRITE (6,34)
  340FORMAT ( 69H  POWER    FT-LB    LBM/SEC     POWER       FT-LB      REF
     1 RPM     LBM/SEC)
      WRITE (6,33) HP,AMOM,WLBM,HP1,AMOM1,RPM1,WLBM1
   33 FORMAT (F7.1,F9.2,F9.3,F10.1,F12.3,F11.1,F10.3)
      ETA5=(ETAI(1)+ETAI(5)+2.*(ETAI(2)+ETAI(3)+ETAI(4)))/8.
      AKIS5=(AKIS(1)+AKIS(5)+2.*(AKIS(2)+AKIS(3)+AKIS(4)))/8.
      RSTAR5=(RSTAR(1)+RSTAR(5)+2.*(RSTAR(2)+RSTAR(3)+RSTAR(4)))/8.
      WRITE (6,95)
   95 FORMAT(/59H                    ETA       PTO/P2  M-STATION O     AKIS      R
     1STAR)
      WRITE(6,96)ETA5,PRAT5,AMC,AKIS5,RSTAR5
   96 FORMAT(11X,F6.4,F11.4,F11.5,F10.3,F10.5)
      IF(IND-1)400,930,930
  930 IF(N11-1)750,400,400
  400 CONTINUE
      END
```

```
      SUBROUTINE PARAB (V,I,J,K,A,B,C,VAR1,VAR2,VAR3)
      DIMENSION V(10)
      COMMON IND
      VAR12=VAR1**2
      VAR22=VAR2**2
      VAR32=VAR3**2
      D=VAR2*VAR32-VAR3*VAR22+VAR1*(VAR22-VAR32)+VAR12*(VAR3-VAR2)
     0DA=V(I)*(VAR2*VAR32-VAR3*VAR22)+VAR1*(VAR22*V(K)-VAR32*V(J))
     1 + VAR12*(V(J)*VAR3-V(K)*VAR2)
      DB=V(J)*VAR32-V(K)*VAR22+V(I)*(VAR22-VAR32)+VAR12*(V(K)-V(J))
      DC= VAR2*V(K)-VAR3*V(J)+VAR1*(V(J)-V(K))+V(I)*(VAR3-VAR2)
      A=DA/D
      B=DB/D
      C=DC/D
      RETURN
      END
```

```
      SUBROUTINE LSQPOL(M,KM,IW,ISW,LP,SIGMA,X,F2,W,Y,DELY,B,SB,T,ST,C,  LSQ
     1SC,A)                                                               LSQ
      REAL*8 X,F2,Y,B,T,C,A,F,P,BM,D,FBAR,XBAR,PXF,PXP,XPXP,XPXPM,XP,     LSQ
     1ALPHA,BETA,PPXF,PPXPP,PT,VARA,POLYF1                                LSQ
      DIMENSION S(30),X(1),F2(1),ST(1),SB(1),F(100),PM(100),P(100),B(1),LSQ
     1DELY(1),W(1),A(30,30),T(1),Y(1),BM(11,11),D(11,11),C(1),SC(1)       LSQ
      COMMON IND
      DO 7 I=1,11                                                         LSQ
      DO 4 J=1,11                                                         LSQ
      D(I,J)=0.0D0                                                        LSQ
    4 CONTINUE                                                            LSQ
    7 CONTINUE                                                            LSQ
      LL=0                                                                LSQ
    9 FM=0.0                                                              LSQ
      SUMEV2=0.0                                                          LSQ
      A(1,1)=1.0                                                          LSQ
      A(2,2)=1.0                                                          LSQ
      FBAR=0.0                                                            LSQ
      XBAR=0.0                                                            LSQ
      DO10I=1,M                                                           LSQ
      IF(IW)1009,1010,1009                                                LSQ
 1010 W2=1.0                                                              LSQ
      W(I)=1.0                                                            LSQ
      GOTO1011                                                            LSQ
 1009 W2=SQRT(W(I))                                                       LSQ
 1011 FM=FM+W(I)                                                          LSQ
      F(I)=W2*F2(I)                                                       LSQ
      PM(I) = W2                                                          LSQ
      FBAR=FBAR+F(I)*PM(I)                                                LSQ
   10 XBAR=XBAR+X(I)*PM(I)**2                                             LSQ
      XBAR=XBAR/FM                                                        LSQ
      T(1)=FBAR/FM                                                        LSQ
      A(2,1)=-XBAR                                                        LSQ
      PXF=0.0                                                             LSQ
      PXP=0.0                                                             LSQ
      DO20I=1,M                                                           LSQ
      P(I)=(X(I)-XBAR)*PM(I)                                              LSQ
      PXF=PXF+P(I)*F(I)                                                   LSQ
   20 PXP=PXP+P(I)*P(I)                                                   LSQ
      T(2)=PXF/PXP                                                        LSQ
      PMXPM=FM                                                            LSQ
      S(1)=PMXPM                                                          LSQ
      KM=KM+1                                                             LSQ
      B(1)=T(1)*A(1,1)+T(2)*A(2,1)                                        LSQ
      B(2)=T(2)*A(2,2)                                                    LSQ
   60 DO190K=2,KM                                                         LSQ
      IF(K-2)40,165,65                                                    LSQ
   40 WRITE(6,4000)                                                       LSQ
```

```
 4000 FORMAT(7HSTOP 40)                                                  LSQ
      STOP                                                               LSQ
   65 XPXP=0.0                                                           LSQ
      XPXPM=0.0                                                          LSQ
      B(K)=0.0                                                           LSQ
      DO70J=1,M                                                          LSQ
      XP=X(J)*P(J)                                                       LSQ
      XPXP=XPXP+XP*P(J)                                                  LSQ
   70 XPXPM=XPXPM+XP*PM(J)                                               LSQ
      ALPHA=XPXP/PXP                                                     LSQ
      BETA=XPXPM/PMXPM                                                   LSQ
      PPXF=0.0                                                           LSQ
      PPXPP=0.0                                                          LSQ
      DO90I=1,M                                                          LSQ
   80 PT=P(I)                                                            LSQ
   81 P(I)=X(I)*PT-ALPHA*PT-BETA*PM(I)                                   LSQ
   82 PPXF=PPXF+P(I)*F(I)                                                LSQ
   83 PPXPP=PPXPP+P(I)*P(I)                                              LSQ
   90 PM(I)=PT                                                           LSQ
      T(K)=PPXF/PPXPP                                                    LSQ
      PMXPM=PXP                                                          LSQ
      PXP=PPXPP                                                          LSQ
      A(K,1)=-ALPHA*A(K-1,1)-BETA*A(K-2,1)                               LSQ
      A(K,K-1)=A(K-1,K-2)-A(K-1,K-1)*ALPHA                               LSQ
      A(K,K)=1.0                                                         LSQ
      IF(K-3)150,150,110                                                 LSQ
  110 K1=K-2                                                             LSQ
      DO120I=2,K1                                                        LSQ
  120 A(K,I)=A(K-1,I-1)-ALPHA*A(K-1,I)-BETA*A(K-2,I)                     LSQ
  150 DO160I=1,K                                                         LSQ
  160 B(I)=B(I)+T(K)*A(K,I)                                              LSQ
  165 SIG3=0.0                                                           LSQ
      DO180I=1,M                                                         LSQ
      Y(I)=POLYE1(X(I),K,B)                                              LSQ
  175 DELY(I)=Y(I)-F2(I)                                                 LSQ
  180 SIG3 = SIG3 + (DELY(I)**2)*W(I)                                    LSQ
      SIG3=SIG3/FM                                                       LSQ
      SIG2=SIG3*FLOAT(M)/FLOAT(M-K)                                      LSQ
      IF(K-2)40,1650,1651                                                LSQ
 1650 FLEV = 0.                                                          LSQ
      GO TO 1652                                                         LSQ
 1651 FLEV=(SUMEV2-SIG3)/SIG2                                            LSQ
 1652 SUMEV2=SIG3                                                        LSQ
      SIGMA=SQRT (SIG2)                                                  LSQ
      S(K) = PXP                                                         LSQ
      DO499I=1,K                                                         LSQ
  499 ST(I)=SIGMA/SQRT(S(I))                                             LSQ
      DO501I=1,K                                                         LSQ
```

```
      SB(I)=0.0                                                          LSQ
      DO500J=I,K                                                         LSQ
  500 SB(I)=SB(I)+(A(J,I)*ST(J))**2                                      LSQ
  501 SB(I)=SQRT(SB(I))                                                  LSQ
      IF(LP)658,183,658                                                  LSQ
  658 IF(K-2)652,651,652                                                 LSQ
  651 D(1,1)=1.0D0                                                       LSQ
      D(2,2)=1.0D0                                                       LSQ
      D(2,1)=0.0D0                                                       LSQ
      D(3,3)=1.5D0                                                       LSQ
      D(3,2)=0.0D0                                                       LSQ
      D(3,1)=-0.5D0                                                      LSQ
      D(4,4)=3.5D0                                                       LSQ
      D(4,3)=0.0D0                                                       LSQ
      D(4,2)=-1.5D0                                                      LSQ
      D(4,1)=0.0D0                                                       LSQ
      D(5,5)=35.0D0/8.0D0                                                LSQ
      D(5,4)=0.0D0                                                       LSQ
      D(5,3)=-30.0D0/8.0D0                                               LSQ
      D(5,2)=0.0D0                                                       LSQ
      D(5,1)=3.0D0/8.0D0                                                 LSQ
      D(6,6)=63.0D0/8.0D0                                                LSQ
      D(6,5)=0.0D0                                                       LSQ
      D(6,4)=-70.0D0/8.0D0                                               LSQ
      D(6,2)=15.0D0/8.0D0                                                LSQ
      D(7,7)=231.0D0/16.0D0                                              LSQ
      D(7,5)=-315.0D0/16.0D0                                             LSQ
      D(7,3)=105.0D0/16.0D0                                              LSQ
      D(7,1)=-5.0D0/16.0D0                                               LSQ
      D(8,8)=429.0D0/16.0D0                                              LSQ
      D(8,6)=-693.0D0/16.0D0                                             LSQ
      D(8,4)=315.0D0/16.0D0                                              LSQ
      D(8,2)=-35.0D0/16.0D0                                              LSQ
      D(9,9)=6435.0D0/128.0D0                                            LSQ
      D(9,7)=-12012.0D0/128.0D0                                          LSQ
      D(9,5)=6930.0D0/128.0D0                                            LSQ
      D(9,3)=-1260.0D0/128.0D0                                           LSQ
      D(9,1)=35.0D0/128.0D0                                              LSQ
      D(10,10)=12155.0D0/128.0D0                                         LSQ
      D(10,8)=-25740.0D0/128.0D0                                         LSQ
      D(10,6)=18018.0D0/128.0D0                                          LSQ
      D(10,4)=-4620.0D0/128.0D0                                          LSQ
      D(10,2)=315.0D0/128.0D0                                            LSQ
      D(11,11)=46189.0D0/256.0D0                                         LSQ
      D(11,9)=-109395.0D0/256.0D0                                        LSQ
      D(11,7)=90090.0D0/256.0D0                                          LSQ
      D(11,5)=-30030.0D0/256.0D0                                         LSQ
      D(11,3)=3465.0D0/256.0D0                                           LSQ
```

```
      D(11,1)=-63.0D0/256.0D0                                              LSQ
  652 DO700II=1,K                                                          LSQ
      J=K-II+1                                                             LSQ
      VARA=0.0                                                             LSQ
      III=K-J                                                              LSQ
      IF(III)702,701,702                                                   LSQ
  702 DO703JJ=1,III                                                        LSQ
      JK=K-JJ+1                                                            LSQ
  703 VARA=VARA+D(JK,J)*BM(K,JK)                                           LSQ
  701 BM(K,J)=(A(K,J)-VARA)/D(J,J)                                         LSQ
      IF(K-2)700,704,700                                                   LSQ
  704 BM(1,1)=A(1,1)/D(1,1)                                                LSQ
  700 CONTINUE                                                             LSQ
  705 DO708I=1,K                                                           LSQ
      C(I)=0.0                                                             LSQ
      SC(I)=0.0                                                            LSQ
      DO707J=1,K                                                           LSQ
      C(I)=C(I)+BM(J,I)*T(J)                                               LSQ
  707 SC(I)=SC(I)+(BM(J,I)*ST(J))**2                                       LSQ
  708 SC(I)=SQRT(SC(I))                                                    LSQ
  183 CONTINUE                                                             LSQ
      IF(IND-1)190,192,192
  192 WRITE(6,600)                                                         LSQ
      WRITE(6,1) (I,B(I),SB(I),I=1,K)                                      LSQ
  185 WRITE(6,186) SIGMA,FLEV,SUMEV2                                       LSQ
      WRITE(6,601) (I,T(I),ST(I),I=1,K)                                    LSQ
      IF(LP)187,670,187                                                    LSQ
  187 WRITE(6,188)                                                         LSQ
      WRITE(6,602) (I,C(I),SC(I),I=1,K)                                    LSQ
  670 WRITE(6,2)                                                           LSQ
      WRITE(6,603) (I,X(I),F2(I),Y(I),DELY(I),W(I),I=1,M)                  LSQ
  190 CONTINUE                                                             LSQ
      IF(IND-1)220,211,211
  211 IF(ISW) 210,220,210                                                  LSQ
  210 DO215I=2,KM                                                          LSQ
  215 WRITE(6,5) I,(A(I,J),J=1,I)                                          LSQ
  220 KM=KM-1                                                              LSQ
      RETURN                                                               LSQ
    1 FORMAT(3H B(0PI2,2H)=1PE15.7,6H ERRB=E10.3,3H B(0PI2,2H)=1PE15.7,    LSQ
     16H ERRB=E10.3,3H B(0PI2,2H)=1PE15.7,6H ERRB=E10.3)                   LSQ
    2 FORMAT(4H0   I 11X 4HX(I) 12X4HF(I)12X4HY(I)12X7HDELY(I)10X4HW(I)/)LSQ
    5 FORMAT(36H0 ORTHOGONAL POLYNOMIAL COEFF FOR K=I5//(1P8E15.6))        LSQ
  186 FORMAT(7H0SIGMA=1PE16.7,9H F LEVEL=1PE16.7,12H SUM SQ DEV=,1PE16.7LSQ
     *                            //  45H COEFFICIENTS OF Y=T1*P1+T2*P2+ETC ANDLSQ
     1 ERRORS/)                                                            LSQ
  188 FORMAT(23H0  LEGENDRE POLYNOMIALS/45H COEFFICIENTS OF Y=C1*L1+C2*LLSQ
     12+ETC AND ERRORS/)                                                   LSQ
  600 FORMAT(41H1COEFFICIENTS OF Y=B1+B2*X+ETC AND ERRORS/)                LSQ
```

```
0186   601 FORMAT(3H T(I2,2H)=1PE15.7,6H ERRT=E10.3,3H T(OPI2,2H)=1PE15.7,6H LSQ
          1ERRT=E10.3,3H T(OPI2,2H)=1PE15.7,6H ERRT=E10.3)                       LSQ
0187   602 FORMAT(3H C(I2,2H)=1PE15.7,6H ERRC=E10.3,3H C(OPI2,2H)=1PE15.7,6H LSQ
          1ERRC=E10.3,3H C(OPI2,2H)=1PE15.7,6H ERRC=E10.3)                       LSQ
0188   603 FORMAT(I6,1P5E16.7)                                                   LSQ
0189       END                                                                   LSQ
```

```
0001       REAL FUNCTION POLYE1*8(X,K,B)                                         LSQ
0002       REAL*8 X,B,S                                                          LSQ
0003       DIMENSION B(30)                                                       LSQ
0004    10 S=B(K)                                                                LSQ
0005       KK=K-1                                                                LSQ
0006    20 DO 40 I=1,KK                                                          LSQ
0007    30 IK=K-I                                                                LSQ
0008    40 S=X*S+B(IK)                                                           LSQ
0009       POLYE1=S                                                              LSQ
0010       RETURN                                                                LSQ
0011        END                                                                  LSQ
```

```
      SUBROUTINE CHAN (TTO,AMC,PTO,RC,WLBM,WCHAN,WPERO)
      DIMENSION RC(10),WPERO(10)
      COMMON IND
      TC=TTO/(1.+.2*AMC**2)
      VC=49.01*SQRT(TC)*AMC
      PC=PTO/(1.+.2*AMC**2)**3.5
      RHO=PC/(53.35*TC)
      AREA= 3.1416*(RC(5)**2-RC(1)**2)
      WLBM=RHO*AREA*VC
      WCHAN=WLBM/(PTO*SQRT(32.174/(53.35*TTO)))
      WPERO(1)=0.
      WPERO(2)=.25
      WPERO(3)=.5
      WPERO(4)=.75
      WPERO(5)=1.
      RETURN
      END
```

```
      SUBROUTINE STATOR (ALFA1,X,TTO,PTO,AM,T,P,V1,VA1,SI1,SI2,Y,S,DSDX,
     1VU1,PRAT,T1IS,SS,DALF,AA1,BA1,CA1,AA2,BA2,CA2,ALFAM,RSF,DELR,
     2CL,CK,ZETAPS,R,RS1,RS3,RS5,ZETA,DR,ZETAS,NS)
     0DIMENSION ALFA1(10),X(10),T(10),P(10),V1(10),VA1(10),SI1(10),
     1SI2(10),Y(10),S(10),DSDX(10),VU1(10),PRAT(10),T1IS(10),SS(10)
     2,DALDX(10),ALFA(10),DALF(10),ALFAM(10),AMS(10),DALFDX(10),DELR(10)
     3,ZETAS(10),ETA(10),ZETAPS(10),R(10),ZETA(10),DR(10)
      COMMON IND
      C8=0.0
      C9=0.0
      C1=2.*32.174*778.16*.24
      C2=VA1(3)**2/(C1*TTO)
      DO 303 I=1,5
      IF(R(I)-RS3)300,301,302
  300 ZETAS(I)=ZETA(1)+(R(I)-RS1)/(RS3-RS1)*(ZETA(3)-ZETA(1))
      ALFA1(I)=ALFA1(3)+(R(I)-RS3)/(RS1-RS3)*DALF(1)
      GO TO 303
  301 ZETAS(I)=ZETA(3)
      ALFA1(I)=ALFA1(3)
      GO TO 303
  302 ZETAS(I)=ZETA(3)+(R(I)-RS3)/(RS5-RS3)*(ZETA(5)-ZETA(3))
      ALFA1(I)=ALFA1(3)+(R(I)-RS3)/(RS5-RS3)*DALF(5)
  303 ZETAPS(I)=ZETAS(I)/2.0
      DO 305 I=1,5
      ETA(I)=1.-ZETAS(I)
      M=I-1
      N=I+1
      IF (I-1)307,307,309
  307 DALFDX(1)=(ALFA1(2)-ALFA1(1))/(X(2)-X(1))
      GO TO 315
  309 IF(I-5)311,313,313
  311 DALFDX(I)=.5*((ALFA1(N)-ALFA1(I))/(X(N)-X(I))+(ALFA1(I)-ALFA1(M))/
     1(X(I)-X(M)))
      GO TO 315
  313 DALFDX(5)=(ALFA1(5)-ALFA1(4))/(X(5)-X(4))
  315 TAN1=-2.*TAN(ALFA1(I))
      PROD=TAN1*DALFDX(I)
      SINSQ=-2.*SIN(ALFA1(I))**2/X(I)
      SI1(I)=PROD+SINSQ
  305 CONTINUE
  304 DO 332 J=1,5
      IF(J-1)306,306,310
  306 IF(NS-1)317,310,310
  317 DO 308 I=1,5
      SS(I)=0.
  308 SI2(I)=SI1(I)
      GO TO 318
  310 DO 312 I=1,5
```

```
      AA=C2*Y(I)**2/COS(ALFA1(I))**2
      AB=(1.-AA)/(1.-AA/ETA(I))
  312 S(I)=ALOG(AB)
  314 DSDX(1)=(S(2)-S(1))/(X(2)-X(1))
      DSDX(2)=0.5*(DSDX(1)+(S(3)-S(2))/(X(3)-X(2)))
      DSDX(3)=0.5*((S(4)-S(3))/(X(4)-X(3))+(S(3)-S(2))/(X(3)-X(2)))
      DSDX(4)=0.5*((S(5)-S(4))/(X(5)-X(4))+(S(4)-S(3))/(X(4)-X(3)))
      DSDX(5)=(S(5)-S(4))/(X(5)-X(4))
      DO 316 I=1,5
      IF(NS-1)319,321,321
  319 SS(I)=(1.-COS(ALFA1(I))**2/(C2*Y(I)**2))*DSDX(I)
      GO TO 316
  321 SS(I)=((-COS(ALFA1(I))**2/(C2*Y(I)**2))+SIN(ALFA1(I))**2+COS(AL
     1FA1(I))**2*(CL**2+(DR(I)/2.0)**2)/CL**2)*DSDX(I)+COS(ALFA1(I))**2*
     2CK*2.*RSF*DELR(I)/CL**2
  316 SI2(I)= SS(I)+SI1(I)
  318 SUM1=(SI2(1)+SI2(2))*(X(2)-X(1))/4.
      SUM2=(SI2(2)+SI2(3))*(X(3)-X(2))/4.
      SUM3=(SI2(3)+SI2(4))*(X(4)-X(3))/4.
      SUM4=(SI2(4)+SI2(5))*(X(5)-X(4))/4.
      EN2=-SUM2
      EN1=-SUM2-SUM1
      EN3=SUM3
      EN4=SUM3+SUM4
      Y(1)=1.+EN1+EN1**2/2.+EN1**3/6.+EN1**4/24.+EN1**5/120.
      Y(2)=1.+EN2+EN2**2/2.+EN2**3/6.+EN2**4/24.+EN2**5/120.
      Y(3)=1.
      Y(4)=1.+EN3+EN3**2/2.+EN3**3/6.+EN3**4/24.+EN3**5/120.
      Y(5)=1.+EN4+EN4**2/2.+EN4**3/6.+EN4**4/24.+EN4**5/120.
      IF(IND-1)332,323,323
  323 IF(J-1)324,324,320
  320 IF(J-3)322,324,322
  322 IF(J-5)332,324,332
  324 WRITE (6,326)
  326 FORMAT (/57H SLINE  C8  C9  ITERATION  I'ALFA  I'DSDX  I'TOTAL
     1  Y)
      DO 330 I=1,5
  328 FORMAT (I4,F4.2,F4.2,I9,F12.4,F9.5,F9.4,2F8.4)
  330 WRITE (6,328) I,C8,C9,J,SI1(I),SS(I),SI2(I),Y(I),ALFA1(I)
  332 CONTINUE
      DO 334 I=1,5
      VA1(I)=VA1(3)*Y(I)
      VU1(I)=VA1(I)*TAN(ALFA1(I))
      V1(I)=VA1(I)/COS(ALFA1(I))
      T(I)=TTO-V1(I)**2/C1
      T1IS(I)=TTO-(TTO-T(I))/ETA(I)
      P(I)=PTO*(T1IS(I)/TTO)**3.5
  334 PRAT(I)=P(I)/PTO
```

```
      C9=C9+1.
      IF(C9-2.)336,356,356
  336 DO 352 I=1,5
      AMS(I)=V1(I)/(49.01*SQRT(T(I)))
      IF (AMS(I)-.75)338,344,346
  338 IF (AMS(I)-.5)340,340,342
  340 ALFA(3)=ALFAM(1)
      GO TO 348
  342 ALFA(3)=AA1+BA1*AMS(I)+CA1*AMS(I)**2
      GO TO 348
  344 ALFA(3)=ALFAM(3)
      GO TO 348
  346 ALFA(3)=AA2+BA2*AMS(I)+CA2*AMS(I)**2
  348 IF(R(I)-RS3)339,350,341
  339 ALFA1(I)=ALFA(3)+(R(I)-RS3)/(RS1-RS3)*DALF(1)
      GO TO 352
  350 ALFA1(I)=ALFA(3)
      GO TO 352
  341 ALFA1(I)=ALFA(3)+(R(I)-RS3)/(RS5-RS3)*DALF(5)
  352 CONTINUE
      DO 354 I=1,5
      M=I-1
      N=I+1
      IF (I-1)347,347,349
  347 DALFDX(1)=(ALFA1(2)-ALFA1(1))/(X(2)-X(1))
      GO TO 355
  349 IF(I-5)351,353,353
  351 DALFDX(I)=.5*((ALFA1(N)-ALFA1(I))/(X(N)-X(I))+(ALFA1(I)-ALFA1(M))/
     1(X(I)-X(M)))
      GO TO 355
  353 DALFDX(5)=(ALFA1(5)-ALFA1(4))/(X(5)-X(4))
  355 TAN1=-2.*TAN(ALFA1(I))
      PROD=TAN1*DALFDX(I)
      SINSQ=-2.*SIN(ALFA1(I))**2/X(I)
      SI1(I)=PROD+SINSQ
  354 CONTINUE
      GO TO 304
  356 RETURN
      END
```

```
      SUBROUTINE FLOWR(PRAT,ZETAP,X,WI,PTE,PTO,TTE,TTO,AS,ZS,RS,AR,ZR,
     1RR,M,WCHAN,VA,WPER,CODE,WLBM,B,R,TIPC,A)
      REAL*8 B
     ODIMENSION PRAT(10),ZETAP(10),X(10),WI(10),PTE(10),TTE(10),
     1VA(10),WPER(10),B(20),A(10),R(10)
      COMMON IND
      GAM=1.4
      G=32.174
      C=0.15
      A(3)=B(1)+B(2)*R(3)+B(3)*R(3)**2+B(4)*R(3)**3+B(5)*R(3)**4
      F1=1./(C+1.)
      F2=1./(3.*C+1.)
      F3=1./(5.*C+1.)
      F4=1./(7.*C+1.)
      F5=1./(9.*C+1.)
      F6=1./(11.*C+1.)
      PRATCR=(2./(GAM+1.))**(GAM/(GAM-1.))
      PHICR=(2./(GAM+1.))**(1./(GAM-1.))*SQRT(2.*GAM/(GAM+1.))
      DO 420 I=1,5
      IF (PRATCR-PRAT(I))400,402,402
  400 XE=1.-PRAT(I)**((GAM-1.)/GAM)
      GO TO 404
  402 XE=1.-PRATCR**((GAM-1.)/GAM)
  404 XE2=XE**2
      XE3=XE**3
      XE4=XE**4
      XEINV=1./(XE-1.)
      HNUM=XEINV+F2+XE*F3+XE2*F4+XE3*F5+XE4*F6
      HDEN=XEINV+F1+XE*F2+XE2*F3+XE3*F4+XE4*F5
      HSTAR=HNUM/HDEN
      XI=(HSTAR-1.)/(HSTAR-1.+ZETAP(I))
      IF (PRATCR-PRAT(I))406,408,408
  406 PHI=SQRT(2.*GAM/(GAM-1.)*(PRAT(I)**(2./GAM)-PRAT(I)**
     1 ((GAM+1.)/GAM)))
      GO TO 410
  408 PHI=PHICR
  410 A(I)=B(I)+B(2)*R(I)+B(3)*R(I)**2+B(4)*R(I)**3+B(5)*R(I)**4
      ARAT=A(I)/A(3)
      IF(M-2)415,412,415
  412 IF(I-5)415,414,414
  414 ARAT=ARAT+2.*3.1416*R(5)*TIPC/(ZR*AR*RR*(X(5)-X(4)))
  415 IF(IND-1)420,416,416
  416 WRITE (6,418) XI,PHI,ARAT
  418 FORMAT (/5H  XI=, F6.4, 6H  PHI=, F7.5, 7H  ARAT=,F6.4)
  420 WI(I)=(PTE(I)/PTO)/SQRT(TTE(I)/TTO)*ARAT*XI*PHI
      SUM1=(WI(1)+WI(2))*(X(2)-X(1))/2.
      SUM2=(WI(2)+WI(3))*(X(3)-X(2))/2.
      SUM3=(WI(3)+WI(4))*(X(4)-X(3))/2.
```

```
      SUM4=(WI(4)+WI(5))*(X(5)-X(4))/2.
      WSUM=SUM1+SUM2+SUM3+SUM4
      IF (M-1)428,426,428
  426 WREQ=WCHAN/(AS*ZS*RS)
      DIFF=ABS(WREQ-WSUM)
      GO TO 430
  428 WREQ=WCHAN/(AR*ZR*RR)
      DIFF=ABS(WREQ-WSUM)
  430 IF (DIFF-.0002)432,432,434
  432 VA(3)=VA(3)
      CODE=20.
      GO TO 442
  434 IF(WSUM-WREQ)436,432,438
  436 VA(3)=VA(3)+DIFF/.00065
      GO TO 442
  438 VA(3)=VA(3)-DIFF/.00065
  442 WPER(1)=0.
      WPER(2)=SUM1/WSUM
      WPER(3)=(SUM1+SUM2)/WSUM
      WPER(4)=(SUM1+SUM2+SUM3)/WSUM
      WPER(5)=1.
      IF(IND-1)450,423,423
  423 WRITE (6,422) (WI(I),I=1,5)
  422 FORMAT (/20H  FLOW INTEGRAND 1-5, 5F10.5)
      WRITE (6,424) SUM1,SUM2,SUM3,SUM4,WSUM
  424 FORMAT (/15H SUMS 1-4, WSUM, 5F10.5)
      WRITE (6,440) WSUM,WREQ,VA(3)
  440 FORMAT(35H REF FLOWS,COMPUTED-REQUIRED,AX VEL,2F10.4,F10.2)
      WRITE (6,444) WCHAN,WLBM
  444 FORMAT(/36H REF FLOW RATE CHANNEL-SQUARE INCHES,F8.5,18H FLOW RATE
     1-LBM/SEC,F8.5)
      WRITE (6,446) M
  446 FORMAT (/30H STREAMLINE FLOW FRACTIONS, M=,I2)
      WRITE (6,448) X(2),WPER(2),X(3),WPER(3),X(4),WPER(4)
  448 FORMAT(6F10.4)
  450 RETURN
      END
```

```
      OSUBROUTINE SLINE (RR,X,DWDX,WPER2,WPER1,HE,U,DHEDX,S,DSDX1,
      1ARF,RRF,FC1,FC2,CODE,M,B)
       REAL*8 B
      ODIMENSICN RR(10),X(10),DWDX(10),WI(10),WPER2(10),WPER1(10),HE(10),
      1DHEDX(10),S(10),DSDX1(10),U(10),B(20)
       COMMON IND
       N7=0
       SAVE=RR(3)
       CODE=1.
       DO 700 I=1,4
       J=I+1
  700  DWDX(I)=(WPER2(J)-WPER2(I))/(X(J)-X(I))
       N=0
       DO 720 I=2,4
       K=I+1
       J=I-1
       IF (ABS(WPER2(I)-WPER1(I))-.002)716,716,702
  702  IF (WPER2(I)-WPER1(I))704,716,708
  704  XN=X(I)+(WPER1(I)-WPER2(I))/DWDX(J)
       IF(M-1)706,712,706
  706  SL=(HE(K)-HE(I))/(X(K)-X(I))
       DEL=2.*(SL-DHEDX(I))/(X(K)-X(I))
       DHEDX(I)=DHEDX(I)+DEL*(XN-X(I))
       HE(I)=HE(I)+DHEDX(I)*(XN-X(I))
       SL=(S(K)-S(I))/(X(K)-X(I))
       DEL=2.*(SL-DSDX1(I))/(X(K)-X(I))
       DSDX1(I)=DSDX1(I)+DEL*(XN-X(I))
       S(I)=S(I)+DSDX1(I)*(XN-X(I))
       GO TO 712
  708  XN=X(I)-(WPER2(I)-WPER1(I))/DWDX(I)
       IF (M-1)710,712,710
  710  SL=(HE(I)-HE(J))/(X(I)-X(J))
       DEL=2.*(DHEDX(I)-SL)/(X(I)-X(J))
       DHEDX(I)=DHEDX(I)+DEL*(XN-X(I))
       HE(I)=HE(I)+DHEDX(I)*(XN-X(I))
       SL=(S(I)-S(J))/(X(I)-X(J))
       DEL=2.*(DSDX1(I)-SL)/(X(I)-X(J))
       DSDX1(I)=DSDX1(I)+DEL*(XN-X(I))
       S(I)=S(I)+DSDX1(I)*(XN-X(I))
  712  RR(I)=XN*SAVE
       GO TO 718
  716  N=N+1
       IF (N-3)720,730,720
  718  U(I)=U(I)*XN/X(I)
  720  CONTINUE
       DO 722 I=1,5
  722  X(I)=RR(I)/RR(3)
       FC1=RR(3)/SAVE
```

```
      FC2=FC1**2
      RRF=RR(3)
      ARF=B(1)+B(2)*RRF+B(3)*RRF**2+B(4)*RRF**3+B(5)*RRF**4
      IF(IND-1)732,721,721
  721 IF (M-1)729,732,729
  729 WRITE (6,724)
  724 FORMAT (/47H SLINE   XNEW    HENEW     DHEDX      S-NEW    DSDX1)
      DO 728 I=1,5
  726 FORMAT (I4,F9.4,F9.2,F9.4,F9.6,F9.5)
  728 WRITE (6,726) I,X(I),HE(I),DHEDX(I),S(I),DSDX1(I)
      GO TO 732
  730 CODE=40.
  732 RETURN
      END
```

```
0001          0SUBROUTINE ROTOR1(VU1,VA1,RPM,U,BETA1,HE,TTE,PTE,X2,P1,T1,W1,WU1,
              1X1,RS,ZETAR,ZETAPR,RR,DHEDX,DSDX,S,U2,OMEG,BR1,BR2,BR3,FS1,FS2,
              2B3,B4,B5,B6,RS1,RS3,RS5,BETO,STALI,BINC)
0002           REAL*8 B3,B4,B5,B6
0003          0DIMENSION VU1(10),VA1(10),U(10),BETA1(10),HE(10),TTE(10),PTE(10),
              1X2(10),P1(10),T1(10),W1(10),WU1(10),X1(10),RS(10),ZETAR(10),
              2ZETAPR(10),RR(10),DHEDX(10),DSDX(10),S(10),U2(10),ZETA(10)
              3,B3(20),B4(20),B5(20),B6(20),BETO(10),STALI(10),BINC(10)
0004           COMMON IND
0005           C=2.*32.174*778.16*.24
0006           OMEG=RPM*3.1416/30.
0007           DO 520 I=1,5
0008           U(I)=OMEG*RS(I)/12.
0009           U2(I)=U(I)*RR(I)/RS(I)
0010           WU1(I)=VU1(I)-U(I)
0011           BETA1(I)=ATAN(WU1(I)/VA1(I))
0012           W1(I)=VA1(I)/COS(BETA1(I))
0013           TTE(I)=T1(I)+W1(I)**2/C+(U2(I)**2-U(I)**2)/C
0014           PTE(I)=P1(I)*(TTE(I)/T1(I))**3.5
0015           HE(I)=TTE(I)*.24
0016           BETO(I)=BR1+FS1*BR2*X1(I)+FS2*BR3*X1(I)**2
0017           STALI(I)=B6(1)+B6(2)*RS(I)+B6(3)*RS(I)**2+B6(4)*RS(I)**3+B6(5)*RS
              1(I)**4
0018           BINC(I)=BETA1(I)-BETO(I)/57.3
0019           RINC=BINC(I)/(STALI(I)/57.3)
0020           IF(IND-1)510,501,501
0021       501 IF(RINC+2.0)500,500,502
0022       500 RINC=-2.0
0023           GO TO 506
0024       502 IF(RINC-1.6)510,504,504
0025       504 RINC=1.6
0026       506 WRITE(6,508)RINC
0027       508 FORMAT (/58H RATIO OF INCIDENCE TO STALL INCIDENCE EXCEEDED, USE I
              1/IS=, F5.1)
0028       510 ZETA(1)=B3(1)+B3(2)*RINC+B3(3)*RINC**2+B3(4)*RINC**3+B3(5)*RINC
              1**4
0029           ZETA(3)=B4(1)+B4(2)*RINC+B4(3)*RINC**2+B4(4)*RINC**3+B4(5)*RINC*
              1*4
0030           ZETA(5)=B5(1)+B5(2)*RINC+B5(3)*RINC**2+B5(4)*RINC**3+B5(5)*RINC
              1**4
0031           IF(RS(I)-RS3)512,514,516
0032       512 ZETAR(I)=ZETA(1)+(RS(I)-RS1)/(RS3-RS1)*(ZETA(3)-ZETA(1))
0033           GO TO 518
0034       514 ZETAR(I)=ZETA(3)
0035           GO TO 518
0036       516 ZETAR(I)=ZETA(3)+(RS(I)-RS3)/(RS5-RS3)*(ZETA(5)-ZETA(3))
0037       518 ZETAPR(I)=ZETAR(I)/2.0
0038       520 CONTINUE
```

```
      DSDX(1)=(S(2)-S(1))/(X2(2)-X2(1))
      DSDX(2)=0.5*(DSDX(1)+(S(3)-S(2))/(X2(3)-X2(2)))
      DSDX(3)=0.5*((S(4)-S(3))/(X2(4)-X2(3))+(S(3)-S(2))/(X2(3)-X2(2)))
      DSDX(5)=(S(5)-S(4))/(X2(5)-X2(4))
      DSDX(4)=0.5*(DSDX(5)+(S(4)-S(3))/(X2(4)-X2(3)))
      DHEDX(1)=(HE(2)-HE(1))/(X2(2)-X2(1))
      DHEDX(2)=0.5*(DHEDX(1)+(HE(3)-HE(2))/(X2(3)-X2(2)))
     0DHEDX(3)=0.5*((HE(3)-HE(2))/(X2(3)-X2(2))+(HE(4)-HE(3))/
     1 (X2(4)-X2(3)))
      DHEDX(5)=(HE(5)-HE(4))/(X2(5)-X2(4))
      DHFDX(4)=0.5*(DHEDX(5)+(HF(4)-HE(3))/(X2(4)-X2(3)))
  522 CONTINUE
      RETURN
      END
```

```
0001          SUBROUTINE ROTOR2 (BETA2,HE,DHEDX,DSDX1,DSDX2,VA2,WU2,W2,VU2,V2,
             1X2,U,YR,ZETAR,RI1,RI2,RI3,RI4,RI,SR1,SR2,AA,SR,TTE,PTE,T2,P2,PRAT2
             2,T2S,INDS,DBET,BETAM,AB1,BB1,CB1,AB2,BB2,CB2,RRF,DELR,CL,CK,DR,R,
             3RR1,RR3,RR5,NS)
0002         ODIMENSION BETA2(10),HE(10),DHEDX(10),DSDX1(10),DSDX2(10),VA2(10),
             1WU2(10),W2(10),VU2(10),V2(10),X2(10),U(10),YR(10),ZETAR(10),
             2RI1(10),RI2(10),RI3(10),RI4(10),RI(10),SR1(10),SR2(10),YOLD(10),
             3AA(10),SR(10),TTE(10),PTE(10),T2(10),P2(10),PRAT2(10),T2S(10),
             4DBET(10),BETAM(10),AMR(10),DBETDX(10),BETA(10),DELR(10),RI5(10)
             5,DR(10),R(10)
0003          COMMON IND
0004          INDS=0
0005          INDS1=0
0006          C=2.*32.174*778.16
0007          GAM=1.4
0008          C1=C/VA2(3)**2
0009          DO 274 I=1,5
0010          IF(R(I)-RR3)270,271,273
0011      270 BETA2(I)=BETA2(3)+(R(I)-RR3)/(RR1-RR3)*DBET(1)
0012          GO TO 274
0013      271 BETA2(I)=BETA2(3)
0014          GO TO 274
0015      273 BETA2(I)=BETA2(3)+(R(I)-RR3)/(RR5-RR3)*DBET(5)
0016      274 CONTINUE
0017          DBETDX(1)=(BETA2(2)-BETA2(1))/(X2(2)-X2(1))
0018          DBETDX(5)=(BETA2(5)-BETA2(4))/(X2(5)-X2(4))
0019          DO 280 I=2,4
0020          M=I-1
0021          N=I+1
0022      280 DBETDX(I)=.5*((BETA2(N)-BETA2(I))/(X2(N)-X2(I))+(BETA2(I)-BETA2
             1(M))/(X2(I)-X2(M)))
0023          DO 10 I=1,5
0024      200 TAN1=-2.*TAN(BETA2(I))
0025          PROD=TAN1*DBETDX(I)
0026          SIN1=-2.*SIN(BETA2(I))**2/X2(I)
0027          RI1(I)=PROD+SIN1+DSDX1(I)
0028          SR1(I)=-4.*U(3)*COS(BETA2(I))*SIN(BETA2(I))/(VA2(3)*YR(I))
0029          SR2(I)=2.*U(3)*U(I)*COS(BETA2(I))**2/(VA2(3)**2*YR(I)**2)
0030          YOLD(I)=YR(I)
0031          AA(I)=(VA2(3)*YR(I)/COS(BETA2(I)))**2/(C*HE(I))
0032          RI3(I)=C*COS(BETA2(I))**2/(VA2(3)*YR(I))**2*DHEDX(I)
0033          IF (INDS1-1)10,250,250
0034       10 CONTINUE
0035      281 IF(IND-1)201,282,282
0036      282 WRITE (6,121)(RI1(I),I=1,5)
0037      121 FORMAT(/23H CONSTANT INTEGRAND 1-5, 5F8.5)
0038          WRITE (6,122)
0039      122 FORMAT(/60H SLINE   INDS1   GRAD S    INT2    INT3     INT4     INT
```

```
     1Y VAL)
 201 DO 20 J=1,13
     DO 30 I=1,5
     AA(I)=AA(I)*(YR(I)/YOLD(I))**2
     ANUM=1.-AA(I)
     ADEN=1.-AA(I)/(1.-ZETAR(I))
     AB=ANUM/ADEN
     IF (AB) 130,130,30
 130 INDS=1
     GO TO 150
  30 SR(I)=ALOG(ANUM/ADEN)
     DSDX2(1)=(SR(2)-SR(1))/(X2(2)-X2(1))
     DSDX2(2)=0.5*(DSDX2(1)+(SR(3)-SR(2))/(X2(3)-X2(2)))
     DSDX2(3)=0.5*((SR(3)-SR(2))/(X2(3)-X2(2))+(SR(4)-SR(3))/
    1 (X2(4)-X2(3)))
     DSDX2(5)=(SR(5)-SR(4))/(X2(5)-X2(4))
     DSDX2(4)=0.5*(DSDX2(5)+(SR(4)-SR(3))/(X2(4)-X2(3)))
     DO 40 I=1,5
     SR1(I)=SR1(I)*YOLD(I)/YR(I)
     SR2(I)=SR2(I)*(YOLD(I)/YR(I))**2
     RI2(I)=SR1(I)-SR2(I)
     RI3(I)=RI3(I)*(YOLD(I)/YR(I))**2
     IF(NS-1)31,32,32
  31 RI4(I)=DSDX2(I)-(DSDX1(I)+DSDX2(I))*C1*HE(I)
    1 *(COS(BETA2(I))/YR(I))**2
     GO TO 40
  32 RI4(I)=-(DSDX1(I)+DSDX2(I))*C1*HE(I)*(COS(BETA2(I))/YR(I))**2
     RI5(I)=(DSDX1(I)+DSDX2(I))*(SIN(BETA2(I))**2+COS(BETA2(I))**2
    1*((CL**2+(DR(I)/2.0)**2)/CL**2))-COS(BETA2(I))**2*(2.*CK*RRF*
    2DELR(I))/CL**2
     RI4(I)=RI4(I)+RI5(I)
  40 RI(I)=RI1(I)+RI2(I)+RI3(I)+RI4(I)
     SUM1=(RI(1)+RI(2))*(X2(2)-X2(1))/4.
     SUM2=(RI(2)+RI(3))*(X2(3)-X2(2))/4.
     SUM3=(RI(3)+RI(4))*(X2(4)-X2(3))/4.
     SUM4=(RI(4)+RI(5))*(X2(5)-X2(4))/4.
     EN1=-(SUM2+SUM1)
     EN2=-SUM2
     EN4=SUM3
     EN5=SUM3+SUM4
     DO 50 I=1,5
  50 YOLD(I)=YR(I)
     YR(1)=1.+EN1+EN1**2/2.+EN1**3/6.+EN1**4/24.+EN1**5/120.
     YR(2)=1.+EN2+EN2**2/2.+EN2**3/6.+EN2**4/24.+EN2**5/120.
     YR(3)=1.0
     YR(4)=1.+EN4+EN4**2/2.+EN4**3/6.+EN4**4/24.+EN4**5/120.
     YR(5)=1.+EN5+EN5**2/2.+EN5**3/6.+EN5**4/24.+EN5**5/120.
     NCOUNT=0
```

```
      DO 110 I=1,5
      TEST=ABS(YCLD(I)-YR(I))
      IF(TEST-.005)110,110,119
  110 NCOUNT=NCOUNT+1
      IF(NCOUNT-5)119,140,119
  119 IF(IND-1)20,120,120
  120 IF (J-3) 80,100,80
   80 IF (J-6) 90,100,90
   90 IF (J-9) 160,100,160
  160 IF (J-12) 20,100,20
  100 DO 60 I=1,5
  123 FORMAT (I4,I7,F10.5,5F8.4)
   60 WRITE (6,123) I,INDS1,DSDX2(I),RI2(I),RI3(I),RI4(I),RI(I),YR(I)
   20 CONTINUE
  140 DO 70 I=1,5
      VA2(I)=YR(I)*VA2(3)
      W2(I)=VA2(I)/COS(BETA2(I))
   70 T2(I)=TTE(I)-W2(I)**2/(0.24*C)
      IF(INDS1-1)251,149,149
  251 INDS1=INDS1+1
      DO 250 I=1,5
      AMR(I)=W2(I)/(49.01*SQRT(T2(I)))
      IF(AMR(I)-.75)1,4,5
    1 IF(AMR(I)-.5)2,2,3
    2 BETA(3)=BETAM(1)
      GO TO 6
    3 BETA(3)=AB1+BB1*AMR(I)+CB1*AMR(I)**2
      GO TO 6
    4 BETA(3)=BETAM(3)
      GO TO 6
    5 BETA(3)=AB2+BB2*AMR(I)+CB2*AMR(I)**2
    6 IF (R(I)-RR3)221,222,223
  221 BETA2(I)=BETA(3)+(R(I)-RR3)/(RR1-RR3)*DBET(1)
      GO TO 250
  222 BETA2(I)=BETA(3)
      GO TO 250
  223 BETA2(I)=BETA(3)+(R(I)-RR3)/(RR5-RR3)*DBET(5)
  250 CONTINUE
      DBETDX(1)=(BETA2(2)-BETA2(1))/(X2(2)-X2(1))
      DBETDX(5)=(BETA2(5)-BETA2(4))/(X2(5)-X2(4))
      DO 224 I=2,4
      M=I-1
      N=I+1
  224 DBETDX(I)=.5*((BETA2(N)-BETA2(I))/(X2(N)-X2(I))+(BETA2(I)-BETA2
     1(M))/(X2(I)-X2(M)))
      DO 225 I=1,5
      TAN1=-2.*TAN(BETA2(I))
      PROD=TAN1*CBETDX(I)
```

```
      SIN1=-2.*SIN(BETA2(I))**2/X2(I)
      RI1(I)=PROD+SIN1+DSDX1(I)
      SR1(I)=-4.*U(3)*COS(BETA2(I))*SIN(BETA2(I))/(VA2(3)*YR(I))
      SR2(I)=2.*U(3)*U(I)*COS(BETA2(I))**2/(VA2(3)**2*YR(I)**2)
      YOLD(I)=YR(I)
      AA(I)=(VA2(3)*YR(I)/COS(BETA2(I)))**2/(C*HE(I))
      RI3(I)=C*COS(BETA2(I))**2/(VA2(3)*YR(I))**2*DHEDX(I)
  225 CONTINUE
      GO TO 281
  149 DO 190 I=1,5
      WU2(I)=VA2(I)*TAN(BETA2(I))
      VU2(I)=WU2(I)+U(I)
      T2S(I)=TTE(I)-(TTE(I)-T2(I))/(1.-ZETAR(I))
      P2(I)=PTE(I)*(T2S(I)/TTE(I))**(GAM/(GAM-1.))
  190 PRAT2(I)=P2(I)/PTE(I)
  150 RETURN
      END
```

STATOR SOLUTION **TABLE V**

SET NO.	PTO	TTO	RPM	PR
1	17.20	568.00	12000.	1.30

SLINE	R1	X1	ZETAS	ZETAPS	Y	A
1	3.300	0.782	0.09040	0.04520	1.01316	0.3801
2	3.799	0.900	0.08411	0.04205	1.00784	0.5082
3	4.220	1.000	0.07924	0.03962	1.00000	0.6161
4	4.600	1.090	0.07620	0.03810	0.98457	0.7123
5	4.949	1.173	0.07340	0.03670	0.96925	0.8017

SLINE	T1	P1	ALFA1	BETA1	U1	W-FRAC	PTO/P1
1	535.65	13.72	76.27	60.35	345.58	0.0	1.2539
2	542.40	14.42	74.61	42.91	397.84	0.2507	1.1932
3	546.54	14.85	73.28	16.90	441.94	0.4998	1.1579
4	549.16	15.13	72.40	-11.09	481.73	0.7503	1.1365
5	551.26	15.36	71.60	-33.20	518.31	1.0000	1.1198

SLINE	VA1	VU1	V1	WU1	W1	M1
1	148.1	605.6	623.5	260.1	299.3	0.550
2	147.3	534.8	554.7	136.9	201.1	0.486
3	146.2	486.3	507.8	44.4	152.7	0.443
4	143.9	453.5	475.8	-28.2	146.6	0.414
5	141.7	425.6	448.6	-92.7	169.3	0.390

ROTOR SOLUTION **TABLE VI**

SET NO.	PTO	TTO	RPM	PR
1	17.20	568.00	12000.	1.30

SLINE	R2	X2	TTE	PTE	ZETAR	ZETAPR	Y	VA2
1	2.979	0.729	541.27	14.23	0.16894	0.08447	0.9085	129.7
2	3.583	0.876	544.35	14.60	0.12121	0.06060	0.9731	138.9
3	4.089	1.000	547.53	14.95	0.10912	0.05456	1.0000	142.8
4	4.552	1.113	550.55	15.27	0.16709	0.08354	1.0454	149.2
5	4.929	1.206	553.46	15.58	0.21749	0.10875	1.1002	157.1

SLINE	T2	P2	PTO/P2	ALFA2	BETA2	U2	W-FRAC	A
1	532.03	13.23	1.300	2.209	-67.104	312.01	0.0	0.3515
2	531.17	13.24	1.299	0.911	-69.578	375.17	0.25023	0.3662
3	530.42	13.19	1.304	-0.871	-71.654	428.18	0.50011	0.3731
4	532.28	13.24	1.299	12.304	-71.432	476.66	0.75143	0.3738
5	533.90	13.25	1.298	20.116	-71.104	516.22	1.00000	0.3639

SLINE	M2	VU2	V2	WU2	W2	BO	STALI	INCID
1	0.295	5.0	129.8	-307.0	333.3	62.44	13.48	-2.09
2	0.352	2.2	138.9	-373.0	398.0	42.12	34.80	0.80
3	0.402	-2.2	142.8	-430.3	453.4	20.84	40.42	-3.94
4	0.414	32.5	152.7	-444.1	468.5	-1.61	38.93	-9.48
5	0.428	57.5	167.3	-458.7	484.8	-24.96	37.17	-8.24

SLINE	DELH	PT1	TT2	PT2	T2IS	T2S
1	8.30	16.84	533.43	13.35	526.96	530.15
2	8.46	16.94	532.73	13.37	527.06	529.35
3	8.62	17.00	532.08	13.34	526.54	528.32
4	8.11	17.03	534.22	13.41	527.12	528.62
5	7.63	17.06	536.23	13.45	527.19	528.46

SLINE	ETAI	ETAS	ETAR	PSIR	RSTAR	AKIS	DELR
1	0.8425	0.9096	0.8310	0.9116	0.13338	4.129	0.07775
2	0.8614	0.9159	0.8788	0.9374	0.31729	3.109	0.05974
3	0.8664	0.9208	0.8909	0.9439	0.43791	2.551	0.03721
4	0.8263	0.9238	0.8329	0.9126	0.50116	2.117	0.01286
5	0.7786	0.9266	0.7325	0.8846	0.55720	1.825	0.01000

HORSE POWER	MOMENT FT-LB	FLORATE LBM/SEC	REF HORSE POWER	REF MOMENT FT-LB	REF RPM	REF FLORATE LBM/SEC
39.2	17.16	3.342	32.0	14.663	11464.1	2.990

ETA	PTO/P2	M-STATION 0	AKIS	RSTAR
0.8412	1.3003	C.12977	2.689	0.40041

INITIAL DISTRIBUTION LIST

		No. Copies
1.	Defense Documentation Center Cameron Station Alexandria, Virginia 22314	20
2.	Library Naval Postgraduate School Monterey, California 93940	2
3.	Commander, Naval Air Systems Command Navy Department Washington, D.C. 20360	1
4.	Commander, Naval Ship Systems Command Navy Department Washington, D.C. 20360	1
5.	Capt. A. Bodnaruk, USN Naval Ship Systems Command (Code 6140) Navy Department Washington, D.C. 20360	1
6.	Office of Naval Research (Power Branch) Attn. Mr. J. K. Patton, Jr. Navy Department Washington, D.C. 20360	1
7.	Mr. R. Beichel Liquid Rocket Plant Aerojet-General Corporation Sacramento, California 95809	1
8.	Chairman, Department of Aeronautics Naval Postgraduate School Monterey, California 93940	2
9.	Professor M. H. Vavra Department of Aeronautics Naval Postgraduate School Monterey, California 93940	3
10.	Lt R. G. Harrison, USN Naval Air Turbine Test Station 1440 Parkway Ave. P.O. Box 1716 Trenton, New Jersey 08628	3

DOCUMENT CONTROL DATA - R&D

(Security classification of title, body of abstract and indexing annotation must be entered when the overall report is classified)

1. ORIGINATING ACTIVITY (Corporate author)
Naval Postgraduate School
Monterey, California 93940

2a. REPORT SECURITY CLASSIFICATION
UNCLASSIFIED

2b. GROUP

3. REPORT TITLE
AN ANALYSIS OF SINGLE STAGE AXIAL-FLOW TURBINE PERFORMANCE USING THREE-DIMENSIONAL CALCULATING METHODS

4. DESCRIPTIVE NOTES (Type of report and inclusive dates)
Engineer Thesis, September 1967

5. AUTHOR(S) (Last name, first name, initial)
HARRISON, Robert G.

6. REPORT DATE	7a. TOTAL NO. OF PAGES	7b. NO. OF REFS
September 1967	144	9

8a. CONTRACT OR GRANT NO.

b. PROJECT NO.

c.

d. Distribution unlimited

9a. ORIGINATOR'S REPORT NUMBER(S)

9b. OTHER REPORT NO(S) (Any other numbers that may be assigned this report)

10. AVAILABILITY/LIMITATION NOTICES

~~Qualified requesters may obtain copies of this report from DDC~~.

11. SUPPLEMENTARY NOTES

-

12. SPONSORING MILITARY ACTIVITY
Naval Air Systems Command
Navy Department
Washington, D.C. 20360

13. ABSTRACT

The method of turbine performance prediction developed by Vavra and Eckert has been refined in this analysis to realize more of the potential of the three-dimensional calculating methods. Mach number and rotor tip clearance effects on blade outlet angles and loss coefficients have been localized rather than averaged over the blade height. An approximation for streamline curvature has been used.

Performance curves were determined for two single stage axial-flow turbines located at the Propulsion Laboratory of the Naval Postgraduate School. Test results were available for one of the turbines. Agreement between predicted and experimental performance values was generally within 3 per cent.

DD FORM 1 JAN 64 1473

UNCLASSIFIED
Security Classification

14 KEY WORDS	LINK A ROLE	LINK A WT	LINK B ROLE	LINK B WT	LINK C ROLE	LINK C WT
ANALYSIS						
SINGLE-STAGE						
AXIAL-FLOW						
TURBINE						
PERFORMANCE						
THREE-DIMENSIONAL						
CALCULATING						
METHODS						